Available online at www.sciencedirect.com

ScienceDirect

ELSEVIER

Palaeogeography, Palaeoclimatology, Palaeoecology 240 (2006) 3–46

PALAEO

www.elsevier.com/locate/palaeo

Evaporites and the salinity of the ocean during the Phanerozoic: Implications for climate, ocean circulation and life

William W. Hay [a,*], Areg Migdisov [b,☆], Alexander N. Balukhovsky [b], Christopher N. Wold [c], Sascha Flögel [d], Emanuel Söding [e]

[a] *2045 Windcliff Dr., Estes Park, CO 80517, USA*

[b] *VI Vernadski Institute of Geochemistry and Analytical Chemistry, Russian Academy of Sciences, Kosygin 19, Moscow 119991, Russia*

[c] *Platte River Associates, 2790 Valmont Road, Boulder, CO 80304, USA*

[d] *Leibniz-Institute of Marine Sciences (IFM-GEOMAR), Wischhofstrasse 1-3, D-24148 Kiel, Germany*

[e] *Integrated Ocean Drilling Program Management International, Inc., Sapporo Office, Creative Research Initiative "Sousei" (CRIS), Hokkaido University, N21W10 Kitaku, Sapporo 001-0021, Japan*

Received 23 March 2005; accepted 24 March 2006

Abstract

A compilation of data on volumes and masses of evaporite deposits is used as the basis for reconstruction of the salinity of the ocean in the past. Chloride is tracked as the only ion essentially restricted to the ocean, and past salinities are calculated from reconstructed chlorine content of the ocean. Models for ocean salinity through the Phanerozoic are developed using maximal and minimal estimates of the volumes of existing evaporite deposits, and using constant and declining volumes of ocean water through the Phanerozoic. We conclude that there have been significant changes in the mean salinity of the ocean accompanying a general decline throughout the Phanerozoic. The greatest changes are related to major extractions of salt into the young ocean basins which developed during the Mesozoic as Pangaea broke apart. Unfortunately, the sizes of these salt deposits are also the least well known. The last major extractions of salt from the ocean occurred during the Miocene, shortly after the large scale extraction of water from the ocean to form the ice cap of Antarctica. However, these two modifications of the masses of H_2O and salt in the ocean followed in sequence and did not cancel each other out. Accordingly, salinities during the Early Miocene were between 37‰ and 39‰. The Mesozoic was a time of generally declining salinity associated with the deep sea salt extractions of the North Atlantic and Gulf of Mexico (Middle to Late Jurassic) and South Atlantic (Early Cretaceous). The earliest of the major extractions of the Phanerozoic occurred during the Permian. There were few large extractions of salt during the earlier Palaeozoic. The models suggest that this was a time of relatively stable but slowly increasing salinities ranging through the upper 40‰'s into the lower 50‰'s.

Higher salinities for the world ocean have profound consequences for the thermohaline circulation of the ocean in the past. In the modern ocean, with an average salinity of about 34.7‰, the density of water is only very slightly affected by cooling as it approaches the freezing point. Consequently, salinization through sea-ice formation or evaporation is usually required to make water dense enough to sink into the ocean interior. At salinities above about 40‰ water continues to become more dense as it approaches the freezing point, and salinization is not required. The energy-consuming phase changes involved in sea-ice formation and evaporation would not be required for vertical circulation in the ocean.

The hypothesized major declines in salinity correspond closely to the evolution of both planktonic foraminifera and calcareous nannoplankton. Both groups were restricted to shelf regions in the Jurassic and early Cretaceous, but spread into the open ocean in

* Corresponding author.
E-mail address: whay@gmx.de (W.W. Hay).

☆ April 3, 2003.

doi:10.1016/j.palaeo.2006.03.044

the mid-Cretaceous. Their availability to inhabit the open ocean may be directly related to the decline in salinity. The Permian extraction may have created stress for marine organisms and may have been a factor contributing to the end-Permian extinction. The modeling also suggests that there was a major salinity decline from the Late Precambrian to the Cambrian, and it is tempting to speculate that this may have been a factor in the Cambrian explosion of life.

Keywords: Salinity; Salt; Palaeoceanography; Phanerozoic; Sedimentary cycling

1. Introduction

The history of the salinity of the ocean has been a matter of inquiry since the end of the 19th century. Irish Physicist John Joly (1899) used the present salinity of the ocean and the present rate of supply of salt by rivers to estimate the age of the Earth. Using the methodology shown in Fig. 1, he determined that these ions would accumulate in the ocean to their present level in about 90 million years. He reasoned that this must therefore be the age of the ocean, and that the planet could not be much older. His estimate for the age of the earth, being in close agreement with that of Lord Kelvin (1864) was widely accepted by the non-geological community. He held to this argument, rejecting even his own radiometric evidence for a much greater age for the planet, through at least the first quarter of the 20th century (Joly, 1925).

The amount of sodium chloride in the ocean is only about 10% that of saturation, so it might be expected that the steady supply of salts to the ocean would cause its salinity to increase continuously. However, it has not been known how the supply of salts might have changed over time. Further, it has been recognized that there were numerous salt deposits in the geologic record and that these must represent extractions of salt from the ocean.

With the lack of quantification of supply and extraction of salts from the ocean, many geologists and palaeontologists have assumed that the salinity of the ocean has remained essentially constant near its

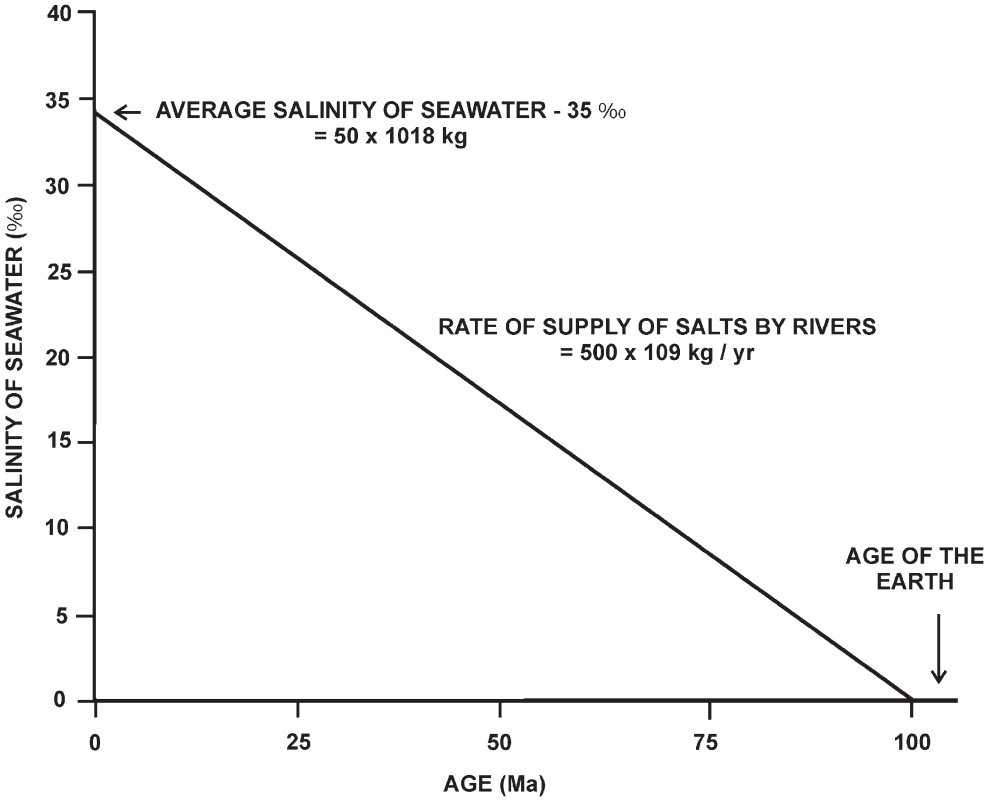

Fig. 1. Schematic version of Joly's (1899) method for determining the age of the Earth from ocean salinity and rate of salt supply.

present value of 34.7‰ through the Phanerozoic (Railsback et al., 1989). Others have made a correction for the present mass of fresh water in glacial ice on Antarctica and Greenland (Shackleton and Kennett, 1975; Shackleton, 1987; Duplessy et al., 1991, 1993), assuming a global mean salinity of 34.03‰ during ice-free times. Others have constructed more complex schemes taking into account the gradual buildup of Antarctic ice (Zachos et al., 1994). However, the extractions of salt from the ocean to form evaporite deposits have been generally disregarded, although it has been recognized that they must have a significant effect on ocean salinity (Southam and Hay, 1981).

In this paper we attempt a quantitative reconstruction of the salinity of the ocean through the Phanerozoic, based solely on deposition and sedimentary cycling of evaporite deposits. However, this may be only part of the salinity history of the ocean because there is another potentially large reservoir of salt stored in brines in the pore space of deeply buried sediments on the continental blocks.

2. Evaporite deposits

2.1. Early estimates of the size of evaporite deposits

The first detailed data on the volumes of evaporite deposits was Zharkov's (1974, 1981) compilation of Palaeozoic salt deposits. It fueled speculation that there might have been changes in salinity of the ocean through time, although it was thought that these could not have been more than a few per parts per thousand (Holland, 1974, 1978). The then known inventory of Palaeozoic salt deposits did not allow for a change in salinity of more than about 10%.

When Sigsbee Knoll was drilled on Leg 1 of the Deep Sea Drilling Project in 1967, a very major discovery was made: much of the Gulf of Mexico was underlain by a vast layer of salt (Ewing et al., 1969). This was soon realized to be the offshore extension of the Jurassic Louann salt known from petroleum drilling in Louisiana and east Texas. The idea that salt could be deposited in basins of oceanic depth was new, and the projected volume of the salt deposit was far larger than any known until then on land. This discovery was soon followed by the discovery that large areas of the Mediterranean and Red Seas were also underlain by salt.

Holland (1974) reported on a series of calculations to determine whether the relative proportions of major ions of seawater might have changed sufficiently to be reflected in an alteration of the sequence and mineralogy of salts deposited as seawater evaporates. He reckoned that the mass of evaporites deposited during the Phanerozoic might be equal to the amount in seawater and so concluded that any salinity changes could not possibly have been greater than a factor of two. He also found it unlikely that the relative proportions of major ions in seawater could have varied by more than a factor of two.

From other compilations of evaporite deposits it became evident that so much salt has been extracted from seawater during the Phanerozoic that the salinity of the ocean during the Palaeozoic must have been higher than it is today (Ronov, 1968; Holser et al., 1980), but a quantitative estimate remained elusive. Holland (1984) discussed the problem of salinity and relative ratios of major ions. He cited a personal communication from Holser in 1981 to the effect that the inventory of halite in sedimentary rocks today amounts to about 30% of the NaCl in the ocean, so that the maximum salinity that might be expected would be about 45‰.

Since Zharkhov's compilation of Palaeozoic salt deposits, a number of other Phanerozoic salt deposits have been described. These include not only new discoveries on land, but very large deposits of Mesozoic salt in the Gulf of Mexico and in the North, Central and South Atlantic, and extensive Miocene salt underlying broad areas of the Mediterranean and Red Seas and Persian Gulf. The present total inventory amounts to a minimum of 9.1×10^{6} km^3 of halite, equal to about 19.6×10^{18} kg or more than 50% of the total of halite dissolved in the ocean today (36.8×10^{18} kg); the maximum estimate is about 16.3×10^{6} km^3 of halite, equal to 35.2×10^{18} kg, or 95% of the present total in the ocean. If all this salt were in the ocean at one time, the salinity would have been 57‰ to 73‰, but as Holland (1984) noted there is no evidence that the total inventory of halite was dissolved in the sea at any one time.

The first comprehensive compilation of evaporite volumes was published by Ronov (1980: Table 13) who extracted the data from the compilations of sediment volumes and masses for the major geologic intervals of the Phanerozoic that had been published in a series of papers by Ronov, Khain, Balukhovsky and Seslavinskiy. The 25 stratigraphic intervals they recognized included subunits of most of the 9 geologic systems of the Palaeozoic and Mesozoic, and the 5 units of the Tertiary. The compilations were made in terms of three tectonic regimes which had distinct erosion–sedimentation histories — (1) platform (cratonic), (2) geosynclinal, and (3) orogenic regions. These tectonic regimes are recognized in the lithologic–palaeogeographic maps for the same time intervals published by Ronov et al.,

1984, 1989). It was recognized that some areas have a transition in time from one tectonic regime to another.

The evaporite data were presented as total volumes of halite, gypsum and anhydrite lumped together. In modern seawater the components of halite (Na^+, Cl^-) and anhydrite/gypsum (Ca^{2+}, SO_4^{2-}) together make up slightly over 80% of the total salts and are at present in the ratio of 1:0.04. However, in evaporite deposits their ratio is more often in the order of 1:0.25. Thus the total evaporite volumes which include all three phases are of limited value in reconstructing ocean salinity in the past.

Holser (1985, Fig. 1) presented an inventory of Phanerozoic evaporite deposits showing volumes of both NaCl and $CaSO_4$. This compilation was based on Zharkov (1981) for the Palaeozoic, and Holser et al. (1980) for the Mesozoic and Cenozoic. He did not speculate on the specifics of changes in ocean salinity through time, but noted that the relative changes in $CaSO_4$ induced by evaporite deposition were much greater than those for NaCl, and are reflected in the temporal distribution of sulfur isotopes.

Continental margin and ocean floor sediments were included in the compilation of Budyko et al. (1987). However, as the purpose of their study was to establish the history of the atmosphere, only the data for total sediment, carbonates, and organic carbon were published. However, it was this landmark compilation that showed clearly the exponential decay of total sediment volumes and masses on a global scale.

Berner and Berner (1987) noted that extractions of salt into evaporite deposits would have resulted in rapid lowerings of salinity, and gradual return of the salt from dissolution of the deposits would have produced longer-term gentle rises in salinity. They suggested that although salinity must have varied through time, the variations were probably about a mean not greatly different from that observed today. Their reason for assuming that salinity must have remained close to its present level throughout the Phanerozoic is based on the fossil record and its diversity since the Early Cambrian.

A more complete compilation was presented by Ronov (1993: Tables 20 and 21). Table 20 presented data for pre-Quaternary Phanerozoic except for Antarctica, recognizing 28 stratigraphic units in the Phanerozoic and 3 in the Late Precambrian. Sedimentary materials are broken down into 18 different deposit types, 12 sediments and 6 volcanics. The amounts of evaporites, broken down into halite and gypsum–anhydrite for the Early Palaeozoic and combined for younger deposits, are expressed as a percent of the total volume of sedimentary and volcanic deposits on the continents. Table 21 presented the information for the Late Jurassic through Pliocene intervals for the continents, offshore regions, and ocean floor in terms of volumes and masses of 32 different kinds of deposit, 26 sediments and 6 volcanics. Ronov made very conservative estimates of the volumes of salt in the deep sea, and also assumed that the majority of the offshore deposits are gypsum/anhydrite. It should be noted that the volumes of the deep sea deposits were estimated at a time when data were still rather incomplete. According to Ronov (1993), the Phanerozoic–Late Precambrian total for all evaporites is 23.77×10^{18} kg. The halite mass was estimated to be 18.39×10^{18} kg.

Land (1995) explored the potential role of saline pore waters in the history of ocean salinity. Using the maximum values of the Holser (1985) evaporite inventory, and adding his own estimate of the volume of halite in the Jurassic Louann Formation (3500×10^3 km^3), he estimated the known inventory of Phanerozoic halite to be approximately 9600×10^3 km^3 or 12.6×10^{18} kg Cl^-. This is almost half the amount of Cl^- dissolved in the ocean today. He noted that the present river flux of Cl^-, given by Drever et al. (1988) as 115×10^9 kg/yr, implies a residence time of Cl^- in the ocean of 220×10^6 years. Further, he noted that if this rate of delivery had been sustained over the entire Phanerozoic (550 my) it would imply dissolution of five times the existing inventory of halite, which seemed unreasonable. He suggested that the deficit could be made up by Cl^- in the pore waters of sedimentary rocks. Using Garrels and Mackenzie's (1971) estimate of the volume of pore water (330×10^{18} kg), and assuming a high pore water salinity with 100,000 mg Cl^-/l, the Cl^- in pore water would contain 30×10^{18} kg of Cl^-, almost three times the amount in halite deposits. This implies a crustal residence time for Cl^- of 420×10^6 years. However, he argued that this still does not solve the problem that the present riverine flux is apparently too large, and he presented evidence that over the long term it may have been about 1/3 of the modern value. This would increase the crustal residence time for Cl to about 1.3×10^9 years, and its oceanic residence time to 680×10^6 years. These calculations were made in a context of assuming that ocean salinity has remained essentially constant as Cl^- is cycled between oceanic and crustal reservoirs.

Knauth (1998) used the same data to speculate on the possibility that more salt has been removed from the ocean into the crustal reservoirs over the course of geologic time. He concluded that the ocean may have had very high salinities (>70‰) in the Precambrian. These projected high salinities have been used by

Table 1
Volumes and masses of halite compiled by Areg Migdisov and Alexander Balukhovsky (Pliocene–Late Devonian, Early Devonian) and from Ronov (1993) (Middle Devonian, older Palaeozoic and Neoproterozoic

Stratigraphic units	Age of top after Ronov (1993)	Volumes of halite								Masses of halite — calculated as 2.16 × volume							
		Platforms	Geosynclines	Orogenic regions	Shelf and slope of platforms	Shelf and slope of geosynclines	Shelf and slope of orogenic regions	Ocean floor	Global total	Platforms	Geosynclines	Orogenic regions	Shelf and slope of platforms	Shelf and slope of geosynclines	Shelf and slope of orogenic regions	Ocean floor	Global total
	Ma	10^3 km^3	10^3 km^3	10^3 km^3	10^3 km^3	10^3 km^3	10^3 km^3	10^3 km^3	10^3 km^3	10^{15} kg	10^{15} kg	10^{15} kg	10^{15} kg	10^{15} kg	10^{15} kg	10^{15} kg	10^{15} kg
Pliocene	1.8	0.00	0.00	4.00	0.00	0.00	0.00	0.00	4.00	0.00	0.00	8.64	0.00	0.00	0.00	0.00	8.64
Miocene	5.3	1.00	0.00	241.00	435.00	0.00	183.00	0.00	860.00	2.16	0.00	520.56	939.60	0.00	395.28	0.00	1857.60
Oligocene	23.7	4.00	0.00	9.00	13.00	1.00	0.00	2.00	29.00	8.64	0.00	19.44	28.08	2.16	0.00	4.32	62.64
Eocene	36.6	0.00	2.00	6.00	8.00	0.00	0.00	0.00	16.00	0.00	4.32	12.96	17.28	0.00	0.00	0.00	34.56
Paleocene	57.8	0.00	0.00	0.00	0.00	0.00	0.00	0.00	0.00	0.00	0.00	0.00	0.00	0.00	0.00	0.00	0.00
Late Cretaceous	66.4	41.00	0.00	0.00	0.00	0.00	0.00	0.00	41.00	88.56	0.00	0.00	0.00	0.00	0.00	0.00	88.56
Early Cretaceous	97.5	182.00	46.00	2.00	231.00	0.00	0.00	300.00	761.00	393.12	99.36	4.32	498.96	0.00	0.00	648.00	1643.76
Late Jurassic	144.0	428.00	49.00	0.00	354.00	12.00	0.00	0.00	843.00	924.48	105.84	0.00	764.64	25.92	0.00	0.00	1820.88
Middle Jurassic	169.0	138.00	0.00	1.00	0.00	0.00	0.00	0.00	139.00	298.08	0.00	2.16	0.00	0.00	0.00	0.00	300.24
Early Jurassic	187.0	42.00	0.00	0.00	0.00	0.00	0.00	0.00	42.00	90.72	0.00	0.00	0.00	0.00	0.00	0.00	90.72
Late Triassic	208.0	384.00	8.00	0.00	0.00	0.00	0.00	0.00	392.00	829.44	17.28	0.00	0.00	0.00	0.00	0.00	846.72
Middle Triassic	230.0	23.50	0.00	0.00	0.00	0.00	0.00	0.00	23.50	50.76	0.00	0.00	0.00	0.00	0.00	0.00	50.76
Early Triassic	240.0	42.50	0.00	0.00	0.00	0.00	0.00	0.00	42.50	91.80	0.00	0.00	0.00	0.00	0.00	0.00	91.80
Late Permian	245.0	180.00	0.00	1.00	0.00	0.00	0.00	0.00	181.00	388.80	0.00	2.16	0.00	0.00	0.00	0.00	390.96
Early Permian	258.0	1046.00	0.00	55.00	0.00	0.00	0.00	0.00	1101.00	2259.36	0.00	118.80	0.00	0.00	0.00	0.00	2378.16
M and L Carboniferous	286.0	129.00	0.00	0.00	0.00	0.00	0.00	0.00	129.00	278.64	0.00	0.00	0.00	0.00	0.00	0.00	278.64
Early Carboniferous	320.0	37.00	0.00	6.30	0.00	0.00	0.00	0.00	43.30	79.92	0.00	13.61	0.00	0.00	0.00	0.00	93.53
Late Devonian	360.0	121.60	2.74	0.00	0.00	0.00	0.00	0.00	124.34	262.66	5.92	0.00	0.00	0.00	0.00	0.00	268.58
Middle Devonian	374.0	168.33	14.58	2.55	0.00	0.00	0.00	0.00	185.46	363.59	31.49	5.52	0.00	0.00	0.00	0.00	400.60
Early Devonian	387.0	1.00	0.00	0.00	0.00	0.00	0.00	0.00	1.00	2.16	0.00	0.00	0.00	0.00	0.00	0.00	2.16
Late Silurian	408.0	27.44	0.00	0.00	0.00	0.00	0.00	0.00	27.44	59.27	0.00	0.00	0.00	0.00	0.00	0.00	59.27
Early Silurian	421.0	0.00	0.00	0.00	0.00	0.00	0.00	0.00	0.00	0.00	0.00	0.00	0.00	0.00	0.00	0.00	0.00
Late Ordovician	438.0	0.00	0.00	0.00	0.00	0.00	0.00	0.00	0.00	0.00	0.00	0.00	0.00	0.00	0.00	0.00	0.00
Middle Ordovician	458.0	17.67	9.41	0.00	0.00	0.00	0.00	0.00	27.08	38.16	20.33	0.00	0.00	0.00	0.00	0.00	58.49
Early Ordovician	478.0	0.00	0.00	0.00	0.00	0.00	0.00	0.00	0.00	0.00	0.00	0.00	0.00	0.00	0.00	0.00	0.00
Late Cambrian	505.0	6.32	0.00	0.00	0.00	0.00	0.00	0.00	6.32	13.65	0.00	0.00	0.00	0.00	0.00	0.00	13.65
Middle Cambrian	523.0	130.59	0.00	0.00	0.00	0.00	0.00	0.00	130.59	282.07	0.00	0.00	0.00	0.00	0.00	0.00	282.07
Early Cambrian	540.0	1155.75	0.00	0.00	0.00	0.00	0.00	0.00	1155.75	2496.42	0.00	0.00	0.00	0.00	0.00	0.00	2496.42
Vendian	570.0	423.09	0.00	0.00	0.00	0.00	0.00	0.00	423.09	913.88	0.00	0.00	0.00	0.00	0.00	0.00	913.88
Late Riphean	680.0	0.00	0.00	0.00	0.00	0.00	0.00	0.00	0.00	0.00	0.00	0.00	0.00	0.00	0.00	0.00	0.00
M and E Riphean	1050.0	0.00	0.00	0.00	0.00	0.00	0.00	0.00	0.00	0.00	0.00	0.00	0.00	0.00	0.00	0.00	0.00

Table 2
Volumes and masses of halite compiled by William Holser and Christopher Wold

Stratiraphic units	Age of top — time scale of Gradstein and Ogg (1996)	Volumes of halite								Masses of halite — calculated as 2.16 * volume							
		Platforms	Geosynclines	Orogenic regions	Shelf and slope of platforms	Shelf and slope of geosynclines	Shelf and slope of orogenic regions	Ocean floor	Global total	Platforms	Geosynclines	Orogenic regions	Shelf and slope of platforms	Shelf and slope of geosynclines	Shelf and slope of orogenic regions	Ocean floor	Global total
	Ma	10^3 km^3	10^3 km^3	10^3 km^3	10^3 km^3	10^3 km^3	10^3 km^3	10^3 km^3	10^3 km^3	10^{15} kg	10^{15} kg	10^{15} kg	10^{15} kg	10^{15} kg	10^{15} kg	10^{15} kg	10^{15} kg
Pliocene	1.8	0.00	0.00	0.00	0.00	0.00	0.00	0.00	0.00	0.00	0.00	0.00	0.00	0.00	0.00	0.00	0.00
Miocene	5.3	0.00	0.00	1000.00	0.00	0.00	0.00	1100.00	2100.00	0.00	0.00	2160.00	0.00	0.00	0.00	2376.00	4536.00
Oligocene	23.8	0.00	0.00	0.00	0.00	0.00	0.00	0.00	0.00	0.00	0.00	0.00	0.00	0.00	0.00	0.00	0.00
Eocene	33.7	0.00	0.00	0.00	0.00	0.00	0.00	0.00	0.00	0.00	0.00	0.00	0.00	0.00	0.00	0.00	0.00
Paleocene	54.8	0.00	0.00	0.00	0.00	0.00	0.00	0.00	0.00	0.00	0.00	0.00	0.00	0.00	0.00	0.00	0.00
Late Cretaceous	65.0	54.50	0.00	0.00	0.00	0.00	0.00	0.00	54.50	117.72	0.00	0.00	0.00	0.00	0.00	0.00	117.72
Early Cretaceous	98.9	0.00	0.00	0.00	0.00	0.00	0.00	2500.00	2500.00	0.00	0.00	0.00	0.00	0.00	0.00	5400.00	5400.00
Late Jurassic	142.0	0.00	0.00	0.00	0.00	0.00	0.00	2100.00	2100.00	0.00	0.00	0.00	0.00	0.00	0.00	4536.00	4536.00
Middle Jurassic	159.4	0.00	0.00	0.00	0.00	0.00	0.00	0.00	0.00	0.00	0.00	0.00	0.00	0.00	0.00	0.00	0.00
Early Jurassic	180.1	0.00	0.00	0.00	0.00	0.00	0.00	1800.00	1800.00	0.00	0.00	0.00	0.00	0.00	0.00	3888.00	3888.00
Late Triassic	205.7	0.00	0.00	0.00	0.00	0.00	0.00	0.00	0.00	0.00	0.00	0.00	0.00	0.00	0.00	0.00	0.00
Middle Triassic	227.4	115.00	0.00	0.00	0.00	0.00	0.00	0.00	115.00	248.40	0.00	0.00	0.00	0.00	0.00	0.00	248.40
Early Triassic	241.7	0.00	0.00	0.00	0.00	0.00	0.00	0.00	0.00	0.00	0.00	0.00	0.00	0.00	0.00	0.00	0.00
Late Permian	248.2	485.00	50.00	0.00	0.00	0.00	560.00	0.00	1095.00	1047.60	108.00	0.00	0.00	0.00	1209.60	0.00	2365.20
Early Permian	256.0	0.00	0.00	0.00	0.00	0.00	0.00	0.00	0.00	0.00	0.00	0.00	0.00	0.00	0.00	0.00	0.00
Pennsylvanian	290.0	69.00	0.00	0.00	0.00	0.00	0.00	0.00	69.00	149.04	0.00	0.00	0.00	0.00	0.00	0.00	149.04
Mississippian	323.0	0.00	0.00	0.00	0.00	0.00	0.00	0.00	0.00	0.00	0.00	0.00	0.00	0.00	0.00	0.00	0.00
Late Devonian	354.0	98.80	62.00	0.00	0.00	0.00	0.00	0.00	160.80	213.41	133.92	0.00	0.00	0.00	0.00	0.00	347.33
Middle Devonian	370.0	0.00	0.00	0.00	0.00	0.00	0.00	0.00	0.00	0.00	0.00	0.00	0.00	0.00	0.00	0.00	0.00
Early Devonian	391.0	2.32	0.00	0.00	0.00	0.00	0.00	0.00	2.32	5.02	0.00	0.00	0.00	0.00	0.00	0.00	5.02
Late Silurian	417.0	26.00	0.00	0.00	0.00	0.00	0.00	0.00	26.00	56.16	0.00	0.00	0.00	0.00	0.00	0.00	56.16
Early Silurian	423.0	0.00	0.00	0.00	0.00	0.00	0.00	0.00	0.00	0.00	0.00	0.00	0.00	0.00	0.00	0.00	0.00
Late Ordovician	443.0	0.00	0.00	0.00	0.00	0.00	0.00	0.00	0.00	0.00	0.00	0.00	0.00	0.00	0.00	0.00	0.00
Middle Ordovician	458.0	0.00	0.00	0.00	0.00	0.00	0.00	0.00	0.00	0.00	0.00	0.00	0.00	0.00	0.00	0.00	0.00
Early Ordovician	880.0	0.00	0.00	0.00	0.00	0.00	0.00	0.00	0.00	0.00	0.00	0.00	0.00	0.00	0.00	0.00	0.00
Late Cambrian	495.0	0.00	0.00	0.00	0.00	0.00	0.00	0.00	0.00	0.00	0.00	0.00	0.00	0.00	0.00	0.00	0.00
Middle Cambrian	505.0	0.00	0.00	0.00	0.00	0.00	0.00	0.00	0.00	0.00	0.00	0.00	0.00	0.00	0.00	0.00	0.00
Early Cambrian	518.0	675.00	0.00	0.00	0.00	0.00	0.00	0.00	675.00	1458.00	0.00	0.00	0.00	0.00	0.00	0.00	1458.00
Vendian	545.0	600.00	0.00	0.00	0.00	0.00	0.00	0.00	600.00	1296.00	0.00	0.00	0.00	0.00	0.00	0.00	1296.00
Late Riphean	680.0	0.00	0.00	0.00	0.00	0.00	0.00	0.00	0.00	0.00	0.00	0.00	0.00	0.00	0.00	0.00	0.00
M and E Riphean	1050.0	0.00	0.00	0.00	0.00	0.00	0.00	0.00	0.00	0.00	0.00	0.00	0.00	0.00	0.00	0.00	0.00

Table 3
Maximum estimates of volumes and masses of halite (compiled from data of Migdisov, Balukhovsky, Ronov, Holser, and Wold)

Stratiraphic units	Age of top — time scale of Gradstein et al. (2004)	Volumes of halite								Masses of halite — calculated as 2.16 * volume							
		Platforms	Geosynclines	Orogenic regions	Shelf and slope of platforms	Shelf and slope of geosynclines	Shelf and slope of orogenic regions	Ocean floor	Global total	Platforms	Geosynclines	Orogenic regions	Shelf and slope of platforms	Shelf and slope of geosynclines	Shelf and slope of orogenic regions	Ocean floor	Global total
	Ma	10^3 km^3	10^3 km^3	10^3 km^3	10^3 km^3	10^3 km^3	10^3 km^3	10^3 km^3	10^3 km^3	10^{15} kg	10^{15} kg	10^{15} kg	10^{15} kg	10^{15} kg	10^{15} kg	10^{15} kg	10^{15} kg
Pliocene	1.81	0.05	0.00	4.00	0.00	0.00	0.00	0.00	4.05	0.11	0.00	8.64	0.00	0.00	0.00	0.00	8.75
Miocene	5.33	1.20	0.00	1000.00	435.00	0.00	183.00	1100.00	2719.20	2.59	0.00	2160.00	939.60	0.00	395.28	2376.00	5873.47
Oligocene	23.03	3.60	0.00	9.20	13.00	1.00	0.00	2.00	28.80	7.78	0.00	19.87	28.08	2.16	0.00	4.32	62.21
Eocene	33.90	0.00	1.30	5.40	8.00	0.00	0.00	0.00	14.70	0.00	2.81	11.66	17.28	0.00	0.00	0.00	31.75
Paleocene	55.80	0.10	0.00	4.20	0.00	0.00	0.00	0.00	4.30	0.22	0.00	9.07	0.00	0.00	0.00	0.00	9.29
Late Cretaceous	65.50	54.50	0.00	0.00	0.00	0.00	0.00	0.00	54.50	117.72	0.00	0.00	0.00	0.00	0.00	0.00	117.72
Early Cretaceous	99.60	177.50	46.20	1.50	231.00	0.00	0.00	2800.00	3256.20	383.40	99.79	3.24	498.96	0.00	0.00	6048.00	7033.39
Late Jurassic	145.50	489.00	11.00	21.00	354.00	12.00	0.00	2100.00	2987.00	1056.24	23.76	45.36	764.64	25.92	0.00	4536.00	6451.92
Middle Jurassic	161.20	138.00	0.00	1.00	0.00	0.00	0.00	0.00	139.00	298.08	0.00	2.16	0.00	0.00	0.00	0.00	300.24
Early Jurassic	175.60	42.00	0.00	0.00	0.00	0.00	0.00	1800.00	1842.00	90.72	0.00	0.00	0.00	0.00	0.00	3888.00	3978.72
Late Triassic	199.60	384.00	8.00	0.00	0.00	0.00	0.00	0.00	392.00	829.44	17.28	0.00	0.00	0.00	0.00	0.00	846.72
Middle Triassic	228.00	115.00	0.00	0.00	0.00	0.00	0.00	0.00	115.00	248.40	0.00	0.00	0.00	0.00	0.00	0.00	248.40
Early Triassic	245.00	42.50	0.00	0.00	0.00	0.00	0.00	0.00	42.50	91.80	0.00	0.00	0.00	0.00	0.00	0.00	91.80
Late Permian	251.00	485.00	50.00	1.00	0.00	0.00	560.00	0.00	1096.00	1047.60	108.00	2.16	0.00	0.00	1209.60	0.00	2367.36
Early Permian	270.60	1046.00	0.00	55.00	0.00	0.00	0.00	0.00	1101.00	2259.36	0.00	118.80	0.00	0.00	0.00	0.00	2378.16
M and L Carboniferous	299.00	129.00	0.00	0.00	0.00	0.00	0.00	0.00	129.00	278.64	0.00	0.00	0.00	0.00	0.00	0.00	278.64
Early Carboniferous	318.10	37.00	0.00	6.30	0.00	0.00	0.00	0.00	43.30	79.92	0.00	13.61	0.00	0.00	0.00	0.00	93.53
Late Devonian	359.20	121.60	62.00	0.00	0.00	0.00	0.00	0.00	183.60	262.66	133.92	0.00	0.00	0.00	0.00	0.00	396.58
Middle Devonian	385.30	168.33	14.58	2.55	0.00	0.00	0.00	0.00	185.46	363.59	31.49	5.52	0.00	0.00	0.00	0.00	400.60
Early Devonian	397.50	2.32	0.00	0.00	0.00	0.00	0.00	0.00	2.32	5.01	0.00	0.00	0.00	0.00	0.00	0.00	5.01
Late Silurian	416.00	27.44	0.00	0.00	0.00	0.00	0.00	0.00	27.44	59.27	0.00	0.00	0.00	0.00	0.00	0.00	59.27
Early Silurian	428.20	0.00	0.00	0.00	0.00	0.00	0.00	0.00	0.00	0.00	0.00	0.00	0.00	0.00	0.00	0.00	0.00
Late Ordovician	443.70	0.00	0.00	0.00	0.00	0.00	0.00	0.00	0.00	0.00	0.00	0.00	0.00	0.00	0.00	0.00	0.00
Middle Ordovician	460.90	17.67	9.41	0.00	0.00	0.00	0.00	0.00	27.08	38.16	20.33	0.00	0.00	0.00	0.00	0.00	58.49
Early Ordovician	471.80	0.00	0.00	0.00	0.00	0.00	0.00	0.00	0.00	0.00	0.00	0.00	0.00	0.00	0.00	0.00	0.00
Late Cambrian	488.30	6.32	0.00	0.00	0.00	0.00	0.00	0.00	6.32	13.65	0.00	0.00	0.00	0.00	0.00	0.00	13.65
Middle Cambrian	501.00	130.59	0.00	0.00	0.00	0.00	0.00	0.00	130.59	282.07	0.00	0.00	0.00	0.00	0.00	0.00	282.07
Early Cambrian	513.00	1155.75	0.00	0.00	0.00	0.00	0.00	0.00	1155.75	2496.42	0.00	0.00	0.00	0.00	0.00	0.00	2496.42
Ediacaran	542.00	600.00	0.00	0.00	0.00	0.00	0.00	0.00	600.00	1296.00	0.00	0.00	0.00	0.00	0.00	0.00	1296.00
Cryogenian–Tonian	630.00	0.00	0.00	0.00	0.00	0.00	0.00	0.00	0.00	0.00	0.00	0.00	0.00	0.00	0.00	0.00	0.00
Middle Proterozoic	1000.00	0.00	0.00	0.00	0.00	0.00	0.00	0.00	0.00	0.00	0.00	0.00	0.00	0.00	0.00	0.00	0.00

Table 4
Minimum estimates of volumes and masses of halite (compiled from data of Migdisov, Balukhovsky, Ronov, Holser, and Wold)

Stratiraphic units	Age of top — time scale of Gradstein et al. (2004)	Volumes of halite								Masses of halite — calculated as 2.16 * volume							
		Platforms	Geosynclines	Orogenic regions	Shelf and slope of platforms	Shelf and slope of geosynclines	Shelf and slope of orogenic regions	Ocean floor	Global total	Platforms	Geosynclines	Orogenic regions	Shelf and slope of platforms	Shelf and slope of geosynclines	Shelf and slope of orogenic regions	Ocean floor	Global total
	Ma	10^3 km^3	10^3 km^3	10^3 km^3	10^3 km^3	10^3 km^3	10^3 km^3	10^3 km^3	10^3 km^3	10^{15} kg	10^{15} kg	10^{15} kg	10^{15} kg	10^{15} kg	10^{15} kg	10^{15} kg	10^{15} kg
Pliocene	1.81	0.05	0.00	4.00	0.00	0.00	0.00	0.00	4.05	0.11	0.00	8.64	0.00	0.00	0.00	0.00	8.75
Miocene	5.33	1.20	0.00	240.80	435.00	0.00	183.00	1100.00	1960.00	2.59	0.00	520.13	939.60	0.00	395.28	2376.00	4233.60
Oligocene	23.03	3.60	0.00	9.20	13.00	1.00	0.00	2.00	28.80	7.78	0.00	19.87	28.08	2.16	0.00	4.32	62.21
Eocene	33.90	0.00	1.30	5.40	8.00	0.00	0.00	0.00	14.70	0.00	2.81	11.66	17.28	0.00	0.00	0.00	31.75
Paleocene	55.80	0.10	0.00	4.20	0.00	0.00	0.00	0.00	4.30	0.22	0.00	9.07	0.00	0.00	0.00	0.00	9.29
Late Cretaceous	65.50	44.40	0.00	0.00	0.00	0.00	0.00	0.00	44.40	95.90	0.00	0.00	0.00	0.00	0.00	0.00	95.90
Early Cretaceous	99.60	177.50	46.20	1.50	231.00	0.00	0.00	300.00	756.20	383.40	99.79	3.24	498.96	0.00	0.00	648.00	1633.39
Late Jurassic	145.50	489.00	11.00	21.00	354.00	12.00	0.00	2100.00	2987.00	1056.24	23.76	45.36	764.64	25.92	0.00	4536.00	6451.92
Middle Jurassic	161.20	138.00	0.00	1.00	0.00	0.00	0.00	0.00	139.00	298.08	0.00	2.16	0.00	0.00	0.00	0.00	300.24
Early Jurassic	175.60	42.00	0.00	0.00	0.00	0.00	0.00	1800.00	1842.00	90.72	0.00	0.00	0.00	0.00	0.00	3888.00	3978.72
Late Triassic	199.60	384.00	8.00	0.00	0.00	0.00	0.00	0.00	392.00	829.44	17.28	0.00	0.00	0.00	0.00	0.00	846.72
Middle Triassic	228.00	23.50	0.00	0.00	0.00	0.00	0.00	0.00	23.50	50.76	0.00	0.00	0.00	0.00	0.00	0.00	50.76
Early Triassic	245.00	42.50	0.00	0.00	0.00	0.00	0.00	0.00	42.50	91.80	0.00	0.00	0.00	0.00	0.00	0.00	91.80
Late Permian	251.00	180.00	50.00	1.00	0.00	0.00	560.00	0.00	791.00	388.80	108.00	2.16	0.00	0.00	1209.60	0.00	1708.56
Early Permian	270.60	1046.00	0.00	55.00	0.00	0.00	0.00	0.00	1101.00	2259.36	0.00	118.80	0.00	0.00	0.00	0.00	2378.16
M and L Carboniferous	299.00	129.00	0.00	0.00	0.00	0.00	0.00	0.00	129.00	278.64	0.00	0.00	0.00	0.00	0.00	0.00	278.64
Early Carboniferous	318.10	37.00	0.00	6.30	0.00	0.00	0.00	0.00	43.30	79.92	0.00	13.61	0.00	0.00	0.00	0.00	93.53
Late Devonian	359.20	121.60	2.74	0.00	0.00	0.00	0.00	0.00	124.34	262.66	5.92	0.00	0.00	0.00	0.00	0.00	268.57
Middle Devonian	385.30	168.33	14.58	2.55	0.00	0.00	0.00	0.00	185.46	363.59	31.49	5.52	0.00	0.00	0.00	0.00	400.60
Early Devonian	397.50	1.00	0.00	0.00	0.00	0.00	0.00	0.00	1.00	2.16	0.00	0.00	0.00	0.00	0.00	0.00	2.16
Late Silurian	416.00	27.44	0.00	0.00	0.00	0.00	0.00	0.00	27.44	59.27	0.00	0.00	0.00	0.00	0.00	0.00	59.27
Early Silurian	428.20	0.00	0.00	0.00	0.00	0.00	0.00	0.00	0.00	0.00	0.00	0.00	0.00	0.00	0.00	0.00	0.00
Late Ordovician	443.70	0.00	0.00	0.00	0.00	0.00	0.00	0.00	0.00	0.00	0.00	0.00	0.00	0.00	0.00	0.00	0.00
Middle Ordovician	460.90	17.67	9.41	0.00	0.00	0.00	0.00	0.00	27.08	38.16	20.33	0.00	0.00	0.00	0.00	0.00	58.49
Early Ordovician	471.80	0.00	0.00	0.00	0.00	0.00	0.00	0.00	0.00	0.00	0.00	0.00	0.00	0.00	0.00	0.00	0.00
Late Cambrian	488.30	6.32	0.00	0.00	0.00	0.00	0.00	0.00	6.32	13.65	0.00	0.00	0.00	0.00	0.00	0.00	13.65
Middle Cambrian	501.00	130.59	0.00	0.00	0.00	0.00	0.00	0.00	130.59	282.07	0.00	0.00	0.00	0.00	0.00	0.00	282.07
Early Cambrian	513.00	1155.75	0.00	0.00	0.00	0.00	0.00	0.00	1155.75	2496.42	0.00	0.00	0.00	0.00	0.00	0.00	2496.42
Ediacaran	542.00	600.00	0.00	0.00	0.00	0.00	0.00	0.00	600.00	1296.00	0.00	0.00	0.00	0.00	0.00	0.00	1296.00
Cryogenian–Tonian	630.00	0.00	0.00	0.00	0.00	0.00	0.00	0.00	0.00	0.00	0.00	0.00	0.00	0.00	0.00	0.00	0.00
Middle Proterozoic	1000.00	0.00	0.00	0.00	0.00	0.00	0.00	0.00	0.00	0.00	0.00	0.00	0.00	0.00	0.00	0.00	0.00

Knauth (2005) in discussing the possible early history of life on Earth.

All of these studies, whether suggesting that the general trend is toward higher ocean salinities with age, or more simply, variations about a mean recognize that ocean salinity must have changed with time. However, quantification of the salinity of the ocean in the past has been elusive because there was no agreement on how to reconstruct the original extractions and the subsequent delivery of dissolved evaporite and pore water salt to the ocean in the past.

2.2. Recent compilations of evaporite deposits

More recently, William Holser and Christopher Wold compiled a list of major evaporite deposits that included several large accumulations that had escaped earlier attention. Estimates of the size of some of the deposits in the deep sea vary significantly. For the South Atlantic, volume estimates range from 4000 km^3 (Southam and Hay, 1981) to 1000 km^3 (Burke, 1975; Burke and Sengor, 1988), and Holser and Wold chose an intermediate value. They were also able to include some recently discovered deposits, such as those in Thailand (Japakasetr and Workman, 1981). This list has been published in terms of masses of NaCl and $CaSO_4$ as Table 1 in Floegel et al. (2000). They found the total mass of evaporite deposits existing today to be 32.02×10^{18} kg and the mass of halite to be 24.40×10^{18} kg.

Areg Migdisov and Alexander Balukhovsky, have gone back to the original data on areas, thicknesses, and volumes of sediment which they worked on as part of the group led by Alexander Ronov and Victor Khain at the Vernadski Institute in the 1960s and '70s. They recompiled the information for the Pliocene though Carboniferous and for the Early Devonian in terms of the original geographical areas defined for the global compilation. The evaporites have been divided into halite and gypsum–anhydrite. These data have been placed in the GERM (Geochemical Earth Reference Model) data bank. The Ronov data for evaporites differ from those of Zharkov (1974, 1981) because they used different maps and also included the additional amounts of halite in diapirs and other salt tectonic features. For this reason estimates from the Ronov database are generally larger than those of Zharkov.

The results of these recent compilations are presented here as four data sets, Tables 1–4. Table 1 shows the Ronov data for halite as revised by Migdisov and Balukhovsky; it still lacks some of the deep sea deposits; Table 2 shows the Holser and Wold data on major evaporite deposits recast into the same format. It includes the deep sea deposits (previously published in Floegel et al., 2000). Table 3 is a combination of Tables 1 and 2 using the smaller number when there are differences between the Ronov/Migdisov/Balukhovsky and Holser/Wold data sets. Table 4 is a combination of Tables 1 and 2, using the larger number whenever there are differences between the data sets, and Table 3 can be regarded as a minimum estimate and Table 4 as a maximum estimate of the size of known halite deposits. It should be noted that these are not the maximum estimates of evaporite volumes proposed; Southam and Hay (1981) gave the volume of the Early Cretaceous South Atlantic halite as 4000 km^3, and Land (1995) cited the volume of the Jurassic Louann salt of the Gulf of Mexico to be 3500 km^3.

We do not know whether these data represent a complete inventory of the world's evaporite deposits. There are no data from Antarctica, and many areas of the ocean basins and marginal seas have not been sufficiently explored to be sure that there are not more deposits to be found. Furthermore, many of the estimates on volumes and masses of halite in the deep sea are based on seismic data, some of which show only diapirs or the top of the salt layer, and none of which have been drilled though except near their edges. However, future discoveries and corrections are not likely to be so large as to invalidate the results presented here.

3. Factors affecting ocean salinity

Two factors are important in determining the salinity of the ocean in the past: 1) the amount of salt, and 2) the amount of water. The salinity of seawater is a measure of the amount of dissolved solids in terms of weight. Today the ocean contains about 1322.746×10^{18} kg H_2O, and about 47.578×10^{18} kg of salts, for a mean salinity of 34.72.The four major anions, Cl^-, SO_4^{2-}, $HCO_3^{?-}$, Br^-, and four major cations Na^+, Mg^{2+}, Ca^{2+}, K^+, make up 99.8% by weight of the dissolved solids. The two most abundant ions, Cl^- and Na^+, comprise 85.1% by weight of the salt in present day seawater. Chloride alone makes up 55% by weight and, as shown in Table 5, there are 17% more moles of Cl^- than Na^+. Of the major ions in seawater, Cl^- is unique in that it is incompatible with almost all minerals and resides almost entirely in seawater, in the pore space of sediments, and in evaporite deposits derived from seawater. Because all of the other major ions can enter into and be exchanged with counterparts in minerals, the only element that can be used as a proxy for salinity in the past is Cl^-.

Table 5
Composition of modern seawater: major ions after Gill (1989) with modifications to make chlorinity (*Cl*) of 19.2 equal to a salinity of 34.72‰

Species	Atomic/ Molecular weight	Concentration o/oo by weight (=g/kg)	Proportion of total salts by weight, as %	Molar concentration	Mass in the ocean (10^{15} kg)	Moles in the ocean (10^{15})
H_2O	18.02	965.28		17,389.8474	1,371,346	76,121,000
Na^+	22.99	10.59	30.51	0.4608	15,049	654,602
Mg^{2+}	24.31	1.27	3.67	0.0524	1810	74,432
Ca^{2+}	40.08	0.41	1.17	0.0102	578	14,422
K^+	39.10	0.38	1.10	0.0097	541	13,836
Sr^{2+}	87.62	0.01	0.04	0.0001	19	211
Cl^-	35.45	19.12	55.08	0.5394	27,168	766,311
SO_4^{2-}	96.06	2.67	7.69	0.0278	3793	39,484
HCO_3^-	61.02	0.12	0.35	0.0020	172	2823
CO_3^{2-}	60.01	0.02	0.05	0.0003	26	427
Br^-	79.91	0.07	0.19	0.0008	94	1176
F^-	19.00	0.03	0.08	0.0015	41	2173
Other	0.00	0.02	0.07		35	
Sum of halides		19.22	55.35		27,303	
Sum of salts		34.72			49,326	1,569,899
Sum of salts + water		1000.00			1,420,671	

Note: The mass of seawater assumes an ocean volume of 1,370,323,000 km^3 with an average temperature of 3.5 °C, average salinity of 34.72‰, and average pressure of 2000 dbar, giving an average density of 1035.8 kg/m^3 (calculated after Millero and Poisson, 1981).

Salinity has a complicated history of definitions. It was intended to be an expression of the weight of salt in a given volume of water. Unfortunately this cannot be determined simply by drying. As the water is evaporated chemical reactions occur, some of the solid salts deposited are hydrated, and gasses other than H_2O vapor are lost. Accordingly, salinity was originally defined to be the total amount of dissolved solids in seawater, when carbonate is converted to oxide; bromide and iodide are converted to chloride; organic matter is oxide; and the remainder dried to 480 °C. It is obviously impossible to determine salinity in the past using this definition. Subsequently, the definition of salinity was changed to accommodate a simpler analytical technique using titration with silver nitrate to determine the amount of halides (Cl^-, Br^-, F^-, and I^-) in the water. This measure is termed the "Chlorinity, *Cl*" and salinity was then redefined as 1.80655 *Cl*. The abundance ratios of these halides in modern seawater are 325,000:1117:22:1. Chlorine is so dominant that for practical purposes the other halides need not be considered. The chloride content of the ocean could be used to make precise estimates of ocean salinity in the past were it not for the fact that we know that the relative proportions and total amounts of the major cations have changed with time (Sandberg, 1983; Hardie, 1996; Stanley and Hardie, 1998, 1999; Lowenstein et al., 2001; Hardie, 2003). Because salinity is expressed in terms of weight, not moles, changing the proportions of cations having different atomic weights could change the salinity without changing the chlorinity.

It should be noted that since the 1970s salinity, or "practical salinity" to be exact, has been defined in terms of electrical conductivity of the seawater sample relative to a KCl solution. Again, this definition cannot be applied to ancient seawater.

The sulfate minerals in evaporite deposits, gypsum and anhydrite, can not be used to reconstruct past ocean salinity because sulfur can also leave the ocean as pyrite. For simplicity we do not report their abundances here, but note that extractions of sulfate from the ocean during the Miocene, Early Cretaceous and Late Jurassic and included in the data sets of Holser (1985), Ronov (1993) and Floegel et al. (2000) appear to have exceeded the entire amount dissolved in the ocean today. In contrast halite extractions rarely exceeded 10% of the amount in solution. The Late Palaeozoic extractions of sulfate, which probably took place in short periods of time, produced significant upward jumps in the value of $\delta^{34}S$, as discussed by Holser (1977), suggesting a strong impact on the dissolved inventory. Berner (2004) reviewed earlier modeling attempts to determine the relative proportions of major ions in seawater, including sulfate. He developed a new model to reconstruct the variation in calcium, magnesium and sulfate content of the ocean throughout the Phanerozoic.

In the discussion of Phanerozoic palaeosalinities below we have assumed that the amount of salt in the

ocean retains its present proportionality of 1.81558 times the amount of the chloride ion. The periodic removal of salts other than NaCl, most importantly $CaCO_3$, $CaMg(CO_3)_2$, $CaSO_4$, $MgSO_4$, KCl, etc., implies that chloride is not an exact but only an approximate proxy for the salinity of seawater.

4. Delivery of salts to the ocean today

Salts can be brought to the ocean by rivers, groundwater, glaciers, and through the atmosphere. Of these potential transport mechanisms, the dissolved load of rivers and groundwater dominate. The dissolved load of rivers is relatively well known (Meybeck, 1979). River water is essentially a bicarbonate solution, with more than 80% of the solutes consisting of HCO_3^-, SO_4^{2-}, Ca^{2+} and H_4SiO_4 (Allen, 1997), but it also contains the other anions and cations that are common is seawater, including Cl^-.

Chlorine is the classic "excess volatile" and is very rare in silicate minerals. Chlorine occurs regularly only in chlorapatite, cerargyrite, lazurite, sodalite, vanadinite, and in the evaporite salts halite, sylvite, kainite, and boracite (Emiliani, 1992). It is not a regular constituent of chlorite or chloritoid although in these and some other minerals it may substitute for OH^-. Cl^- is released in the weathering of shales (Meybeck, 1987), it is presumably bound with the interlayer water. NaCl must be contained in magmas because NaCl brine is present in fluid inclusions in silicate minerals, but it must be a relatively minor constituent because there is no record of NaCl as a primary magmatic precipitate (Mueller and Saxena, 1977).

Determining the global average concentration of Cl^- in river waters, $[Cl^-]$, is difficult because concentrations vary through three (Meybeck, 1979) and possibly even five orders of magnitude (Feth, 1981). Essentially there have only been two attempts to determine an average value, that of Livingston (1963): 7.8 mg/l = 0.220 mmol; subsequently cited by Garrels and Mackenzie (1971), Lisitzin (1974), Holland (1978), and Brown et al. (1989) among others, and that of Meybeck (1979): 8.3 mg/l = 0.233 mmol, subsequently cited by Drever et al. (1988), Berner and Berner (1987) and others. The estimates of average values were determined by averaging the $[Cl^-]$ in major rivers. Meybeck (1979) averaged data from 61 rivers or regional groups of rivers, having a total discharge of 23,413 km^3/yr. This value for the concentration is then multiplied by estimates of the total water discharge from land to extrapolate the total amount of Cl^- delivered from land to the sea each year.

Estimates of the total discharge of rivers to the ocean range between 32,500 km^3/yr (Garrels and Mackenzie, 1971) and 37,500 km^3/yr (Marcinek and Rosenkranz, 1989); Berner and Berner (1987) use a value of 37,400 km^3/yr. From the values for concentration and discharge, the total flux of Cl^- from land to sea via rivers may range between 254×10^9 kg and 311×10^9 kg; Berner and Berner (1987) give the flux as 308×10^9 kg. Meybeck's (1979) global average for $[Cl^-]$ in rivers is dominated by those rivers which drain areas with large evaporite deposits in the continental interior (see Fig. 1 in Feth, 1981). The total discharge of the rivers for which he had reliable data is only about 60% of the global discharge from land to sea, and the assumption that Cl^- has the same average concentration in the other 40% of the world's rivers, which drain more coastal areas mostly lacking evaporite deposits, may not be justified.

The origin of the Cl^- in river and groundwater is controversial. There are four potential sources of riverine Cl^-: 1) recycled directly from the ocean via the atmosphere, 2) from volcanic emissions, including juvenile chloride outgassed from the mantle, 3) from human activities, 4) from introduction of saline groundwaters, and 5) from dissolution of evaporites.

4.1. The atmospheric recycling correction for chloride in rivers

The bursting of bubbles generated by breaking waves injects droplets of seawater from the sea surface into the air. Evaporation of the water leaves the salt as an aerosol. Sea salt aerosol is concentrated below 1 to 2 km above the ocean surface and decreases exponentially with height (Ryan and Mukherjee, 1975). The salt is hygroscopic, and serves as a nucleus for raindrops. Hence rainwater has a small content of sea salt, the amount decreasing away from its source. The $[Cl^-]$ ranges from >8 mg/l over the ocean to 1 mg/l in coastal regions, to 0.1 mg/l or less in the continental interiors (Junge and Werby, 1958; Stallard and Edmond, 1981; Drever, 1982; Berner and Berner, 1987). Because concentrations of Cl^- in rainwater vary through two or more orders of magnitude (Feth, 1981), a global average is difficult to determine. Garrels and Mackenzie (1971) give a $[Cl^-]$ of 3.8 mg/l in rainwater as a global average; this seems to be generally accepted (Brown et al., 1989).

Estimates of the proportion of riverine Cl^- due to atmospheric recycling vary greatly. Sverdrup et al. (1942) made a first attempt to separate salts atmospherically recycled from the ocean from those derived from weathering on land. As a simplification they assumed

that all of the Cl^- in rivers is atmospherically recycled. Using this assumption, the amount of non-atmospherically recycled solutes in river water can be determined by setting [Cl^-] equal to 0 and subtracting the amounts of the other ions proportional to their abundance in seawater. Feth (1981) noted that subsequent authors have sometimes dropped the modifying statements and stated assumptions of Sverdrup et al. (1942), with the result that the idea that all Cl^- in river water is recycled from the sea has appeared in some textbooks (e.g. Rankama and Sahama, 1950; Brown et al., 1989).

Garrels and Mackenzie (1971) cited the amount of atmospherically recycled Cl^- in river water to be 55%. Holland (1978) presented a more detailed argument. He concluded that if the Cl^- in North American rivers were derived solely from atmospheric precipitation, [Cl^-] would be 1–4 ppm depending on the distance from the coast rather than the average of 8 ppm observed. He interpreted this to mean that at present about 27% of the salt in rivers comes from the sea through atmospheric cycling. Meybeck (1983) estimated the proportion of Cl^- dissolved in rivers that is atmospherically recycled from the ocean is 72%. However Berner and Berner (1987) argue that most of the rivers on which Meybeck's estimate is based are short and strongly affected by precipitation coming directly from the ocean. In contrast, Berner and Berner (1987) use a value of 13% for atmospherically recycled salt, based on studies of the Amazon by Stallard and Edmond (1981). It can also be argued that this is too small because very little of the Amazon Basin is close to the coast. It is important to recall that the 100 largest rivers deliver about 60% of the water entering the ocean. The remaining 40% comes from smaller rivers that are shorter and closer to the coast.

Using maximum and minimum estimates for the atmospherically recycled component of river water and the total Cl^- flux of rivers, the short-term atmospherically recycled flux ranges between 183×10^9 kg/yr and 40×10^9 kg/yr. The flux from other sources would then be between 71×10^9 kg/yr and 271×10^9 kg/yr, a very large uncertainty.

4.2. Chloride from volcanic emissions

The chloride emitted from volcanoes comes from two possible sources: subducted seawater, and outgassing from the Earth's mantle. The total amount of Cl^- in the oceans, pore waters in sediments, and salt deposits is probably between 55 and 65×10^{18} kg or 1.25 and 1.60×10^{21} mol. It is not known whether this has been at the surface of the Earth since early in its history, or has been gradually added through time. If added steadily since the accretion of the Earth, this would require a flux of 12 to 14×10^9 kg Cl^-/yr.

HCl is emitted by volcanoes, but many of these are situated along subduction zones and it can be argued that the emissions are simply returning the salt dissolved in subducted seawater. Present volcanic emissions of Cl^- into the troposphere and stratosphere are thought to be about 500 times smaller than the input of Cl^- into the ocean from rivers. Prior to the advent of plate tectonics, Correns (1956) evaluated the role of magmatic sources, and concluded that they were inadequate to maintain the balance observed today. Subsequently, Bartels (1972) estimated annual volcanic emissions of 7.6×10^9 kg Cl^-/yr from chlorine measurements for the Greenland icecap. This is half the rate expected if the rate of outgassing were constant over geologic time. Over the Phanerozoic this amounts to 4142×10^{15} kg, or almost 16% of the present amount in the ocean. Anderson (1974) arrived at a much lower estimate of 1.7×10^9 kg Cl^-/yr in total volcanic emissions, which over the course of the Phanerozoic would amount to only 3.5% of the oceans' Cl^-. Unfortunately, the rate of addition of juvenile Cl^- to the total inventory remains an open question.

4.3. Chloride from human activities

The amount of Cl^- introduced into rivers and groundwater is also difficult to estimate. Meybeck (1979) proposed that the amount of Cl^- "pollution" of rivers is about 30%. This estimate was based on a comparison of Cl^- concentrations in river in the early and late 20th century. Applying this value to the estimate of non-atmospherically recycled Cl^-, the residual "natural" Cl^- flux might range between 50×10^9 kg/yr and 190×10^9 kg/yr. However, salt has been an important commodity since prehistoric times (Kurlansky, 2002). Originally salt was used in food preparation and storage (e.g. salt cod, in which the salt used for preservation may outweigh the fish!), and more recently for the chlorination of water supplies and deicing of roads. According to the Salt Institute (www.saltinstitute.org) global salt production increased during the 20th century from 10×10^9 kg/yr early in the century to 183×10^9 kg/yr in 1990 and reached 225×10^9 kg/yr in 2002. These correspond to Cl^- masses of 6×10^9 kg/yr, 110×10^9 kg/yr, and 135×10^9 kg/yr. Only a fraction of this salt is extracted from evaporite deposits. The major portion comes from coastal salt evaporation pans. Wold et al. (1999) give the locations of 690 solar salt production facilities located in low and mid-latitude

coastal regions of all continents except Antarctica. Human recycling of salt from the ocean is probably greater than atmospheric recycling. Because of its solubility and ways in which it is used, the human recycling begins to approach the residual "natural" fluxes cited above. Wilkinson (2005, p. 161) stated that "Humans are now an order of magnitude more important at moving sediment than the sum of all other natural processes operating on the surface of the planet." It appears that the human effect on salt may be just as great as or greater than it is on sedimentary materials generally.

4.4. Chloride from of saline groundwaters

It is well known that the salinity of pore waters tends to increase with depth (Feth, 1981; Land, 1995). On the continental blocks, deeper groundwaters may have [Cl^-] as high as 100 g/l, 5 times the concentration in seawater. The source of this Cl^- is uncertain, part of it may be from dissolution of evaporite deposits, but such saline waters also occur in basins that are not known to contain halite as a solid phase. Speculation is that clay minerals may act as osmotic membranes allowing escape of water but retaining Cl^- as compaction occurs (Feth, 1981). As noted above, Land (1995) suggested that the amount of Cl^- in brines could equal that in evaporite deposits.

Although the brines may approach the land surface in arid regions, they are ordinarily overlain by fresh, circulating groundwater. Because of the density differences the two water masses do not readily mix, but it is thought that upward diffusion gradually introduces salt into the fresher layer from which it eventually enters rivers. The rates of these processes are unknown.

4.5. Chloride from evaporite deposits

Holland (1978) was the first geochemist to recognize the importance of evaporites in river water chemistry. He noted that there is an obvious relation between elevated chloride and sulfate in rivers and the presence of evaporites in the drainage basin. He estimated the average chloride [Cl^-] in North American rivers to be 8 ppm. He estimated that 75% of this comes from the erosion of evaporites. On a global scale this implies an annual delivery of about 225×10^9 kg/yr from the erosion of evaporites. Berner and Berner (1987) concluded that, after correcting for atmospherically recycled salt and pollution (using the value of 30% from Meybeck, 1979), the delivery from evaporites would be about 188×10^9 kg/yr.

Allen (1997), working from the Oxford Global Sediment Flux Database, concluded that evaporites contribute 18% of the total solute load of rivers, although they are only 1% of the outcrop area.

5. Water

Critical to evaluation ocean salinity in the past is information on the amounts of water in the ocean and other reservoirs.

5.1. The total amount of free water on Earth

Free water is H_2O that is not incorporated into the solid phases of minerals. It occurs on the surface of the Earth as a solid: ice; as a liquid: fresh water in rivers and lakes, seawater, pore water in sediments on land and in the ocean, water in fissure and cracks in igneous and metamorphic rocks, water in the biosphere; and as a gas, vapor (Table 6). Three of these reservoirs, ice, seawater, and pore water, are large; all of the others are small and can be neglected. The possible exception is that the Arctic Ocean basin may have been isolated from the world ocean and filled with fresh or brackish water at times during the Late Cretaceous and Palaeogene forming by far the largest "lake" on Earth. Its present volume is about 16.7×10^6 km^3, and its volume at the beginning of the Late Cretaceous would have been about 15.6×10^6 km^3. Both values are smaller than the present volume of ice on Antarctica (23.56×10^6 km^3 = 21.6×10^6 km^3 water).

Some water is bound in sedimentary minerals, such as gypsum (-600×10^{15} kg), and in hydrated clays. The amount in clay is unknown but probably small. Potentially very large amounts of water, possibly several ocean equivalents, are incorporated into the mineral wadsleyite which is stable in the Earth's mantle.

Table 6
Water at or near the surface of the Earth (from various sources)

	Mass (10^{15} kg)	Moles (10^{15})
Free water		
Ice	27,820.0	1,544,269
Rivers and lakes	225.0	12,490
Oceans	1,371,345.7	76,122,437
Pore water	58,613.0	3,253,566
Fissures in crystalline rocks	75.0	4163
Atmosphere	13.0	722
Biosphere	0.6	33
Bound water (speculative values)		
in Gypsum	600	33,306
in clays	7500	416,320

There are two ultimate sources for water being supplied to the surface of the earth: outgassing from the earth's interior, "juvenile water", and water carried by incoming extraterrestrial objects, particularly comets. Based on consideration of 'excess volatiles,' Rubey (1951) estimated the rate of outgassing of water from the earth's interior at 0.370×10^{12} kg/yr, making the assumption that it had occurred at the same rate throughout geologic time and that the oceans had been generated through this process. However, in the context of plate tectonics most of the "outgassed" H_2O, especially that of volcanic arc systems, is now thought to be the result of recycling of seawater through subduction zones.

Turekian (1968) proposed that the oceans originated as saline water condensed in the last phases of Earth accretion and hence have always had roughly their present volume. Others have argued that bombardment of the early Earth by asteroids would have vaporized any early ocean, and that the water accumulated later from comets colliding with the Earth.

Wallmann (2001) has estimated the outgassing rate of juvenile water from the mantle to be 0.11×10^{12} kg/yr into ocean crustal rocks, and about 0.04×10^{12} kg/yr into the atmosphere, mostly through intraplate volcanoes.

Geologists had generally assumed that cometary delivery of water would occur as rare events largely restricted to the early history of the Earth, but Frank et al. (1986) suggested that the Earth might be continuously bombarded by cosmic snowballs. On the basis of observations from satellites they estimated that small comets could bring in water at a rate of about 1×10^{12} kg; this would fill the oceans in about 1.3 billion years. At first their idea was ridiculed as being a misinterpretation of the instrumental data, but more recently there seems to be additional evidence from ground-based telescopes that this might be the case (Frank and Sigwarth, 2001). However, even if there is an influx of water from space, the rate of supply remains highly controversial. Where it has been possible to make measurements, the water in comets has about twice as much Deuterium as ocean water, suggesting that the cometary contribution is small.

The other side of the equation is losses of free water; there are three possibilities: subduction into the mantle, loss into space, and incorporation into minerals.

Southam and Hay (1981) estimated the water lost to subduction to be 0.26×10^{12} kg/yr but suggested that most, if not all, of this is returned as volcanic water emissions. Von Huene and Scholl (1991) estimated the global long-term rate of subduction of sediment to be 1 km^3 solid per year. If the pore space is 30%, the mass of subducted water is 0.30×10^{12} kg/yr. These numbers for subducted water so closely balance estimates of outgassing that it is evident that the contribution of truly juvenile water must be small or negligible. Thus until recently it seemed likely that the volume of the oceans was essentially in a steady state.

Another method of estimating the amount of pore water subducted is to assume that the amount of sediment on the ocean floor is in a steady state, i.e. what is delivered from the continents is ultimately subducted. The age–area distribution of the ocean floor is not an exponential decay, as might be expected, but is more nearly linear. It can be fit by a second order polynomial equation

$$A = 0.077t^2 - 2.98t + 281.54 \quad (1)$$

where A is the area of ocean floor older than age t (my) still in existence today. Using the data of Hay et al. (1988), on the modern mass–age distribution of sediment on the ocean floor, and making the correction for the loss of ocean floor with age, it works out that the long-term average mass of sediment delivered to the ocean floor is 3.08×10^{12} kg/yr. For the sediment mass to be in steady state, this amount must be subducted each year. Assuming an average density of the solid phase to be 2700 kg/m^3, the volume subducted would be 1.14 km^3 solid/yr, very close to the estimate of Von Huene and Scholl (1991).

Wallmann (2001) has reevaluated the data on subduction, taking into account not only pore water, which he estimates to be between 1.08 and 1.80×10^{12} kg/yr, but also the structurally bound water in the sediments, 0.09×10^{12} kg/yr, pore water in the uppermost 0.5 km of ocean crust, 0.07×10^{12} kg/yr, water in the upper ocean crustal rocks, 0.11×10^{12} kg/yr, water in the deeper ocean crust and peridotites from 0.5 to 7 km, between 0.36 and 1.26×10^{12} kg/yr, and water from the mantle trapped in the ocean crust 0.11×10^{12} kg/yr. These total between 1.82 and 3.33×10^{12} kg/yr as an estimate of water subducted. The difference between his estimate of pore water subducted and those given above is largely related to differences in the assumed porosity of the sediment being subducted.

Wallmann (2001) estimates the amounts returned at subduction zones: cool submarine water reflux, 1.08 to 1.80×10^{12} kg/yr, and recycling through arc volcanoes, 0.14 to 1.21×10^{12} kg/yr, for a total between 1.22 and 2.90×10^{12} kg/yr. He estimates that the net amount of water subducted into the deeper mantle (>250 km) is between 0.16 and 0.41×10^{12} kg/yr.

In addition to the water subducted, there is flow through the mid-ocean ridge basalts and older ocean crust, estimated to be of the order of 130×10^{12} kg/yr (Humphris and McCollom, 1998). Although this water is altered chemically, it is returned to the ocean and Cl^- is not affected.

The loss of water to space comes from dissociation of H_2O into its components by radiation at the top of the atmosphere, and subsequent loss of the hydrogen into space. This may have been an important process in the Earth's early history, but today the presence of ozone in the atmosphere makes an effective cold trap, the stratosphere, through which H_2O vapor from the surface cannot pass. The presence of significant quantities of free oxygen in the atmosphere, a prerequisite to making ozone, was essential to ending the loss of water to space, and in this respect the present oceans may owe their existence to the development of life on this planet.

It is possible that water brought by small comets today is dissociated and the hydrogen escapes back into space.

It is obvious that the uncertainties concerning supply and loss of free water from the surface of the Earth are so great that it is impossible to make a balance or even know the sign of the change. However, there is another possible source of information on the volume of the ocean basins — palaeogeography. It has long been recognized that there are long-term episodes of continental flooding and emergence on the scale of hundreds of millions of years. A long-term trend was already evident in the data on continental flooding of Budyko et al. (1987), shown in Fig. 2.

The greatest flooding occurred in the Early Ordovician and Late Cretaceous and the greatest emergence in the Late Triassic and at present. These long-term trends are thought to reflect changes in the rate of sea-floor spreading. However, Tardy et al. (1989), in compiling areas of land on the palaeogeographic maps (redrawn from Scotese et al., 1979; Parrish et al., 1982), noted that there appeared to be a secular decline in sea level on which these episodes of flooding and emergence were superimposed. They considered the possibility of a long-term loss of water from the oceans, but concluded that the observations were more likely to reflect a loss of information through erosion of older deposits. They assumed that the sedimentary cycling known from the

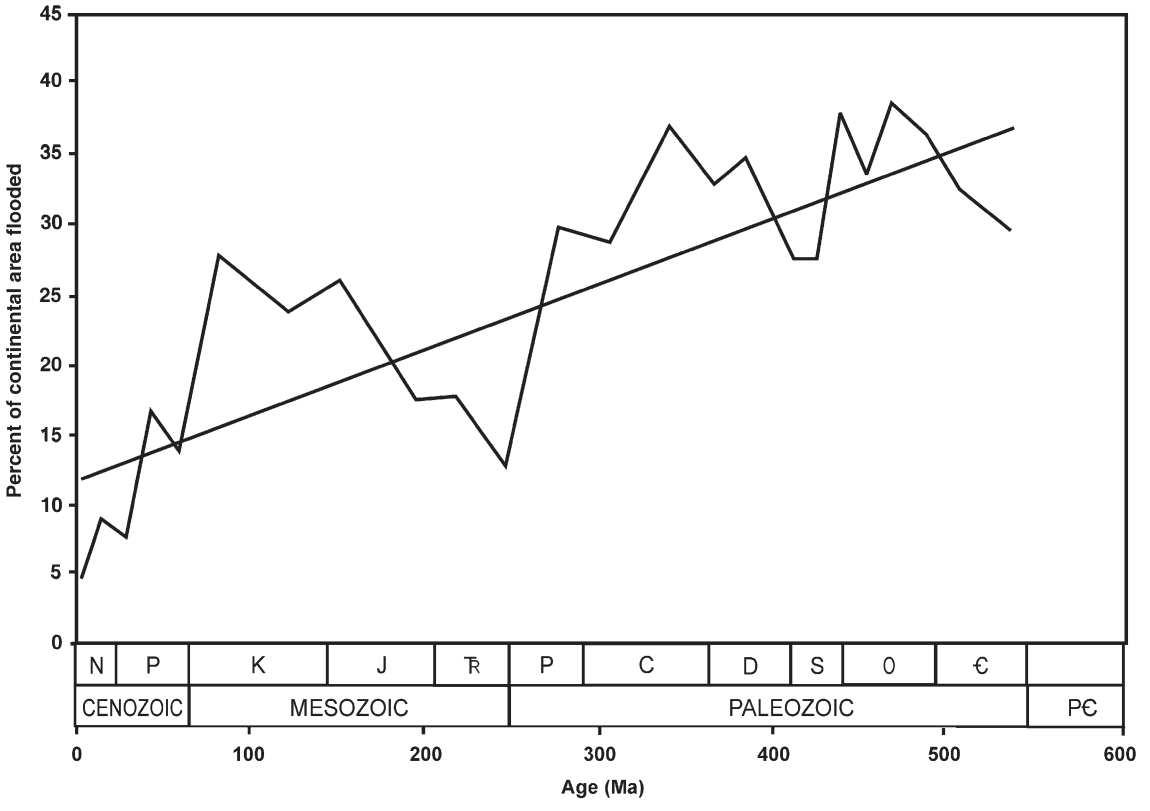

Fig. 2. Percent of continental area flooded during the Phanerozoic, based on data in Budyko et al. (1987). Diagonal line is linear regression through the Phanerozoic, showing an apparent decline in the volume of seawater with time.

mass–age distribution of sediments also applied to the apparent areas of the continents on palaeogeographic maps. They calculated the palaeoland area A (in 10^3 km^2) to decrease exponentially as a function of time t (in my) following the formula

$$A = \mathrm{EXP}(-0.00122t + 11.941) \quad (2)$$

Hallam (1992) assumed that the observed secular decline is not an artifact of the loss of information with age. He estimated that the oceans had lost about 10% of their water over the course of the Phanerozoic. This amounts to 0.25×10^{12} kg seawater/yr, in the middle of the range of Wallmann's (2001) estimates of the net water subducted into the deep mantle.

There is a problem in the quantitative evaluation of the long-term trend, noted by Ronov (1994). From the palaeogeographic maps one can measure the area of continent flooded, but any assumption about the absolute magnitude of the sea level change requires knowledge of the hypsography of the continents at the time. The assumption usually made is that the hypsography does not change with time. However, Ronov (1994) showed that the sea level trends are similar but not exactly the same for the Gondwanan and Laurasian continents. More importantly, the degree of flooding of the Gondwanan continents is only about half that of the Laurasian continents. This implies that the two regions have had different hypsographies (or hypsographic histories) throughout the Phanerozoic. Because this problem remains unsolved, and because we know nothing about the possible variations in the rate of loss of water to the mantle, we have used a constant rate of decline of 256×10^{15} kg/my throughout the Phanerozoic, based on Hallam (1992) and Wallmann (2001), for our "long-term trend" model.

In our calculations of palaeosalinity we use two models for the total amount of free water on Earth, a steady-state model assuming that the amount of free water has remained constant over the Phanerozoic, and a "long-term trend" model another assuming that it has declined at the rate of 0.256×10^{12} kg/yr.

Table 7
Late Cenozoic ice volumes — after Flint (1971) and Denton and Hughes (1981a,b)

Region	Age	Area	Average thickness	Ice volume	Water volume	Sea level
		10^{12} m^2	km	10^6 km^3	10^6 km^3	m
Antarctic						
	Present	12.53	1.88	23.56	21.60	59.84
	Glacial	13.81	1.88	25.96	23.81	65.95
Greenland						
	Present	1.73	1.52	2.63	2.41	6.68
	Glacial	2.30	1.52	3.50	3.21	8.88
Arctic ocean						
	Present	15.00	0.00	0.05	0.04	0.00
	Glacial	15.00	1.36	20.40	18.71	0.00
Laurentide						
	Present	0.00	0.00	0.00	0.00	0.00
	Glacial	13.39	2.20	29.46	27.01	74.83
Cordilleran						
	Present	0.30	0.30	0.09	0.08	0.23
	Glacial	2.37	1.50	3.56	3.26	9.03
British–Scandinavian–Barents–Kara						
	Present	0.30	0.30	0.09	0.08	0.23
	Glacial	8.37	2.00	16.74	15.35	42.52
Other						
	Present	0.64	0.30	0.19	0.18	0.49
	Glacial	5.20	0.30	1.56	1.43	3.96
Totals with thick Arctic ice (Denton and Hughes' "Outrageous hypothesis")						
	Present	30.50		26.60	24.39	67.46
	Glacial	60.44		101.17	92.77	205.17
Glacial–Present		29.94		74.57	68.38	137.71
Totals without thick Arctic ice						
	Present	30.50		26.60	24.39	67.46
	Glacial	60.44		80.82	74.11	205.17
Glacial–Present		29.94		54.21	49.71	137.71

5.2. The amount of water in the ocean

There are two reservoirs of free water outside the ocean large enough to significantly affect the ocean volume: ice and groundwater. The volumes of ice at present and during the last glacial maximum are shown in Table 7. The estimates are from Flint (1971), partially revised by Denton and Hughes (1981a). The amount of water currently present as ice is about 24.4×10^6 km^3. It is mostly in the Antarctic and Greenland ice sheets, but there are also lesser amounts in the Cordillera of North America, the mountains of Scandinavia, and elsewhere.

During the Quaternary as much as 2% of the total ocean volume may have been incorporated into ice sheets. During the Last Glacial Maximum the mean salinity of the ocean was probably about 36.0‰, but if the Denton and Hughes (1981b) "outrageous hypothesis" of a thick sheet of ice floating on the Arctic Ocean is true, the ocean salinity could have been as high as 37.6‰.

The amount of water stored in the pore space of sediments is larger that the amount in ice sheets, but varies on a much longer time scale (10^6 years) and only as the total mass of sedimentary rocks increases or decreases. If the total sedimentary mass remains constant, the pore space, and hence the amount of water stored in it, also remain constant. This is because the rate at which older sediments are being eroded and releasing pore water is the same as the rate at which new sediments are being formed and enclosing pore water. Of course, young sediments contain more pore space than older, more deeply buried sediments, but over the long term the dewatering of sediments through compaction has almost no effect on the fluxes. However, there are both marine and non-marine sediments. The pore space in the former is filled with seawater which may be altered by reactions with the minerals. Pore space in the latter is filled with rainwater and salts derived from weathering. Although the long-term net pore water flux into and out of sediments changes only with the total sedimentary mass, the associated fluxes of fresh water from non-marine sediments and of salt water flux from marine sediments may change on the time scale of 10^6 years.

On the shorter term (10^4–10^3 years) the portion of the pore space that is filled with water may vary. However, the effects of variations in groundwater storage in response to climate change are much less

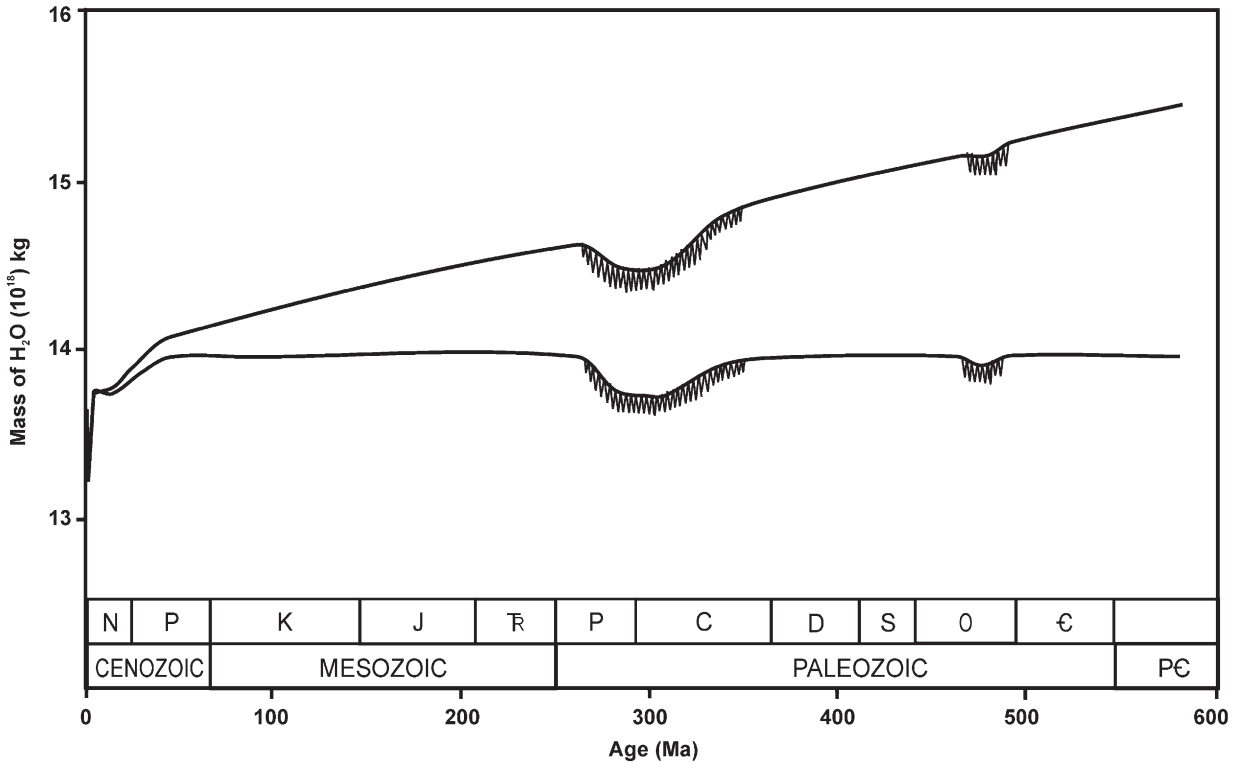

Fig. 3. Mass of water in the oceans through the Phanerozoic taking glaciations into account. Upper sloping line assumes that there has been loss of water to the mantle at a constant rate, lower quasi-horizontal line assumes that the mass of free water at the Earth's surface has remained constant.

well known. It is probably about an order of magnitude less than the volume changes due to buildup and melting of ice sheets. The possibility of relatively short-term changes in the volume of groundwater has been explored by Hay and Leslie (1990), who concluded that changes in storage equivalent to 30 m of sea level (10.8×10^{18} kg H_2O) were possible and changes equaling 10 m of sea level (3.6×10^{18} kg H_2O) were probable. The maximum possible salinity change due to variations in groundwater storage would be in the order of 0.3‰.

Fig. 3 shows two models for the mass of H_2O in the ocean through the Phanerozoic, taking into account the fluxes into and out of ice sheets and the possible long-term flux of water from the ocean into the mantle via subduction. The calculations are given in Table 8. The net fluxes of water into and out of the pore space in sediments are so small that they cannot be shown in this figure. The upper, sloping line includes the long-term loss of water to the mantle at a steady rate, and includes the fluctuations due to glacial buildup and decay. The lower, quasi-horizontal line assumes that there has been a constant mass of free water on the surface of the earth and shows only the effect of fluxes into and out of ice. For the Palaeozoic glaciations, the amounts of ice are speculative; we assume that the Late Palaeozoic Gondwanan glaciation involved ice masses comparable to today's Antarctic ice sheets, and that the Ordovician glaciation was much smaller. The steep declines in all models approaching the present are related to both the buildup of ice sheets, first on Antarctica and then in the northern hemisphere.

Table 8
Masses of water (H_2O only) in the ocean during the Phanerozoic according to two different models

Stratigraphic unit	Time scale of Gradstein et al. (2004)				Masses of water			
	Age of top	Age of base	Length	Age of mid-point	Mass of water in ice	Ocean water — taking only glacial changes into account — Model A	Water in ocean and ice with long-term trend	Ocean water — with both long-term trend and glacial variations — Model B
	Ma	Ma	my	Ma	10^{15} kg	10^{15} kg	10^{15} kg	10^{15} kg
Holocene	0	0.01	0.01	0.01	24,390	1,371,346	1,395,736	1,371,346
Pleistocene	0.01	1.81	1.80	0.91	74,110	1,321,626	1,395,969	1,321,859
Pliocene	1.81	5.33	3.52	3.57	22,000	1,373,736	1,396,649	1,374,649
Miocene	5.33	23.03	17.70	14.18	22,000	1,373,736	1,399,365	1,377,365
Oligocene	23.03	33.90	10.87	28.47	10,000	1,385,736	1,403,020	1,393,020
Eocene	33.90	55.80	21.90	44.85	0	1,395,736	1,407,213	1,407,213
Paleocene	55.80	65.50	9.70	60.65	0	1,395,736	1,411,257	1,411,257
Late Cretaceous	65.50	99.60	34.10	82.55	0	1,395,736	1,416,861	1,416,861
Early Cretaceous	99.60	145.50	45.90	122.55	0	1,395,736	1,427,097	1,427,097
Late Jurassic	145.50	161.20	15.70	153.35	0	1,395,736	1,434,979	1,434,979
Middle Jurassic	161.20	175.60	14.40	168.40	0	1,395,736	1,438,831	1,438,831
Early Jurassic	175.60	199.60	24.00	187.60	0	1,395,736	1,443,744	1,443,744
Late Triassic	199.60	228.00	28.40	213.80	0	1,395,736	1,450,449	1,450,449
Middle Triassic	228.00	245.00	17.00	236.50	0	1,395,736	1,456,258	1,456,258
Early Triassic	245.00	251.00	6.00	248.00	0	1,395,736	1,459,201	1,459,201
Late Permian	251.00	270.60	19.60	260.80	0	1,395,736	1,462,477	1,462,477
Early Permian	270.60	299.00	28.40	284.80	20,000	1,375,736	1,468,619	1,448,619
M and L Carboniferous	299.00	318.10	19.10	308.55	25,000	1,370,736	1,474,697	1,449,697
Early Carboniferous	318.10	359.20	41.10	338.65	5000	1,390,736	1,482,400	1,477,400
Late Devonian	359.20	385.30	26.10	372.25	0	1,395,736	1,490,998	1,490,998
Middle Devonian	385.30	397.50	12.20	391.40	0	1,395,736	1,495,899	1,495,899
Early Devonian	397.50	416.00	18.50	406.75	0	1,395,736	1,499,827	1,499,827
Late Silurian	416.00	428.20	12.20	422.10	0	1,395,736	1,503,755	1,503,755
Early Silurian	428.20	443.70	15.50	435.95	0	1,395,736	1,507,300	1,507,300
Late Ordovician	443.70	460.90	17.20	452.30	0	1,395,736	1,511,484	1,511,484
Middle Ordovician	460.90	471.80	10.90	466.35	0	1,395,736	1,515,079	1,515,079
Early Ordovician	471.80	488.30	16.50	480.05	5000	1,390,736	1,518,585	1,513,585
Late Cambrian	488.30	501.00	12.70	494.65	0	1,395,736	1,522,322	1,522,322
Middle Cambrian	501.00	513.00	12.00	507.00	0	1,395,736	1,525,482	1,525,482
Early Cambrian	513.00	542.00	29.00	527.50	0	1,395,736	1,530,728	1,530,728

6. Reconstructing sediment masses and fluxes in the past

6.1. Reconstructing the total sediment masses originally deposited

The reconstruction of the masses of sediment that existed in the past and of ancient sediment fluxes rests on the resemblance of the mass–age distribution to an exponential decay. Gilluly (1969) was the first geologist to realize (on the basis of area–age distribution of sediments on geologic maps of North and South America) that younger sediments are formed mostly from the erosion of older sediments, and that the distribution has the form of a decay curve. Veizer and Jansen (1979, 1985) have shown that the exponential decay with age holds for: 1) the age/area distribution of continental basement; 2) the thicknesses of both sedimentary and volcanogenic units; 3) the thickness, area and volume of sedimentary rocks; and 4) the cumulative reserves of most mineral commodities. They concluded that "the described exponential relationship is a fundamental law of the present day age distribution of geologic entities" (Veizer and Jansen, 1979, p. 342).

Wold and Hay (1990) described how to use a simple exponential decay having the form

$$y = Ae^{-bt} \tag{3}$$

fit through the data to represent the long-term average sedimentary cycle, as shown in Fig. 4. Here y is the remnant of the original sediment deposited at time t, after t my of cycling at a constant rate of erosion b (decay constant, or "average recycling proportionality parameter" of Veizer and Jansen, 1985), and A is the long-term average rate at which sediment was deposited. For this study we used the Ronov (1993) data set on global sediment masses for both continents and ocean basins supplemented with data for the Quaternary from Hay (1994), and adjusted to include a projection of Antarctic values. Table 9 shows these data in terms of

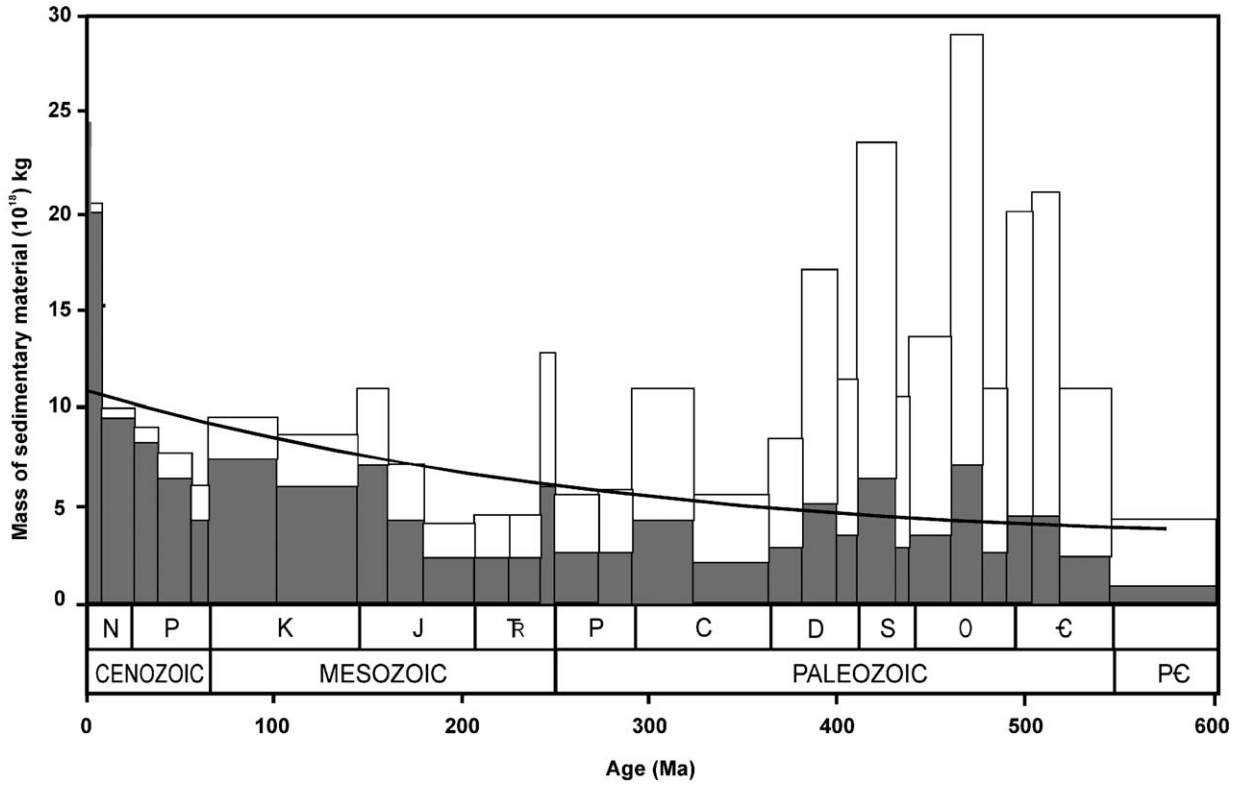

Fig. 4. Existing masses of sediment on the continental blocks and in the ocean basins (shaded areas), exponential decay curve fit through the data (solid curve), and reconstructed original masses of sediment deposited (open areas). The exponential is fit through the total existing sedimentary mass, so the reconstruction of original masses includes sediment that would have been deposited on the ocean floor and has been lost to subduction. Because, except for evaporites, sedimentary material cannot be stored in the ocean, the dashed line can also be interpreted as the detrital and dissolved flux from erosion of older sediments. Note the high sediment volumes reconstructed for the early Palaeozoic, reflecting erosion and sedimentation before the spread of land plants, and the unusually low sediment masses preserved from the Late Precambrian (Ediacarian) possibly reflecting the weathering system after the "snowball Earth."

Table 9
Reconstruction of original masses of sediment deposited during given geologic intervals

Stratigraphic unit	Time scale of Gradstein et al. (2004)				Masses of sedimentary material (after Ronov, 1993; Hay, 1994)						Calculations for reconstruction				
	Age of top	Age of base	Length	Age of mid-point	Platforms	Geosynclines	Orogenic regions	Offshore and ocean floor	Estimated Antarctic	Estimated Global total	Total sediment in interval normalized to time	Exponential curve fit to data[a]	Ratio observed/ exponential	Reconstructed original rate of deposition	Reconstructed original sediment mass deposited during interval
	Ma	Ma	my	Ma	10^{18} kg	10^{18} kg	10^{18} kg	10^{18} kg	10^{18} kg	10^{18} kg	10^{18} kg/my	10^{18} kg/my		10^{18} kg/my	10^{18} kg
Holocene	0	0.01	0.01	0.01								9.549			
Pleistocene	0.01	1.81	1.80	0.91	2.996	5.060	9.434	25.220	1.836	44.546	24.748	9.523	2.599	24.818	44.673
Pliocene	1.81	5.33	3.52	3.57	5.076	2.253	16.014	44.808	2.451	70.502	20.029	9.444	2.121	20.253	71.289
Miocene	5.33	23.03	17.70	14.18	9.193	6.794	29.696	117.234	4.797	167.714	9.475	9.138	1.037	9.903	175.275
Oligocene	23.03	33.90	10.87	28.47	6.993	6.543	9.999	62.297	2.471	88.303	8.124	8.741	0.929	8.876	96.477
Eocene	33.90	55.80	21.90	44.85	17.720	20.564	11.878	82.048	5.267	138.477	6.323	8.306	0.761	7.270	159.204
Paleocene	55.80	65.50	9.70	60.65	7.111	3.768	5.134	23.663	1.681	41.357	4.264	7.908	0.539	5.149	49.942
Late Cretaceous	65.50	99.60	34.10	82.55	41.873	57.247	20.817	118.203	12.593	250.733	7.353	7.387	0.995	9.505	324.122
Early Cretaceous	99.60	145.50	45.90	122.55	45.160	70.941	11.194	124.581	13.366	265.242	5.779	6.523	0.886	8.460	388.298
Late Jurassic	145.50	161.20	15.70	153.35	18.180	29.202	6.580	48.305	5.666	107.933	6.875	5.927	1.160	11.076	173.891
Middle Jurassic	161.20	175.60	14.40	168.40	13.502	27.463	12.214		5.584	58.763	4.081	5.656	0.721	6.890	99.209
Early Jurassic	175.60	199.60	24.00	187.60	14.866	23.970	9.460		5.071	53.367	2.224	5.328	0.417	3.985	95.644
Late Triassic	199.60	228.00	28.40	213.80	16.864	34.109	6.390		6.023	63.386	2.232	4.912	0.454	4.340	123.244
Middle Triassic	228.00	245.00	17.00	236.50	10.738	19.138	2.433		3.392	35.701	2.100	4.577	0.459	4.382	74.493
Early Triassic	245.00	251.00	6.00	248.00	17.966	13.220	1.006		3.380	35.572	5.929	4.416	1.343	12.821	76.926
Late Permian	251.00	270.60	19.60	260.80	12.767	23.391	6.009		4.428	46.595	2.377	4.244	0.560	5.350	104.854
Early Permian	270.60	299.00	28.40	284.80	18.201	30.879	13.338		6.554	68.972	2.429	3.938	0.617	5.889	167.240
M and L Carboniferous	299.00	318.10	19.10	308.55	24.130	28.056	19.301		7.506	78.993	4.136	3.658	1.131	10.797	206.222
Early Carboniferous	318.10	359.20	41.10	338.65	16.158	46.505	7.074		7.322	77.059	1.875	3.331	0.563	5.375	220.915
Late Devonian	359.20	385.30	26.10	372.25	18.670	34.032	8.890		6.467	68.065	2.608	3.001	0.869	8.300	216.624
Middle Devonian	385.30	397.50	12.20	391.40	13.060	36.362	6.386		5.860	61.914	5.075	2.827	1.795	17.143	209.139
Early Devonian	397.50	416.00	18.50	406.75	9.631	34.248	9.559		5.611	59.049	3.192	2.695	1.184	11.309	209.214
Late Silurian	416.00	428.20	12.20	422.10	8.381	22.952	3.285		3.635	38.253	6.375	2.570	2.481	23.693	142.160
Early Silurian	428.20	443.70	15.50	435.95	13.446	30.209	5.172		5.127	53.948	2.697	2.461	1.096	10.466	209.311
Late Ordovician	443.70	460.90	17.20	452.30	9.039	36.156	0.548		4.803	50.546	3.370	2.339	1.440	13.756	206.342
Middle Ordovician	460.90	471.80	10.90	466.35	14.440	59.523	0.606		7.830	82.399	6.867	2.239	3.066	29.283	351.398
Early Ordovician	471.80	488.30	16.50	480.05	14.340	39.771	0.962		5.783	60.856	2.434	2.146	1.134	10.833	270.822
Late Cambrian	488.30	501.00	12.70	494.65	15.629	22.536	1.109		4.124	43.398	4.340	2.051	2.116	20.210	202.101
Middle Cambrian	501.00	513.00	12.00	507.00	17.903	30.936	2.717		5.413	56.969	4.382	1.973	2.221	21.207	275.692
Early Cambrian	513.00	542.00	29.00	527.50	21.063	27.620	1.872		5.308	55.863	2.069	1.851	1.117	10.672	288.136
Ediacaran	542.00	630.00	88.00	586.00	27.247	41.820	6.125		7.895	83.087	0.615	1.543	0.399	3.808	514.065
Cryogenian–Tonian	630.00	1000.00	370.00	815.00	25.530	107.112	0.337		13.963	146.942	0.397	0.757	0.524	5.009	1853.232
Mesoproterozoic	1000.00	1600.00	600.00	1300.00	39.271	36.854	0.546		8.050	84.721	0.141	0.168	0.843	8.048	4828.875

[a] $y = 9.5496e^{(-0.0031t)}$.

existing masses of sediment representing time intervals of differing length. It also shows step by step the calculations involved in reconstructing the original masses of sediment deposited during each interval of time. In order to use Eq. (3), the volumes/masses must be normalized by dividing by the length of each time interval, so that they are expressed in terms of mass per unit time. We have taken t to be expressed as millions of years. The exponential curve is then fit to the time-normalized mass age data using the age mid-point of each stratigraphic interval.

Assuming a constant total sedimentary mass, and plotted against the Gradstein et al. (2004) time scale, $A = 9549.63 \times 10^{15}$ kg/my and $b = -0.0031$/my (Fig. 4). However, the original data show strong temporal deviations from the exponential decay curve. Wold and Hay (1990) proposed that these temporal variations in the rates of erosion and deposition shown by the data can be described in terms of proportional deviations from the decay curve, and that the original fluxes of both erosion and deposition can be reconstructed by multiplying these proportions by the long-term average rate of sediment deposition, A, as given by:

$$M_t = M_o / M_p \tag{4}$$

where M_t is the mass/my of sediment originally deposited at time t, M_o is the mass/my of sediment of that age existing today, and M_p is the mass/my predicted by the exponential decay for that age. The mass in each stratigraphic interval can then be determined by multiplying the mass/my by the length of the interval, expressed in my.

There still remain possible complications. Wold and Hay (1993) noted that the mass represented by the area under the curve is not equal to the mass of sediment observed, and successive reconstructions based on this method yield a varying total mass of sediment. They suggested that variations from the average rate of erosion and deposition involve variations in both the rate of deposition A, and the decay constant b, with time. They showed how correction for these changes can be made assuming either a constant mass of sediment through time, or growth or decline of the sedimentary mass due to imbalances between the formation of new sediment from weathering of igneous and metamorphic rocks and losses due to subduction and metamorphism. However, they found that the corrections are small and do not affect general trends. To keep the calculations here as simple as possible we have not made corrections for the assumption of a constant or steadily increasing or decreasing sediment mass.

Implicit in the reconstructions of ancient sediment masses is the assumption that the Earth as a whole can be considered a quasi-closed system with regard to sediment. In reality, the Earth itself is not a closed system because new sediments are generated from the weathering of igneous rocks and sediments deposited on the sea floor may be subducted. However for the Earth as a whole these processes probably nearly balance, so that assumption of the Earth as a closed system used for the calculations is a reasonable approximation. Hay (1999) showed that the assumption of constant growth of sedimentary mass since the Early Precambrian versus a constant mass throughout the Proterozoic and Phanerozoic makes very little difference in terms of masses reconstructed for the Phanerozoic.

Evidence that the reconstructions of past sediment fluxes are realistic has come from an unexpected source. McArthur et al. (2001) noted that there is a strong similarity between the reconstructions of original sediment masses and the strontium isotope curve for the Phanerozoic. Because most sediment cannot be stored, original sediment masses are a direct reflection of erosion rates. Wold and Hay (1990) had suggested that times of high deposition rates were times of uplift and erosion of the continents. This fits with the hypothesis that changes in the Sr-isotope ratio also reflect uplift and erosion. A more precise correlation between the two phenomena is presented in Hay et al. (2001).

6.2. Reconstructing the original masses of evaporite deposits

Ancient masses of detrital sediments, such as sands and shales, can be reconstructed in the same way as the total sedimentary mass. Being a particulate material, they are eroded from one site and deposited at another in a brief period of time. For detrital matter, the rate of erosion must equal the rate of deposition on geological time scales. The same applies to carbonates because carbonate is stored only briefly in solution in the ocean. Since they cannot be stored, the proportions of most sediment types within the total sediment mass change only slowly with time as they evolve (Ronov, 1972, 1982).

Evaporites, which constitute about 1.33% of the total existing sedimentary mass, present a special case because they can be stored in solution for long periods of time in the ocean. As shown in Fig. 5, their deposition is episodic and depends on the existence of restricted passages between basins and the open ocean, and the requirement that the basin must be located in a

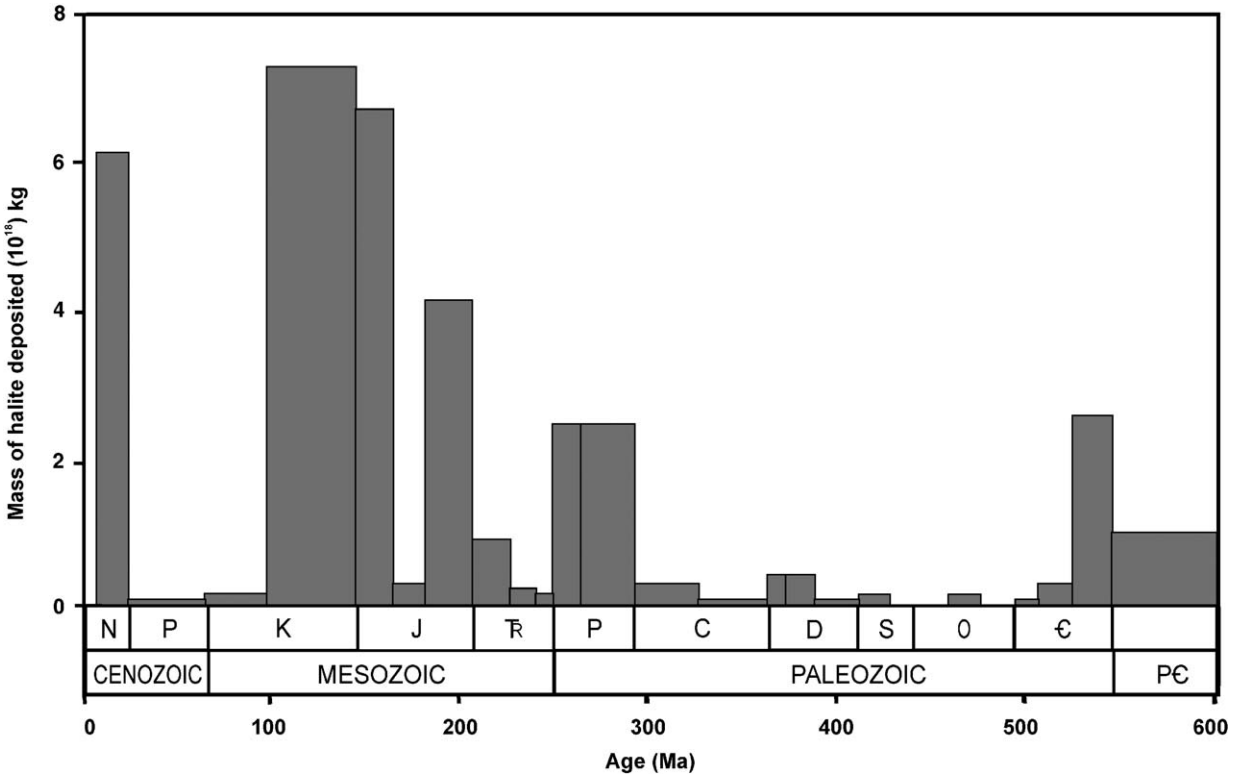

Fig. 5. Distribution of existing halite deposits through the Phanerozoic showing the sporadic nature of deposition. Masses are maximum values, taken from Table 5. Total mass is proportional to the area of the bar; mass for an interval is equal to the value shown on the abscissa times the length of the interval in my. Solid bars are existing masses. Open bars are halite masses subsequently eroded. It is evident that more halite has been deposited than has been eroded.

region where evaporation exceeds precipitation and runoff. Because of their episodic deposition the proportion of evaporites in the total existing sediment of a particular age varies significantly with stratigraphic interval. For the reconstruction of original halite masses we assume that all halite deposits on or within the continental blocks are recycled at the same rate as the total sediment and that their original mass had the same proportion to the total sediment deposited at that time as the existing mass has to the total sediment of that age existing today. We also assume that evaporites deposited in the continental margins and in the deep sea (Mediterranean, Red Sea, Gulf of Mexico and the North and South Atlantic) have not been involved in recycling and retain their original size. This latter assumption is not strictly true: in some places the Mediterranean evaporites are near the sediment surface and are being dissolved. The Gulf of Mexico evaporites have been mobilized by the weight of sediments deposited above them, particularly during the Late Neogene and Quaternary, forming diapirs that approach the sediment surface and undergo dissolution. In both cases the amounts of evaporite lost to dissolution are unknown and difficult to estimate. Tables 10a and b show the reconstruction of minimum and maximum estimates of original halite masses based on the assumptions as to whether they are recyclable or not. For those involved in recycling, their original mass is calculated assuming their proportion of the sediment of each stratigraphic interval has remained constant.

This latter assumption might be questioned because evaporites are much more soluble than other rock types. Garrels and Mackenzie (1971) postulated that because of their solubility evaporites are preferentially eroded. Meybeck (1979), on the basis of data on rivers draining terrains having different geology, concluded that evaporites were 80 times more soluble than silicic rocks and 50 times more soluble than crystalline (igneous and metamorphic) rocks. Einsele (1992) stated that halite has a chemical denudation rate three orders of magnitude greater than most igneous and metamorphic rocks. It is also evident that halite, once deposited, may subsequently be dissolved in the subsurface and

Table 10a
Reconstruction of original masses of halite and amounts eroded since deposition — minimum estimates

Age	Time scale of Gradstein et al. (2004)				Minimum halite masses					
	Age of top	Length	Age of mid-point	Length between mid-points	Total existing halite mass	Halite on ocean floor — not recyclable	Total recyclable halite mass	Recyclable halite mass as proportion of total existing sediment	Reconstructed original recyclable halite mass	Mass of haite eroded since deposition
	Ma	my	Ma	my	10^{15} kg	10^{15} kg	10^{15} kg		10^{15} kg	10^{18} kg
Holocene	0	0.01	0.005							
Pleistocene	0.01	1.80	0.91	0.905	0.000	0.000	0.000	0.000000	0.000	0.000
Pliocene	1.81	3.52	3.57	2.66	8.748	0.000	8.748	0.000124	8.846	0.098
Miocene	5.33	17.70	14.18	10.61	4233.600	2376.000	1857.600	0.011076	1941.353	83.753
Oligocene	23.03	10.87	28.47	14.29	62.208	4.320	57.888	0.000656	63.246	5.358
Eocene	33.90	21.90	44.85	16.39	31.752	0.000	31.752	0.000229	36.505	4.753
Paleocene	55.80	9.70	60.65	15.80	9.288	0.000	9.288	0.000225	11.216	1.928
Late Cretaceous	65.50	34.10	82.55	21.90	95.904	0.000	95.904	0.000382	123.975	28.071
Early Cretaceous	99.60	45.90	122.55	40.00	1633.392	648.000	985.392	0.003715	1442.553	457.161
Late Jurassic	145.50	15.70	153.35	30.80	6451.920	4536.000	1915.920	0.017751	3086.743	1170.823
Middle Jurassic	161.20	14.40	168.40	15.05	300.240	0.000	300.240	0.005109	506.896	206.656
Early Jurassic	175.60	24.00	187.60	19.20	3978.720	3888.000	90.720	0.001700	162.587	71.867
Late Triassic	199.60	28.40	213.80	26.20	846.720	0.000	846.720	0.013358	1646.304	799.584
Middle Triassic	228.00	17.00	236.50	22.70	50.760	0.000	50.760	0.001422	105.914	55.154
Early Triassic	245.00	6.00	248.00	11.50	91.800	0.000	91.800	0.002581	198.520	106.720
Late Permian	251.00	19.60	260.80	12.80	1708.560	0.000	1708.560	0.036669	3844.867	2136.307
Early Permian	270.60	28.40	284.80	24.00	2378.160	0.000	2378.160	0.034480	5766.441	3388.281
M and L Carboniferous	299.00	19.10	308.55	23.75	278.640	0.000	278.640	0.003527	727.425	448.785
Early Carboniferous	318.10	41.10	338.65	30.10	93.528	0.000	93.528	0.001214	268.127	174.599
Late Devonian	359.20	26.10	372.25	33.60	268.574	0.000	268.574	0.003946	854.764	586.190
Middle Devonian	385.30	12.20	391.40	19.15	400.602	0.000	400.602	0.006470	1353.194	952.592
Early Devonian	397.50	18.50	406.75	15.35	2.160	0.000	2.160	0.000037	7.653	5.493
Late Silurian	416.00	12.20	422.10	15.35	59.270	0.000	59.270	0.001549	220.267	160.997
Early Silurian	428.20	15.50	435.95	13.85	0.000	0.000	0.000	0.000000	0.000	0.000
Late Ordovician	443.70	17.20	452.30	16.35	0.000	0.000	0.000	0.000000	0.000	0.000
Middle Ordovician	460.90	10.90	466.35	14.05	58.492	0.000	58.492	0.000710	249.447	190.954
Early Ordovician	471.80	16.50	480.05	13.70	0.000	0.000	0.000	0.000000	0.000	0.000
Late Cambrian	488.30	12.70	494.65	14.60	13.647	0.000	13.647	0.000314	63.553	49.906
Middle Cambrian	501.00	12.00	507.00	12.35	282.074	0.000	282.074	0.004951	1365.043	1082.968
Early Cambrian	513.00	29.00	527.50	20.50	2496.420	0.000	2496.420	0.044688	12,876.227	10,379.807
Ediacaran	542.00	88.00	586.00	58.50	1296.000	0.000	1296.000	0.015598	8018.430	6722.430
Cryogenian–Tonian	630.00	370.00	815.00	229.00	0.000	0.000	0.000	0.000000	0.000	0.000
Mesoproterozoic	1000.00	600.00	1300.00	485.00	0.0000	0.000	0.000	0.000000	0.000	0.000

contribute to the saline brines found in most sedimentary basins. Land (1995) cited abundance evidence for dissolution of halite at depth, including collapse breccias.

However, Wold and Hay (1993) argued that the amount of evaporites dissolved and eroded must be closely related to the general rate of sedimentary cycling. For them to be selectively eroded they must be close enough to the surface so that the groundwaters circulate. We assume that on the time scale of the major stratigraphic units in the Ronov database (average length 18.7 my) little selective erosion of older deposits takes place. Interestingly, the half-life of all sediment, calculated from the equation and values given above, is

Table 10b
Reconstruction of original masses of halite and amounts eroded since deposition — maximum estimates

Age	Time scale of Gradstein et al. (2004)				Maximum halite masses					
	Age of top	Length	Age of mid-point	Length between mid-points	Total existing halite mass	Halite on ocean floor — not recyclable	Total recyclable halite mass	Recyclable halite mass as proportion of total existing sediment	Reconstructed original recyclable halite mass	Mass of haite eroded since deposition
	Ma	my	Ma	my	10^{15} kg	10^{15} kg	10^{15} kg		10^{15} kg	10^{18} kg
Holocene	0	0.01	0.005							
Pleistocene	0.01	1.80	0.91	0.905	0.000	0.000	0.000	0.000000	0.000	0.000
Pliocene	1.81	3.52	3.57	2.66	8.748	0.000	8.748	0.000124	8.846	0.098
Miocene	5.33	17.70	14.18	10.61	5873.472	2376.000	3497.472	0.020854	3655.161	157.689
Oligocene	23.03	10.87	28.47	14.29	62.208	4.320	57.888	0.000656	63.246	5.358
Eocene	33.90	21.90	44.85	16.39	31.752	0.000	31.752	0.000229	36.505	4.753
Paleocene	55.80	9.70	60.65	15.80	9.288	0.000	9.288	0.000225	11.216	1.928
Late Cretaceous	65.50	34.10	82.55	21.90	117.720	0.000	117.720	0.000470	152.176	34.456
Early Cretaceous	99.60	45.90	122.55	40.00	7033.392	6048.000	985.392	0.003715	1442.553	457.161
Late Jurassic	145.50	15.70	153.35	30.80	6451.920	4536.000	1915.920	0.017751	3086.743	1170.823
Middle Jurassic	161.20	14.40	168.40	15.05	300.240	0.000	300.240	0.005109	506.896	206.656
Early Jurassic	175.60	24.00	187.60	19.20	3978.720	3888.000	90.720	0.001700	162.587	71.867
Late Triassic	199.60	28.40	213.80	26.20	846.720	0.000	846.720	0.013358	1646.304	799.584
Middle Triassic	228.00	17.00	236.50	22.70	248.400	0.000	248.400	0.006958	518.301	269.901
Early Triassic	245.00	6.00	248.00	11.50	91.800	0.000	91.800	0.002581	198.520	106.720
Late Permian	251.00	19.60	260.80	12.80	2367.360	0.000	2367.360	0.050808	5327.401	2960.041
Early Permian	270.60	28.40	284.80	24.00	2378.160	0.000	2378.160	0.034480	5766.441	3388.281
M and L Carboniferous	299.00	19.10	308.55	23.75	278.640	0.000	278.640	0.003527	727.425	448.785
Early Carboniferous	318.10	41.10	338.65	30.10	93.528	0.000	93.528	0.001214	268.127	174.599
Late Devonian	359.20	26.10	372.25	33.60	396.576	0.000	396.576	0.005826	1262.142	865.566
Middle Devonian	385.30	12.20	391.40	19.15	400.602	0.000	400.602	0.006470	1353.194	952.592
Early Devonian	397.50	18.50	406.75	15.35	5.011	0.000	5.011	0.000085	17.755	12.744
Late Silurian	416.00	12.20	422.10	15.35	59.270	0.000	59.270	0.001549	220.267	160.997
Early Silurian	428.20	15.50	435.95	13.85	0.000	0.000	0.000	0.000000	0.000	0.000
Late Ordovician	443.70	17.20	452.30	16.35	0.000	0.000	0.000	0.000000	0.000	0.000
Middle Ordovician	460.90	10.90	466.35	14.05	58.492	0.000	58.492	0.000710	249.447	190.954
Early Ordovician	471.80	16.50	480.05	13.70	0.000	0.000	0.000	0.000000	0.000	0.000
Late Cambrian	488.30	12.70	494.65	14.60	13.647	0.000	13.647	0.000314	63.553	49.906
Middle Cambrian	501.00	12.00	507.00	12.35	282.074	0.000	282.074	0.004951	1365.043	1082.968
Early Cambrian	513.00	29.00	527.50	20.50	2496.420	0.000	2496.420	0.044688	12,876.227	10,379.807
Ediacaran	542.00	88.00	586.00	58.50	1296.000	0.000	1296.000	0.015598	8018.430	6722.430
Cryogenian–Tonian	630.00	370.00	815.00	229.00	0.000	0.000	0.000	0.000000	0.000	0.000
Mesoproterozoic	1000.00	600.00	1300.00	485.00	0.0000	0.000	0.000	0.000000	0.000	0.000

224 my, very close to the 220 my half-life of evaporites determined by Garrels and Mackenzie (1971).

A remaining problem is that our calculations are based solely on still existing evaporite deposits. Global sedimentary recycling implies that only half of the sediment deposited in the Late Palaeozoic is still in existence, and that 2/3 of the sediments originally present in the Early Palaeozoic have been destroyed, and some of them would surely have been evaporites. It is likely that many older evaporite deposits have been completely destroyed by erosion. Correspondingly, estimates for variations in salinity of the ocean in the past, particularly in the Palaeozoic, may well be minimal.

Table 11a
Reconstruction of original masses of sediment and halite and amounts eroded since deposition — minimum estimates

Stratigraphic unit	Time to mid-Holocene since unit's mid-point age	Amount of unit's sediment remaining	Amount of unit's sediment eroded during each interval	Halite fluxes from unit during each interval	Time to mid-Holocene since unit's mid-point age	Amount of unit's sediment remaining	Amount of unit's sediment eroded during each interval	Halite fluxes from unit during each interval	Time to mid-Holocene since unit's mid-point age	Amount of unit's sediment remaining	Amount of unit's sediment eroded during each interval	Halite fluxes from unit during each interval
	my	10^{15} kg	10^{15} kg	10^{15} kg	my	10^{15} kg	10^{15} kg	10^{15} kg	my	10^{15} kg	10^{15} kg	10^{15} kg
	Ediacaran				Early Cambrian				Middle Cambrian			
Holocene	*586.00*	83,088.45	234.19	3.65	*527.50*	55,864.14	157.45	7.04	*507.00*	56,970.27	160.57	0.80
Pleistocene	*585.09*	83,322.64	692.15	10.80	*526.59*	56,021.60	465.37	20.80	*506.09*	57,130.84	474.58	2.35
Pliocene	*582.43*	84,014.79	2818.49	43.96	*523.93*	56,486.96	1895.00	84.68	*503.43*	57,605.42	1932.52	9.57
Miocene	*571.82*	86,833.28	3944.66	61.53	*513.32*	58,381.96	2652.17	118.52	*492.82*	59,537.94	2704.69	13.39
Oligocene	*557.54*	90,777.94	4745.69	74.02	*499.04*	61,034.14	3190.74	142.59	*478.54*	62,242.63	3253.92	16.11
Eocene	*541.15*	95,523.63	4811.08	75.04	*482.65*	64,224.88	3234.70	144.55	*462.15*	65,496.55	3298.75	16.33
Paleocene	*525.35*	100,334.71	7071.79	110.31	*466.85*	67,459.59	4754.69	212.48	*446.35*	68,795.30	4848.83	24.01
Late Cretaceous	*503.45*	107,406.50	14,228.01	221.93	*444.95*	72,214.27	9566.14	427.49	*424.45*	73,644.13	9755.55	48.30
Early Cretaceous	*463.45*	121,634.50	12,227.40	190.72	*404.95*	81,780.41	8221.03	367.38	*384.45*	83,399.68	8383.81	41.51
Late Jurassic	*432.65*	133,861.90	6414.42	100.05	*374.15*	90,001.44	4312.70	192.73	*353.65*	91,783.49	4398.10	21.78
Middle Jurassic	*417.60*	140,276.32	8631.31	134.63	*359.10*	94,314.15	5803.22	259.33	*338.60*	96,181.59	5918.13	29.30
Early Jurassic	*398.40*	148,907.63	12,641.32	197.18	*339.90*	100,117.37	8499.33	379.82	*319.40*	102,099.71	8667.62	42.92
Late Triassic	*372.20*	161,548.95	11,817.09	184.32	*313.70*	108,616.70	7945.17	355.05	*293.20*	110,767.34	8102.48	40.12
Middle Triassic	*349.50*	173,366.04	6312.65	98.47	*291.00*	116,561.87	4244.28	189.67	*270.50*	118,869.82	4328.32	21.43
Early Triassic	*338.00*	179,678.69	7296.92	113.82	*279.50*	120,806.15	4906.05	219.24	*259.00*	123,198.14	5003.19	24.77
Late Permian	*325.20*	186,975.61	14,489.90	226.01	*266.70*	125,712.20	9742.22	435.36	*246.20*	128,201.33	9935.11	49.19
Early Permian	*301.20*	201,465.51	15,444.09	240.90	*242.70*	135,454.42	10,383.77	464.03	*222.20*	138,136.45	10,589.37	52.43
M and L Carboniferous	*277.45*	216,909.60	21,285.88	332.02	*218.95*	145,838.19	14,311.46	639.55	*198.45*	148,725.81	14,594.83	72.26
Early Carboniferous	*247.35*	238,195.48	26,237.46	409.25	*188.85*	160,149.65	17,640.64	788.33	*168.35*	163,320.65	17,989.92	89.07
Late Devonian	*213.75*	264,432.94	16,227.12	253.11	*155.25*	177,790.29	10,910.23	487.56	*134.75*	181,310.57	11,126.25	55.09
Middle Devonian	*194.60*	280,660.06	13,723.25	214.06	*136.10*	188,700.52	9226.76	412.33	*115.60*	192,436.83	9409.46	46.59
Early Devonian	*179.25*	294,383.31	14,394.26	224.52	*120.75*	197,927.28	9677.92	432.49	*100.25*	201,846.28	9869.54	48.87
Late Silurian	*163.90*	308,777.57	13,590.73	211.99	*105.40*	207,605.20	9137.67	408.34	*84.90*	211,715.83	9318.59	46.14
Early Silurian	*150.05*	322,368.30	16,815.85	262.29	*91.55*	216,742.86	11,306.06	505.25	*71.05*	221,034.42	11,529.92	57.09
Late Ordovician	*133.70*	339,184.15	15,149.39	236.30	*75.20*	228,048.92	10,185.62	455.18	*54.70*	232,564.34	10,387.30	51.43
Middle Ordovician	*119.65*	354,333.54	15,423.33	240.57	*61.15*	238,234.55	10,369.80	463.41	*40.65*	242,951.64	10,575.13	52.36
Early Ordovician	*105.95*	369,756.87	17,176.18	267.92	*47.45*	248,604.35	11,548.33	516.07	*26.95*	253,526.77	11,776.99	58.31
Late Cambrian	*91.35*	386,933.05	15,150.61	236.32	*32.85*	260,152.68	10,186.44	455.21	*12.35*	265,303.76	10,388.14	51.44
Middle Cambrian	*79.00*	402,083.66	26,469.67	412.88	*20.50*	270,339.12	17,796.76	795.30	*0.00*	275,691.90		
Early Cambrian	*58.50*	428,553.33	85,511.91	1333.82	*0.00*	288,135.88						
Ediacaran	*0.00*	514,065.24										
Total flux from unit through mid-Holocene				6722.41				10,379.77				1082.96

6.3. Reconstructing chlorine fluxes to the ocean in the past

As discussed above, the long-term chlorine fluxes to the ocean in the past have four possible sources: 1) from volcanic emissions, 2) from the weathering of crystalline rocks, 3) from release of saline pore waters through erosion of sediments and 4) from erosion of evaporite deposits. As noted above, the Cl^- from volcanic emissions is mostly, if not entirely, recycled from subducted ocean water, and any contribution of juvenile Cl^- from the mantle is probably negligible. Further, we neglect the contribution of the weathering of crystalline rocks which contain little Cl, most of which is probably also derived from subduction processes. The effect of saline waters both as a sink and source for Cl^- is more speculative, but as a first approximation we will assume that the total sedimentary mass and its contained pore space have remained almost constant during the Proterozoic and Phanerozoic (cf. Hay, 1999). We also assume that the proportions of saline brine and fresh water in the pore space have remained approximately constant. Hence the fluxes into and out of this reservoir would remain equal and have little effect on oceanic salinity, so we assume here that they can also be neglected. Consequently we base our calculations solely on the removal of halite into evaporite deposits and its subsequent recycling.

6.4. Flux of chlorine from the erosion of halite deposits

To determine the amount of halite eroded during each interval of time a series of exponential decays are recalculated starting with the mid-point age of the interval $t_a - t_b$ during which deposition occurred and calculating the flux rate at the mid-points of each subsequent stratigraphic interval. As discussed above, the total amount of sediment originally deposited during the interval $t_a - t_b$ is calculated using Eq. (3) (Table 9). The original amount of halite deposited is assumed to have the same proportional relation to the total sediment as exists today (Tables 10a–b). For each successive interval after deposition, the amount of sediment of interval remaining is determined with Eq. (3) using the time since deposition as t. The detailed calculations for the interval by interval erosion of sediment originally deposited during $t_a - t_b$ are shown in Tables 11a–g. The difference between the amounts remaining in successive stratigraphic intervals is the amount of sediment eroded from $t_a - t_b$ during that time. Analogous to the reconstruction of the amount of halite originally deposited, the amount of halite eroded during each of the successive intervals is determined by multiplying the amount of $t_a - t_b$ sediment eroded by the proportion of halite originally deposited in interval $t_a - t_b$. Tables 11a–g are based on the minimum estimates of recyclable halite. Table 12 shows the fluxes for those intervals for which the maximum estimates of recyclable halite differ from the minimum estimates. The total fluxes from each stratigraphic unit shown at the bottom of Tables 11a–g and 12 are slightly smaller than the masses of halite shown to be eroded since deposition in Tables 10a–b because they are calculated for the mid-Holocene (0.005 Ma) rather than for present as in Tables 10a–b.

As is evident from Tables 9 and 10a–b, at any time the youngest sediments are most likely to be eroded. The greatest amount of erosion will occur immediately after deposition, before the deposits are protected by burial, and in each successive time interval less and less will be eroded. We assume this to be true not only for detrital sediment, but for evaporites as well. The erosional fluxes from halite deposits in each stratigraphic interval are then summed to obtain the flux of halite and Cl^- ($0.607 \times NaCl$) returned to the ocean, and are shown in Table 13 and Fig. 6. While the removal of salt from the ocean into evaporites is sporadic, the return is continuous but varies by a factor of three with time. The possible rates of Cl^- delivery by rivers during the Phanerozoic are hindcast by our calculations to vary between 13 and 42×10^9 kg/yr. For the Quaternary/Holocene the minimum and maximum flux estimates are 29.6×10^9 kg/yr and 34.6×10^9 kg/yr. Although only about 10% of the present Cl^- flux of rivers, these values are appropriate for the range of uncertainties for the "natural" Cl^- flux in rivers discussed above.

7. Reconstructing ocean salinity in the past

As discussed above, the salinity of the ocean depends on two variables, the amount of water in the ocean, and the amount of salts dissolved in the water. Although changes in any of the reservoirs of water shown in Table 6 would affect the mass of water in the ocean, only three of the reservoirs are potentially large enough to affect ocean salinity: ice, pore water, and fresh water lakes. Buildup and decay of the mostly northern hemisphere ice sheets during the Quaternary can cause an oscillation of ocean salinity from 34.7‰ to 36‰, almost a 4% increase. In contrast, although the pore water reservoir is large, it cannot change rapidly and its effect on ocean salinity has been neglected in our calculations. The amount of water in lakes is trivial throughout most of geologic time, but if the Arctic ocean were a fresh water lake in the Eocene, with a mass of 16.5×10^{18} kg it

Table 11b
Reconstruction of original masses of sediment and halite and amounts eroded since deposition — minimum estimates

Stratigraphic unit	Time to mid-Holocene since unit's mid-point age	Amount of unit's sediment remaining	Amount of unit's sediment eroded during each interval	Halite fluxes from unit during each interval	Time to mid-Holocene since unit's mid-point age	Amount of unit's sediment remaining	Amount of unit's sediment eroded during each interval	Halite fluxes from unit during each interval	Time to mid-Holocene since unit's mid-point age	Amount of unit's sediment remaining	Amount of unit's sediment eroded during each interval	Halite fluxes from unit during each interval
	my	10^{15} kg	10^{15} kg	10^{15} kg	my	10^{15} kg	10^{15} kg	10^{15} kg	my	10^{15} kg	10^{15} kg	10^{15} kg
	Late Cambrian				Middle Ordovician				Late Silurian			
Holocene	*494.65*	43,398.44	122.32	0.04	*466.35*	82,400.03	232.25	0.16	*422.10*	38,253.48	107.82	0.17
Pleistocene	*493.74*	43,520.76	361.52	0.11	*465.44*	82,632.27	686.42	0.49	*421.19*	38,361.30	318.66	0.49
Pliocene	*491.08*	43,882.29	1472.14	0.46	*462.78*	83,318.69	2795.14	1.98	*418.53*	38,679.97	1297.62	2.01
Miocene	*480.47*	45,354.43	2060.36	0.65	*452.17*	86,113.83	3911.98	2.78	*407.92*	39,977.58	1816.10	2.81
Oligocene	*466.19*	47,414.79	2478.75	0.78	*437.89*	90,025.81	4706.37	3.34	*393.64*	41,793.69	2184.89	3.39
Eocene	*449.80*	49,893.54	2512.90	0.79	*421.50*	94,732.18	4771.21	3.39	*377.25*	43,978.58	2214.99	3.43
Paleocene	*434.00*	52,406.44	3693.71	1.16	*405.70*	99,503.39	7013.20	4.98	*361.45*	46,193.57	3255.81	5.04
Late Cretaceous	*412.10*	56,100.15	7431.52	2.34	*383.80*	106,516.59	14,110.12	10.02	*339.55*	49,449.38	6550.50	10.15
Early Cretaceous	*372.10*	63,531.67	6386.57	2.01	*343.80*	120,626.71	12,126.09	8.61	*299.55*	55,999.88	5629.43	8.72
Late Jurassic	*341.30*	69,918.24	3350.35	1.05	*313.00*	132,752.79	6361.27	4.52	*268.75*	61,629.31	2953.16	4.58
Middle Jurassic	*326.25*	73,268.59	4508.27	1.42	*297.95*	139,114.06	8559.80	6.08	*253.70*	64,582.48	3973.81	6.16
Early Jurassic	*307.05*	77,776.87	6602.77	2.08	*278.75*	147,673.86	12,536.58	8.90	*234.50*	68,556.29	5820.00	9.02
Late Triassic	*280.85*	84,379.63	6172.26	1.94	*252.55*	160,210.44	11,719.18	8.32	*208.30*	74,376.28	5440.53	8.43
Middle Triassic	*258.15*	90,551.89	3297.20	1.04	*229.85*	171,929.62	6260.35	4.44	*185.60*	79,816.81	2906.31	4.50
Early Triassic	*246.65*	93,849.09	3811.30	1.20	*218.35*	178,189.97	7236.47	5.14	*174.10*	82,723.12	3359.47	5.21
Late Permian	*233.85*	97,660.39	7568.31	2.38	*205.55*	185,426.43	14,369.84	10.20	*161.30*	86,082.58	6671.07	10.34
Early Permian	*209.85*	105,228.70	8066.70	2.54	*181.55*	199,796.27	15,316.13	10.87	*137.30*	92,753.66	7110.38	11.02
M and L Carboniferous	*186.10*	113,295.40	11,117.96	3.50	*157.80*	215,112.41	21,109.52	14.99	*113.55*	99,864.04	9799.91	15.18
Early Carboniferous	*156.00*	124,413.36	13,704.25	4.31	*127.70*	236,221.92	26,020.07	18.47	*83.45*	109,663.94	12,079.59	18.72
Late Devonian	*122.40*	138,117.61	8475.69	2.67	*94.10*	262,241.99	16,092.67	11.42	*49.85*	121,743.53	7470.88	11.58
Middle Devonian	*103.25*	146,593.30	7167.87	2.25	*74.95*	278,334.66	13,609.54	9.66	*30.70*	129,214.41	6318.11	9.79
Early Devonian	*87.90*	153,761.17	7518.36	2.36	*59.60*	291,944.21	14,275.00	10.13	*15.35*	135,532.52	6627.04	10.27
Late Silurian	*72.55*	161,279.53	7098.66	2.23	*44.25*	306,219.21	13,478.12	9.57	*0.00*	142,159.56		
Early Silurian	*58.70*	168,378.19	8783.19	2.76	*30.40*	319,697.33	16,676.52	11.84				
Late Ordovician	*42.35*	177,161.38	7912.77	2.49	*14.05*	336,373.86	15,023.87	10.66				
Middle Ordovician	*28.30*	185,074.15	8055.85	2.53	*0.00*	351,397.73						
Early Ordovician	*14.60*	193,130.00	8971.40	2.82								
Late Cambrian	*0.00*	202,101.40										
Total flux from unit through mid-Holocene				49.91				190.95				161.00

Table 11c
Reconstruction of original masses of sediment and halite and amounts eroded since deposition — minimum estimates

Stratigraphic unit	Time to mid-Holocene since unit's mid-point age	Amount of unit's sediment remaining	Amount of unit's sediment eroded during each interval	Halite fluxes from unit during each interval	Time to mid-Holocene since unit's mid-point age	Amount of unit's sediment remaining	Amount of unit's sediment eroded during each interval	Halite fluxes from unit during each interval	Time to mid-Holocene since unit's mid-point age	Amount of unit's sediment remaining	Amount of unit's sediment eroded during each interval	Halite fluxes from unit during each interval
	my	10^{15} kg	10^{15} kg	10^{15} kg	my	10^{15} kg	10^{15} kg	10^{15} kg	my	10^{15} kg	10^{15} kg	10^{15} kg
	Early Devonian				Middle Devonian				Late Devonian			
Holocene	*406.75*	59,049.91	166.43	0.01	*391.395*	61,914.80	174.51	1.13	*372.25*	68,066.22	191.85	0.76
Pleistocene	*405.84*	59,216.34	491.90	0.02	*390.490*	62,089.31	515.77	3.34	*371.34*	68,258.06	567.01	2.24
Pliocene	*403.18*	59,708.25	2003.06	0.07	*387.830*	62,605.08	2100.25	13.59	*368.68*	68,825.08	2308.91	9.11
Miocene	*392.57*	61,711.31	2803.42	0.10	*377.220*	64,705.33	2939.43	19.02	*358.07*	71,133.99	3231.47	12.75
Oligocene	*378.29*	64,514.73	3372.70	0.12	*362.935*	67,644.76	3536.33	22.88	*343.79*	74,365.46	3887.68	15.34
Eocene	*361.90*	67,887.43	3419.17	0.13	*346.550*	71,181.09	3585.06	23.20	*327.40*	78,253.14	3941.24	15.55
Paleocene	*346.10*	71,306.60	5025.83	0.18	*330.750*	74,766.15	5269.67	34.10	*311.60*	82,194.38	5793.22	22.86
Late Cretaceous	*324.20*	76,332.43	10,111.66	0.37	*308.850*	80,035.82	10,602.25	68.60	*289.70*	87,987.61	11,655.61	45.99
Early Cretaceous	*284.20*	86,444.10	8689.86	0.32	*268.850*	90,638.06	9111.46	58.95	*249.70*	99,643.22	10,016.71	39.52
Late Jurassic	*253.40*	95,133.95	4558.64	0.17	*238.050*	99,749.52	4779.81	30.93	*218.90*	109,659.92	5254.70	20.73
Middle Jurassic	*238.35*	99,692.60	6134.16	0.22	*223.000*	104,529.33	6431.77	41.62	*203.85*	114,914.63	7070.79	27.90
Early Jurassic	*219.15*	105,826.76	8984.02	0.33	*203.800*	110,961.11	9419.90	60.95	*184.65*	121,985.41	10,355.79	40.86
Late Triassic	*192.95*	114,810.79	8398.26	0.31	*177.600*	120,381.00	8805.71	56.98	*158.45*	132,341.21	9680.58	38.20
Middle Triassic	*170.25*	123,209.04	4486.32	0.16	*154.900*	129,186.71	4703.98	30.44	*135.75*	142,021.79	5171.33	20.41
Early Triassic	*158.75*	127,695.36	5185.83	0.19	*143.400*	133,890.69	5437.43	35.18	*124.25*	147,193.12	5977.65	23.59
Late Permian	*145.95*	132,881.19	10,297.79	0.38	*130.600*	139,328.12	10,797.40	69.86	*111.45*	153,170.78	11,870.15	46.84
Early Permian	*121.95*	143,178.98	10,975.92	0.40	*106.600*	150,125.52	11,508.44	74.46	*87.45*	165,040.93	12,651.83	49.92
M and L Carboniferous	*98.20*	154,154.90	15,127.60	0.55	*82.850*	161,633.95	15,861.54	102.63	*63.70*	177,692.76	17,437.43	68.81
Early Carboniferous	*68.10*	169,282.50	18,646.63	0.68	*52.750*	177,495.50	19,551.30	126.50	*33.60*	195,130.19	21,493.78	84.81
Late Devonian	*34.50*	187,929.13	11,532.41	0.42	*19.150*	197,046.80	12,091.92	78.24	*0.00*	216,623.97		
Middle Devonian	*15.35*	199,461.54	9752.94	0.36	*0.000*	209,138.72						
Early Devonian	*0.00*	209,214.48										
Total flux from unit through mid-Holocene				5.49				952.59				586.19

Table 11d
Reconstruction of original masses of sediment and halite and amounts eroded since deposition — minimum estimates

Stratigraphic unit	Time to mid-Holocene since unit's mid-point age	Amount of unit's sediment remaining	Amount of unit's sediment eroded during each interval	Halite fluxes from unit during each interval	Time to mid-Holocene since unit's mid-point age	Amount of unit's sediment remaining	Amount of unit's sediment eroded during each interval	Halite fluxes from unit during each interval	Time to mid-Holocene since unit's mid-point age	Amount of unit's sediment remaining	Amount of unit's sediment eroded during each interval	Halite fluxes from unit during each interval
	my	10^{15} kg	10^{15} kg	10^{15} kg	my	10^{15} kg	10^{15} kg	10^{15} kg	my	10^{15} kg	10^{15} kg	10^{15} kg
	Mississippian				Pennsylvanian				Early Permian			
Holocene	*338.65*	77,060.58	217.20	0.26	*308.545*	78,994.36	222.65	0.79	*284.80*	68,972.96	194.40	6.70
Pleistocene	*337.74*	77,277.78	641.94	0.78	*307.640*	79,217.01	658.05	2.32	*283.89*	69,167.36	574.57	19.81
Pliocene	*335.08*	77,919.72	2614.02	3.17	*304.980*	79,875.06	2679.61	9.45	*281.23*	69,741.93	2339.67	80.67
Miocene	*324.47*	80,533.73	3658.48	4.44	*294.370*	82,554.67	3750.29	13.23	*270.62*	72,081.60	3274.52	112.91
Oligocene	*310.19*	84,192.22	4401.40	5.34	*280.085*	86,304.96	4511.85	15.92	*256.34*	75,356.12	3939.47	135.83
Eocene	*293.80*	88,593.62	4462.04	5.42	*263.700*	90,816.81	4574.02	16.13	*239.95*	79,295.59	3993.75	137.70
Paleocene	*278.00*	93,055.66	6558.75	7.96	*247.900*	95,390.83	6723.34	23.72	*224.15*	83,289.34	5870.40	202.41
Late Cretaceous	*256.10*	99,614.41	13,195.80	16.02	*226.000*	102,114.16	13,526.94	47.71	*202.25*	89,159.73	11,810.88	407.24
Early Cretaceous	*216.10*	112,810.21	11,340.33	13.76	*186.000*	115,641.10	11,624.91	41.01	*162.25*	100,970.61	10,150.14	349.98
Late Jurassic	*185.30*	124,150.54	5949.07	7.22	*155.200*	127,266.01	6098.35	21.51	*131.45*	111,120.76	5324.70	183.60
Middle Jurassic	*170.25*	130,099.61	8005.13	9.72	*140.150*	133,364.36	8206.01	28.95	*116.40*	116,445.46	7164.98	247.05
Early Jurassic	*151.05*	138,104.74	11,724.22	14.23	*120.950*	141,570.38	12,018.43	42.39	*97.20*	123,610.44	10,493.75	361.83
Late Triassic	*124.85*	149,828.96	10,959.79	13.30	*94.750*	153,588.81	11,234.82	39.63	*71.00*	134,104.19	9809.54	338.23
Middle Triassic	*102.15*	160,788.74	5854.68	7.11	*72.050*	164,823.62	6001.60	21.17	*48.30*	143,913.73	5240.22	180.68
Early Triassic	*90.65*	166,643.43	6767.55	8.21	*60.550*	170,825.22	6937.38	24.47	*36.80*	149,153.96	6057.28	208.86
Late Permian	*77.85*	173,410.98	13,438.69	16.31	*47.750*	177,762.60	13,775.92	48.59	*24.00*	155,211.24	12,028.28	414.74
Early Permian	*53.85*	186,849.66	14,323.66	17.38	*23.750*	191,538.52	14,683.10	51.79	*0.00*	167,239.52		
M and L Carboniferous	*30.10*	201,173.33	19,741.64	23.96	*0.000*	206,221.63						
Early Carboniferous	*0.00*	220,914.97										
Total flux from unit through mid-Holocene				174.60				448.78				3388.24

Table 11e
Reconstruction of original masses of sediment and halite and amounts eroded since deposition — minimum estimates

Stratigraphic unit	Time to mid-Holocene since unit's mid-point age	Amount of unit's sediment remaining	Amount of unit's sediment eroded during each interval	Halite fluxes from unit during each interval	Time to mid-Holocene since unit's mid-point age	Amount of unit's sediment remaining	Amount of unit's sediment eroded during each interval	Halite fluxes from unit during each interval	Time to mid-Holocene since unit's mid-point age	Amount of unit's sediment remaining	Amount of unit's sediment eroded during each interval	Halite fluxes from unit during each interval
	my	10^{15} kg	10^{15} kg	10^{15} kg	my	10^{15} kg	10^{15} kg	10^{15} kg	my	10^{15} kg	10^{15} kg	10^{15} kg
	Late Permian				Early Triassic				Middle Triassic			
Holocene	*260.80*	46,595.26	131.33	4.82	*247.995*	35,572.71	100.26	0.26	*236.50*	35,702.00	100.63	0.14
Pleistocene	*259.89*	46,726.59	388.15	14.23	*247.090*	35,672.98	296.33	0.76	*235.59*	35,802.63	297.41	0.42
Pliocene	*257.23*	47,114.74	1580.58	57.96	*244.430*	35,969.31	1206.68	3.11	*232.93*	36,100.04	1211.07	1.72
Miocene	*246.62*	48,695.33	2212.13	81.12	*233.820*	37,175.99	1688.83	4.36	*222.32*	37,311.10	1694.97	2.41
Oligocene	*232.34*	50,907.46	2661.34	97.59	*219.535*	38,864.82	2031.78	5.24	*208.04*	39,006.07	2039.16	2.90
Eocene	*215.95*	53,568.80	2698.01	98.93	*203.150*	40,896.60	2059.77	5.32	*191.65*	41,045.23	2067.26	2.94
Paleocene	*200.15*	56,266.81	3965.80	145.42	*187.350*	42,956.36	3027.65	7.81	*175.85*	43,112.49	3038.65	4.32
Late Cretaceous	*178.25*	60,232.60	7978.94	292.58	*165.450*	45,984.01	6091.45	15.72	*153.95*	46,151.14	6113.58	8.69
Early Cretaceous	*138.25*	68,211.54	6857.01	251.44	*125.450*	52,075.46	5234.92	13.51	*113.95*	52,264.72	5253.95	7.47
Late Jurassic	*107.45*	75,068.55	3597.15	131.90	*94.650*	57,310.38	2746.21	7.09	*83.15*	57,518.67	2756.19	3.92
Middle Jurassic	*92.40*	78,665.70	4840.36	177.49	*79.600*	60,056.59	3695.33	9.54	*68.10*	60,274.86	3708.76	5.27
Early Jurassic	*73.20*	83,506.06	7089.14	259.95	*60.400*	63,751.92	5412.14	13.97	*48.90*	63,983.62	5431.81	7.72
Late Triassic	*47.00*	90,595.20	6626.92	243.00	*34.200*	69,164.06	5059.26	13.06	*22.70*	69,415.43	5077.65	7.22
Middle Triassic	*24.30*	97,222.12	3540.08	129.81	*11.500*	74,223.31	2702.64	6.97	*0.00*	74,493.07		
Early Triassic	*12.80*	100,762.20	4092.05	150.05	*0.000*	76,925.95						
Late Permian	*0.00*	104,854.25										
Total flux from unit through mid-Holocene				2136.28				106.72				55.15

Table 11f
Reconstruction of original masses of sediment and halite and amounts eroded since deposition — minimum estimates

Stratigraphic unit	Time to mid-Holocene since unit's mid-point age	Amount of unit's sediment remaining	Amount of unit's sediment eroded during each interval	Halite fluxes from unit during each interval	Time to mid-Holocene since unit's mid-point age	Amount of unit's sediment remaining	Amount of unit's sediment eroded during each interval	Halite fluxes from unit during each interval	Time to mid-Holocene since unit's mid-point age	Amount of unit's sediment remaining	Amount of unit's sediment eroded during each interval	Halite fluxes from unit during each interval
	my	10^{15} kg	10^{15} kg	10^{15} kg	my	10^{15} kg	10^{15} kg	10^{15} kg	my	10^{15} kg	10^{15} kg	10^{15} kg
	Late Triassic				Early Jurassic				Middle Jurassic			
Holocene	*213.80*	63,387.10	178.66	2.39	*187.595*	53,367.91	150.42	0.26	*168.40*	58,763.71	165.63	0.85
Pleistocene	*212.89*	63,565.76	528.04	7.05	*186.690*	53,518.33	444.57	0.76	*167.49*	58,929.34	489.52	2.50
Pliocene	*210.23*	64,093.79	2150.19	28.72	*184.030*	53,962.90	1810.32	3.08	*164.83*	59,418.86	1993.36	10.18
Miocene	*199.62*	66,243.98	3009.33	40.20	*173.420*	55,773.22	2533.66	4.31	*154.22*	61,412.21	2789.83	14.25
Oligocene	*185.34*	69,253.31	3620.43	48.36	*159.135*	58,306.89	3048.17	5.18	*139.94*	64,202.05	3356.36	17.15
Eocene	*168.95*	72,873.74	3670.31	49.03	*142.750*	61,355.06	3090.17	5.25	*123.55*	67,558.40	3402.60	17.39
Paleocene	*153.15*	76,544.05	5394.98	72.07	*126.950*	64,445.22	4542.23	7.72	*107.75*	70,961.00	5001.47	25.55
Late Cretaceous	*131.25*	81,939.02	10,854.36	144.99	*105.050*	68,987.45	9138.68	15.54	*85.85*	75,962.47	10,062.65	51.41
Early Cretaceous	*91.25*	92,793.38	9328.12	124.61	*65.050*	78,126.13	7853.69	13.35	*45.85*	86,025.13	8647.74	44.18
Late Jurassic	*60.45*	102,121.51	4893.48	65.37	*34.250*	85,979.82	4120.00	7.00	*15.05*	94,672.86	4536.55	23.18
Middle Jurassic	*45.40*	107,014.98	6584.72	87.96	*19.200*	90,099.81	5543.91	9.42	*0.00*	99,209.41		
Early Jurassic	*26.20*	113,599.70	9643.90	128.82	*0.000*	95,643.72						
Late Triassic	*0.00*	123,243.59										
Total flux from unit through mid-Holocene				799.57				71.87				206.65

Stratigraphic unit	Time to mid-Holocene since unit's mid-point age	Amount of unit's sediment remaining	Amount of unit's sediment eroded during each interval	Halite fluxes from unit during each interval	Time to mid-Holocene since unit's mid-point age	Amount of unit's sediment remaining	Amount of unit's sediment eroded during each interval	Halite fluxes from unit during each interval	Time to mid-Holocene since unit's mid-point age	Amount of unit's sediment remaining	Amount of unit's sediment eroded during each interval	Halite fluxes from unit during each interval
	my	10^{15} kg	10^{15} kg	10^{15} kg	my	10^{15} kg	10^{15} kg	10^{15} kg	my	10^{15} kg	10^{15} kg	10^{15} kg
	Late Jurassic				Early Cretaceous				Late Cretaceous			
Holocene	*153.35*	107,934.69	304.22	5.40	*122.545*	265,246.10	747.60	2.78	*82.55*	250,737.28	706.71	0.27
Pleistocene	*152.44*	108,238.90	899.13	15.96	*121.640*	265,993.70	2209.59	8.21	*81.64*	251,443.99	2088.72	0.80
Pliocene	*149.78*	109,138.03	3661.31	64.99	*118.980*	268,203.29	8997.56	33.43	*78.98*	253,532.71	8505.40	3.25
Miocene	*139.17*	112,799.35	5124.25	90.96	*108.370*	277,200.85	12,592.67	46.78	*68.37*	262,038.11	11,903.86	4.55
Oligocene	*124.89*	117,923.59	6164.81	109.43	*94.085*	289,793.52	15,149.83	56.28	*54.09*	273,941.97	14,321.14	5.48
Eocene	*108.50*	124,088.41	6249.75	110.94	*77.700*	304,943.35	15,358.56	57.06	*37.70*	288,263.12	14,518.46	5.55
Paleocene	*92.70*	130,338.15	9186.49	163.07	*61.900*	320,301.91	22,575.51	83.87	*21.90*	302,781.57	21,340.65	8.16
Late Cretaceous	*70.80*	139,524.65	18,482.66	328.09	*40.000*	342,877.43	45,420.55	168.74	*0.00*	324,122.22		
Early Cretaceous	*30.80*	158,007.30	15,883.80	281.95	*0.000*	388,297.98						
Late Jurassic	*0.00*	173,891.10										
Total flux from unit through mid-Holocene				1170.79				457.15				28.07

Table 11g
Reconstruction of original masses of sediment and halite and amounts eroded since deposition — minimum estimates

Stratigraphic unit	Time to mid-Holocene since unit's mid-point age	Amount of unit's sediment remaining	Amount of unit's sediment eroded during each interval	Halite fluxes from unit during each interval	Time to mid-Holocene since unit's mid-point age	Amount of unit's sediment remaining	Amount of unit's sediment eroded during each interval	Halite fluxes from unit during each interval	Time to mid-Holocene since unit's mid-point age	Amount of unit's sediment remaining	Amount of unit's sediment eroded during each interval	Halite fluxes from unit during each interval
	my	10^{15} kg	10^{15} kg	10^{15} kg	my	10^{15} kg	10^{15} kg	10^{15} kg	my	10^{15} kg	10^{15} kg	10^{15} kg
	Paleocene				Eocene				Oligocene			
Holocene	*60.65*	41,358.01	116.57	0.03	*44.845*	138,479.16	390.31	0.09	*28.46*	88,304.55	248.89	0.16
Pleistocene	*59.74*	41,474.58	344.53	0.08	*43.940*	138,869.47	1153.58	0.26	*27.56*	88,553.44	735.61	0.48
Pliocene	*57.08*	41,819.10	1402.93	0.32	*41.280*	140,023.05	4697.43	1.08	*24.90*	89,289.04	2995.43	1.96
Miocene	*46.47*	43,222.03	1963.49	0.44	*30.670*	144,720.47	6574.36	1.51	*14.29*	92,284.47	4192.30	2.75
Oligocene	*32.19*	45,185.52	2362.21	0.53	*16.385*	151,294.83	7909.39	1.81	*0.00*	96,476.77		
Eocene	*15.80*	47,547.73	2394.76	0.54	*0.000*	159,204.23						
Paleocene	*0.00*	49,942.48										
Total flux from unit through mid-Holocene				1.90				4.66				5.19

Stratigraphic unit	Time to mid-Holocene since unit's mid-point age	Amount of unit's sediment remaining	Amount of unit's sediment eroded during each interval	Halite fluxes from unit during each interval	Time to mid-Holocene since unit's mid-point age	Amount of unit's sediment remaining	Amount of unit's sediment eroded during each interval	Halite fluxes from unit during each interval
	my	10^{15} kg	10^{15} kg	10^{15} kg	my	10^{15} kg	10^{15} kg	10^{15} kg
	Miocene				Pliocene			
Holocene	*14.18*	167,716.32	472.71	5.24	*3.565*	70,503.11	198.71	0.02
Pleistocene	*13.27*	168,189.03	1397.13	15.47	*2.660*	70,701.83	587.31	0.07
Pliocene	*10.61*	169,586.17	5689.20	63.01	*0.000*	71,289.14		
Miocene	*0.00*	175,275.36						
Total flux from unit through mid-Holocene				83.72				0.10

Table 12
Reconstruction of amounts of halite eroded since deposition — only for those stratigraphic units in which maximum estimates for recyclable halite differ from minimum estimates

Stratigraphic unit	Time to mid-Holocene since unit's mid-point age	Halite fluxes from unit during each interval	Time to mid-Holocene since unit's mid-point age	Halite fluxes from unit during each interval	Time to mid-Holocene since unit's mid-point age	Halite fluxes from unit during each interval	Time to mid-Holocene since unit's mid-point age	Halite fluxes from unit during each interval	Time to mid-Holocene since unit's mid-point age	Halite fluxes from unit during each interval	Time to mid-Holocene since unit's mid-point age	Halite fluxes from unit during each interval
	my	10^{15} kg	my	10^{15} kg	my	10^{15} kg	my	10^{15} kg	my	10^{15} kg	my	10^{15} kg
	Early Devonian		Late Devonian		Late Permian		Middle Triassic		Late Cretaceous		Miocene	
Holocene	*406.75*	0.01	*372.25*	1.12	*260.795*	6.67	*236.50*	0.70	*82.55*	0.33	*14.18*	9.86
Pleistocene	*405.84*	0.04	*371.34*	3.30	*259.890*	19.72	*235.59*	2.07	*81.64*	0.98	*13.27*	29.14
Pliocene	*403.18*	0.17	*368.68*	13.45	*257.230*	80.31	*232.93*	8.43	*78.98*	3.99	*10.61*	118.64
Miocene	*392.57*	0.24	*358.07*	18.83	*246.620*	112.39	*222.32*	11.79	*68.37*	5.59	*0.00*	
Oligocene	*378.29*	0.29	*343.79*	22.65	*232.335*	135.22	*208.04*	14.19	*54.09*	6.72		
Eocene	*361.90*	0.29	*327.40*	22.96	*215.950*	137.08	*191.65*	14.38	*37.70*	6.82		
Paleocene	*346.10*	0.43	*311.60*	33.75	*200.150*	201.49	*175.85*	21.14	*21.90*	10.02		
Late Cretaceous	*324.20*	0.86	*289.70*	67.91	*178.250*	405.39	*153.95*	42.54	*0.00*			
Early Cretaceous	*284.20*	0.74	*249.70*	58.36	*138.250*	348.39	*113.95*	36.56				
Late Jurassic	*253.40*	0.39	*218.90*	30.62	*107.450*	182.76	*83.15*	19.18				
Middle Jurassic	*238.35*	0.52	*203.85*	41.20	*92.400*	245.93	*68.10*	25.80				
Early Jurassic	*219.15*	0.76	*184.65*	60.34	*73.200*	360.18	*48.90*	37.79				
Late Triassic	*192.95*	0.71	*158.45*	56.40	*47.000*	336.70	*22.70*	35.33				
Middle Triassic	*170.25*	0.38	*135.75*	30.13	*24.300*	179.86	*0.00*					
Early Triassic	*158.75*	0.44	*124.25*	34.83	*12.800*	207.91						
Late Permian	*145.95*	0.87	*111.45*	69.16	*0.000*							
Early Permian	*121.95*	0.93	*87.45*	73.71								
M and L Carboniferous	*98.20*	1.28	*63.70*	101.60								
Early Carboniferous	*68.10*	1.58	*33.60*	125.23								
Late Devonian	*34.50*	0.98	*0.00*									
Middle Devonian	*15.35*	0.83										
Early Devonian	*0.00*											
Total flux from unit through mid-Holocene		12.74		865.56		2960.00		269.90		34.45		157.63

Table 13
Reconstructions of fluxes of halite and chloride from evaporite deposits to ocean

Stratigraphic unit	Age of mid-point	Halite and chloride fluxes to ocean-minimum estimates				Halite and chloride fluxes to ocean-maximum estimates			
		Total return flux of halite to ocean in each time interval	Return flux rate of halite	Total return flux of chloride to ocean in each time interval	Return flux rate of chloride	Total return flux of halite to ocean in each time interval	Return flux rate of halite	Total return flux of chloride to ocean in each time interval	Return flux rate of chloride
	Ma	10^{15} kg	10^{15} kg/my	10^{15} kg	10^{15} kg/my	10^{15} kg	10^{15} kg/my	10^{15} kg	10^{15} kg/my
Holocene	0.01	44.192	48.831	26.824	29.640	51.658	57.081	31.356	34.648
Pleistocene	0.91	130.612	49.102	79.282	29.805	152.679	57.398	92.676	34.841
Pliocene	3.57	531.563	50.100	322.659	30.411	621.422	58.569	377.203	35.552
Miocene	14.18	655.765	45.906	398.050	27.865	703.674	49.260	427.130	29.901
Oligocene	28.47	785.623	47.948	476.873	29.104	843.260	51.465	511.859	31.239
Eocene	44.85	794.609	50.292	482.327	30.527	853.040	53.990	517.795	32.772
Paleocene	60.65	1167.203	53.297	708.492	32.351	1253.091	57.219	760.626	34.732
Late Cretaceous	82.55	2331.918	58.298	1415.474	35.387	2500.984	62.525	1518.097	37.952
Early Cretaceous	122.55	1859.012	60.358	1128.420	36.637	2004.305	65.075	1216.613	39.500
Late Jurassic	153.35	827.315	54.971	502.180	33.367	903.535	60.036	548.446	36.442
Middle Jurassic	168.40	1082.055	56.357	656.807	34.209	1184.617	61.699	719.063	37.451
Early Jurassic	187.60	1570.962	59.960	953.574	36.396	1721.174	65.694	1044.753	39.876
Late Triassic	213.80	1348.109	59.388	818.302	36.049	1488.526	65.574	903.536	39.803
Middle Triassic	236.50	716.298	62.287	434.793	37.808	776.293	67.504	471.210	40.975
Early Triassic	248.00	819.922	64.056	497.693	38.882	889.272	69.474	539.788	42.171
Late Permian	260.80	1330.202	55.425	807.432	33.643	1353.022	56.376	821.284	34.220
Early Permian	284.80	975.751	41.084	592.281	24.938	1000.074	42.108	607.045	25.560
M and L Carboniferous	308.55	1273.448	42.307	772.983	25.680	1306.971	43.421	793.331	26.357
Early Carboniferous	338.65	1540.147	45.838	934.869	27.823	1581.468	47.067	959.951	28.570
Late Devonian	372.25	900.083	47.002	546.351	28.530	900.640	47.031	546.689	28.548
Middle Devonian	391.40	695.033	45.279	421.885	27.484	695.504	45.310	422.171	27.503
Early Devonian	406.75	728.643	47.469	442.286	28.813	728.643	47.469	442.286	28.813
Late Silurian	422.10	678.273	48.973	411.712	29.726	678.273	48.973	411.712	29.726
Early Silurian	435.95	839.229	51.329	509.412	31.157	839.229	51.329	509.412	31.157
Late Ordovician	452.30	756.061	53.812	458.929	32.664	756.061	53.812	458.929	32.664
Middle Ordovician	466.35	758.875	55.392	460.637	33.623	758.875	55.392	460.637	33.623
Early Ordovician	480.05	845.120	57.885	512.988	35.136	845.120	57.885	512.988	35.136
Late Cambrian	494.65	742.968	60.159	450.981	36.517	742.968	60.159	450.981	36.517
Middle Cambrian	507.00	1208.178	58.936	733.364	35.774	1208.178	58.936	733.364	35.774
Early Cambrian	527.50	1333.821	22.800	809.630	13.840	1333.821	22.800	809.630	13.840

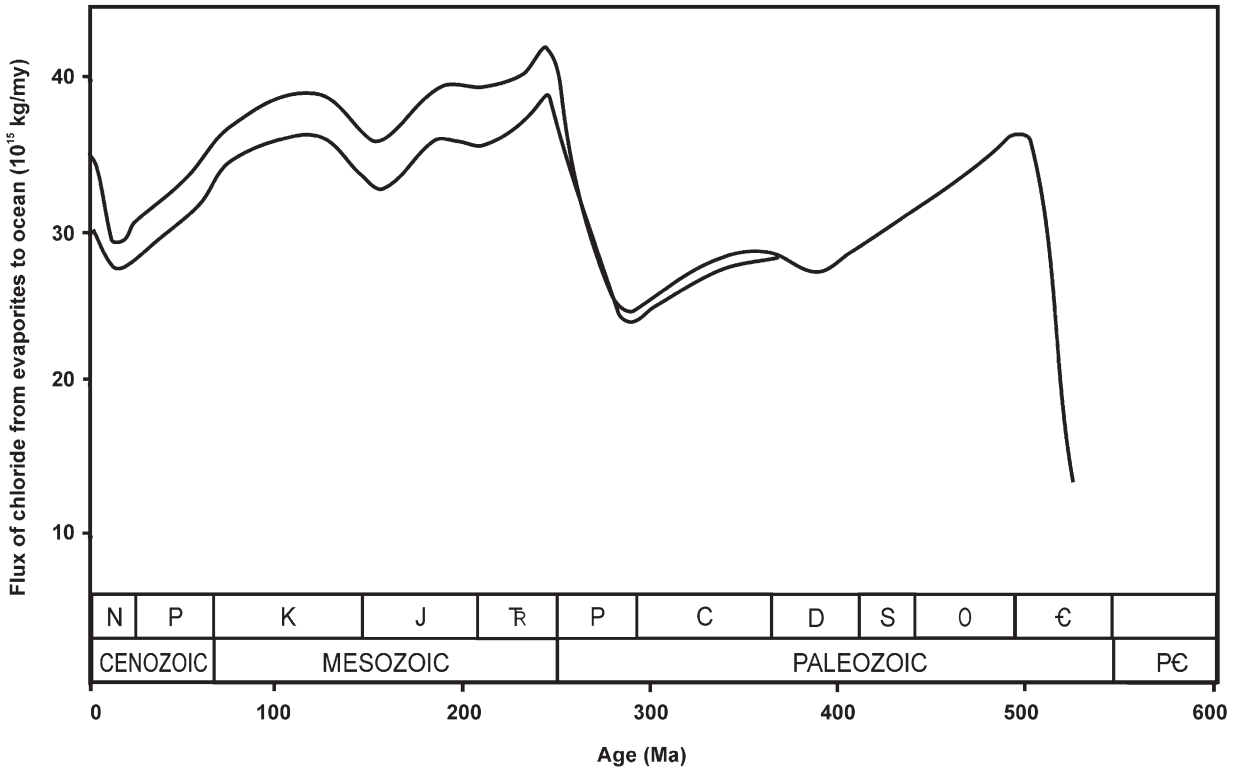

Fig. 6. Fluxes of Cl to the ocean during the Phanerozoic resulting from the erosion of evaporite deposits. Calculations based on both minimum (Tables 3, 14a) and maximum (Tables 4, 14a) estimates are shown, the upper line being based on the maximum estimates. The peaks in flux reflect general increases in erosion rates. Fluxes are maximal if high erosion rates occur in the time interval immediately after halite has been deposited on a continental block and is vulnerable to erosion before it becomes deeply buried.

would have increased the salinity of the world ocean by only slightly more than 1‰.

Table 8 summarizes two models of the amount of water in the ocean through the Phanerozoic and Late Precambrian. The first, termed model A, assumes a constant mass of free water on the surface of the Earth divided between ice sheets and the ocean. The second, model B, assumes that in addition there has been a continuous steady loss of water from the surface to the mantle through subduction at a rate of 256×10^{15} kg/my. It is important to note that Model B assumes that only H_2O and none of the salts in seawater are subducted over the long term. Tables 14a–b include these two models as part of our calculations of the past salinity of the ocean based on removal and return of Cl^-.

Table 14a is based on the existing amounts of halite in evaporite deposits using the minimum estimates of Ronov/Migdisov/Balukhovsky/Holser/Wold (Table 3). The total mass of Na^+ and Cl^- in the ocean today is $42{,}217\times10^{15}$ kg, but as shown in Table 5, there are more moles of Cl^- than there are of Na^+. Today the total chloride in the ocean is $27{,}168\times10^{15}$ kg. Including bromine, fluorine and iodine, the total halides in the ocean are $27{,}303\times10^{15}$ kg. The modern concentration of halides by weight ("chlorinity, *Cl*") is 19.22. The salinity of the ocean today is $1.80655\times Cl$. Unfortunately, this formula cannot be used to determine the salinity of the ocean in the past because it is the ratio between the total halides and the mass of seawater, which includes both H_2O and salts (Table 5). The removal of NaCl as halite into evaporite deposits and its return though dissolution with time means that the relative molar proportions of Na^+ and Cl^- in the ocean will have changed during the Phanerozoic and the relative proportions of the major anions and cations will undoubtedly have changed as well (Hardie, 1996; Stanley and Hardie, 1998; Lowenstein et al., 2001; Hardie, 2003). As a close approximation, we assume that the salinity (mass of salts:mass of seawater) of the ocean varies directly with the proportional relation between Cl^- and H_2O today in terms of mass (1:50.476).

Table 14a shows the masses of water in the ocean for the two models, A and B, through the Phanerozoic, the minimum and maximum fluxes of chlorine into and out of evaporite deposits, assuming Cl^- to be 60.7% of the

Table 14a
Masses of ocean water — models A and B [a], minimum and maximum chloride fluxes from and to the ocean, and minimum and maximum estimates of mass of chloride in the ocean

Stratigraphic unit	Age of mid-point	Length	Mass of ocean water — taking only glacial changes into account — Model A	Mass of ocean water — with both long-term trend and glacial variations — Model B	Chloride flux from ocean into evaporite deposits — minimum rate	Chloride flux from ocean into evaporite deposits — maximum rate	Chloride flux from evaporite deposits to ocean — minimum rate	Chloride flux from evaporite deposits to ocean — maximum rate	Mass of chloride in the ocean — minimum estimate	Mass of chloride in the ocean — maximum estimate
	Ma	my	10^{15} kg	10^{15} kg	10^{15} kg/my	10^{15} kg/my	10^{15} kg/my	10^{15} kg/my	10^{15} kg	10^{15} kg
Recent	0.000	0.00	1,371,346	1,371,346	0.00	0.00	29.64	34.65	27,168	27,168
Holocene	0.005	0.01	1,371,346	1,371,346	0.00	0.00	29.64	34.65	27,168	27,168
Pleistocene	0.910	1.80	1,321,626	1,321,859	0.00	0.00	29.81	34.84	27,114	27,105
Pliocene	3.570	3.52	1,373,736	1,374,649	1.53	1.53	30.41	35.55	27,012	26,985
Miocene	14.180	17.70	1,373,736	1,377,365	148.06	206.83	27.86	29.90	29,140	30,117
Oligocene	28.465	10.87	1,385,736	1,393,020	3.77	3.77	29.10	31.24	28,864	29,818
Eocene	44.850	21.90	1,395,736	1,407,213	1.01	1.01	30.53	32.77	28,218	29,123
Paleocene	60.650	9.70	1,395,736	1,411,257	0.70	0.70	32.35	34.73	27,911	28,793
Late Cretaceous	82.550	34.10	1,395,736	1,416,861	2.21	2.71	35.39	37.95	26,780	27,591
Early Cretaceous	122.550	45.90	1,395,736	1,427,097	27.65	99.06	36.64	39.50	26,367	30,325
Late Jurassic	153.350	15.70	1,395,736	1,434,979	294.71	294.71	33.37	36.44	30,470	34,379
Middle Jurassic	168.400	14.40	1,395,736	1,438,831	21.37	21.37	34.21	37.45	30,285	34,148
Early Jurassic	187.600	24.00	1,395,736	1,443,744	102.45	102.45	36.40	39.88	31,870	35,649
Late Triassic	213.800	28.40	1,395,736	1,450,449	35.19	35.19	36.05	39.80	31,846	35,518
Middle Triassic	236.500	17.00	1,395,736	1,456,258	3.78	18.51	37.81	40.97	31,267	35,136
Early Triassic	248.000	6.00	1,395,736	1,459,201	20.08	20.08	38.88	42.17	31,155	35,004
Late Permian	260.800	19.60	1,395,736	1,462,477	119.07	164.99	33.64	34.22	32,829	37,567
Early Permian	284.800	28.40	1,375,736	1,448,619	123.25	123.25	24.94	25.56	35,621	40,341
M and L Carboniferous	308.550	19.10	1,370,736	1,449,697	23.12	23.12	25.68	26.36	35,572	40,279
Early Carboniferous	338.650	41.10	1,390,736	1,477,400	3.96	3.96	27.82	28.57	34,591	39,268
Late Devonian	372.250	26.10	1,395,736	1,490,998	19.88	29.35	28.53	28.55	34,366	39,289
Middle Devonian	391.400	12.20	1,395,736	1,495,899	67.33	67.33	27.48	27.50	34,852	39,775
Early Devonian	406.750	18.50	1,395,736	1,499,827	0.25	0.58	28.81	28.81	34,323	39,253
Late Silurian	422.100	12.20	1,395,736	1,503,755	10.96	10.96	29.73	29.73	34,094	39,024
Early Silurian	435.950	15.50	1,395,736	1,507,300	0.00	0.00	31.16	31.16	33,611	38,541
Late Ordovician	452.300	17.20	1,395,736	1,511,484	0.00	0.00	32.66	32.66	33,050	37,979
Middle Ordovician	466.350	10.90	1,395,736	1,515,079	13.89	13.89	33.62	33.62	32,834	37,764
Early Ordovician	480.050	16.50	1,390,736	1,513,585	0.00	0.00	35.14	35.14	32,255	37,184
Late Cambrian	494.650	12.70	1,395,736	1,522,322	3.04	3.04	36.52	36.52	31,830	36,759
Middle Cambrian	507.000	12.00	1,395,736	1,525,482	69.05	69.05	35.77	35.77	32,229	37,158
Early Cambrian	527.500	29.00	1,395,736	1,530,728	269.51	269.51	13.84	13.84	39,643	44,573

[a] From Table 8.

weight of the halite, and minimum and maximum estimates of the mass of chloride in the ocean. Table 14b shows the minimum and maximum estimates of the total mass of salts in the ocean assuming the total mass of salts to be 1.81558 times the mass of chloride, the minimum and maximum estimates of the mass of seawater, and minimum and maximum estimates of salinity for water models A and B.

Fig. 7 summarizes these results for both the minimum and maximum models. The short-dash lines are the minimum and maximum estimates of salinity assuming water model A, with no loss of water to the mantle. The upper solid line is the average of these values. The long-dash lines are the minimum and maximum estimates of salinity assuming water model B, with loss only of water to the mantle. The lines slope sharply downward toward the present as extractions occurred, and slope gently upward toward present as evaporite deposits are eroded and salts returned to the ocean. Glaciations have little effect except for the Late Palaeozoic where they cause a broad depression in the lines, and for the Neogene. There were significantly

Table 14b
Mass of salts in the ocean, masses of seawater for ocean water models A and B, and minimum and maximum salinities calculated for ocean water models A and B

Stratigraphic unit	Age of mid-point	Length	Mass of salts in ocean — minimum estimate	Mass of salts in ocean — maximum estimate	Mass of seawater — Model A — minimum estimate	Mass of seawater — Model A — maximum estimate	Salinity — Model A minimum estimate	Salinity — Model A maximum estimate	Mass of seawater — Model B — minimum estimate	Mass of seawater — Model B — maximum estimate	Salinity — Model B minimum estimate	Salinity — Model B maximum estimate
	Ma	my	10^{15} kg	10^{15} kg	10^{15} kg	10^{15} kg			10^{15} kg	10^{15} kg		
Recent	0.000	0.00	49,326	49,326	1,420,672	1,420,672	34.72	34.72	1,420,672	1,420,672	34.72	34.72
Holocene	0.005	0.01	49,325	49,325	1,420,671	1,420,671	34.72	34.72	1,420,671	1,420,671	34.72	34.72
Pleistocene	0.910	1.80	49,228	49,212	1,370,854	1,370,837	35.91	35.90	1,371,087	1,371,070	35.90	35.89
Pliocene	3.570	3.52	49,043	48,994	1,422,779	1,422,730	34.47	34.44	1,423,693	1,423,643	34.45	34.41
Miocene	14.180	17.70	52,906	54,680	1,426,642	1,428,416	37.08	38.28	1,430,270	1,432,044	36.99	38.18
Oligocene	28.465	10.87	52,406	54,138	1,438,1,42	1,439,874	36.44	37.60	1,445,426	1,447,158	36.26	37.41
Eocene	44.850	21.90	51,232	52,875	1,446,968	1,448,611	35.41	36.50	1,458,446	1,460,088	35.13	36.21
Paleocene	60.650	9.70	50,675	52,276	1,446,411	1,448,011	35.04	36.10	1,461,932	1,463,532	34.66	35.72
Late Cretaceous	82.550	34.10	48,621	50,094	1,444,357	1,445,829	33.66	34.65	1,465,482	1,466,955	33.18	34.15
Early Cretaceous	122.550	45.90	47,872	55,057	1,443,607	1,450,793	33.16	37.95	1,474,969	1,482,154	32.46	37.15
Late Jurassic	153.350	15.70	55,321	62,419	1,451,057	1,458,155	38.12	42.81	1,490,301	1,497,398	37.12	41.68
Middle Jurassic	168.400	14.40	54,986	61,998	1,450,721	1,457,734	37.90	42.53	1,493,816	1,500,829	36.81	41.31
Early Jurassic	187.600	24.00	57,864	64,725	1,453,599	1,460,461	39.81	44.32	1,501,608	1,508,469	38.53	42.91
Late Triassic	213.800	28.40	57,819	64,487	1,453,555	1,460,223	39.78	44.16	1,508,268	1,514,936	38.33	42.57
Middle Triassic	236.500	17.00	56,769	63,793	1,452,505	1,459,529	39.08	43.71	1,513,027	1,520,052	37.52	41.97
Early Triassic	248.000	6.00	56,564	63,553	1,452,300	1,459,288	38.95	43.55	1,515,766	1,522,754	37.32	41.74
Late Permian	260.800	19.60	59,604	68,206	1,455,340	1,463,942	40.96	46.59	1,522,081	1,530,683	39.16	44.56
Early Permian	284.800	28.40	64,673	73,243	1,440,409	1,448,979	44.90	50.55	1,513,292	1,521,862	42.74	48.13
M and L Carboniferous	308.550	19.10	64,584	73,131	1,435,320	1,443,867	45.00	50.65	1,514,281	1,522,828	42.65	48.02
Early Carboniferous	338.650	41.10	62,804	71,294	1,453,539	1,462,030	43.21	48.76	1,540,203	1,548,694	40.78	46.04
Late Devonian	372.250	26.10	62,394	71,333	1,458,130	1,467,068	42.79	48.62	1,553,392	1,562,331	40.17	45.66
Middle Devonian	391.400	12.20	63,276	72,215	1,459,012	1,467,950	43.37	49.19	1,559,175	1,568,114	40.58	46.05
Early Devonian	406.750	18.50	62,317	71,267	1,458,053	1,467,002	42.74	48.58	1,562,144	1,571,094	39.89	45.36
Late Silurian	422.100	12.20	61,901	70,851	1,457,637	1,466,587	42.47	48.31	1,565,657	1,574,606	39.54	45.00
Early Silurian	435.950	15.50	61,024	69,974	1,456,760	1,465,710	41.89	47.74	1,568,324	1,577,274	38.91	44.36
Late Ordovician	452.300	17.20	60,004	68,954	1,455,740	1,464,690	41.22	47.08	1,571,488	1,580,438	38.18	43.63
Middle Ordovician	466.350	10.90	59,614	68,563	1,455,350	1,464,299	40.96	46.82	1,574,693	1,583,643	37.86	43.29
Early Ordovician	480.050	16.50	58,561	67,511	1,449,297	1,458,247	40.41	46.30	1,572,147	1,581,096	37.25	42.70
Late Cambrian	494.650	12.70	57,789	66,739	1,453,525	1,462,475	39.76	45.63	1,580,111	1,589,061	36.57	42.00
Middle Cambrian	507.000	12.00	58,514	67,464	1,454,250	1,463,200	40.24	46.11	1,583,996	1,592,946	36.94	42.35
Early Cambrian	527.500	29.00	71,976	80,926	1,467,712	1,476,661	49.04	54.80	1,602,704	1,611,654	44.91	50.21

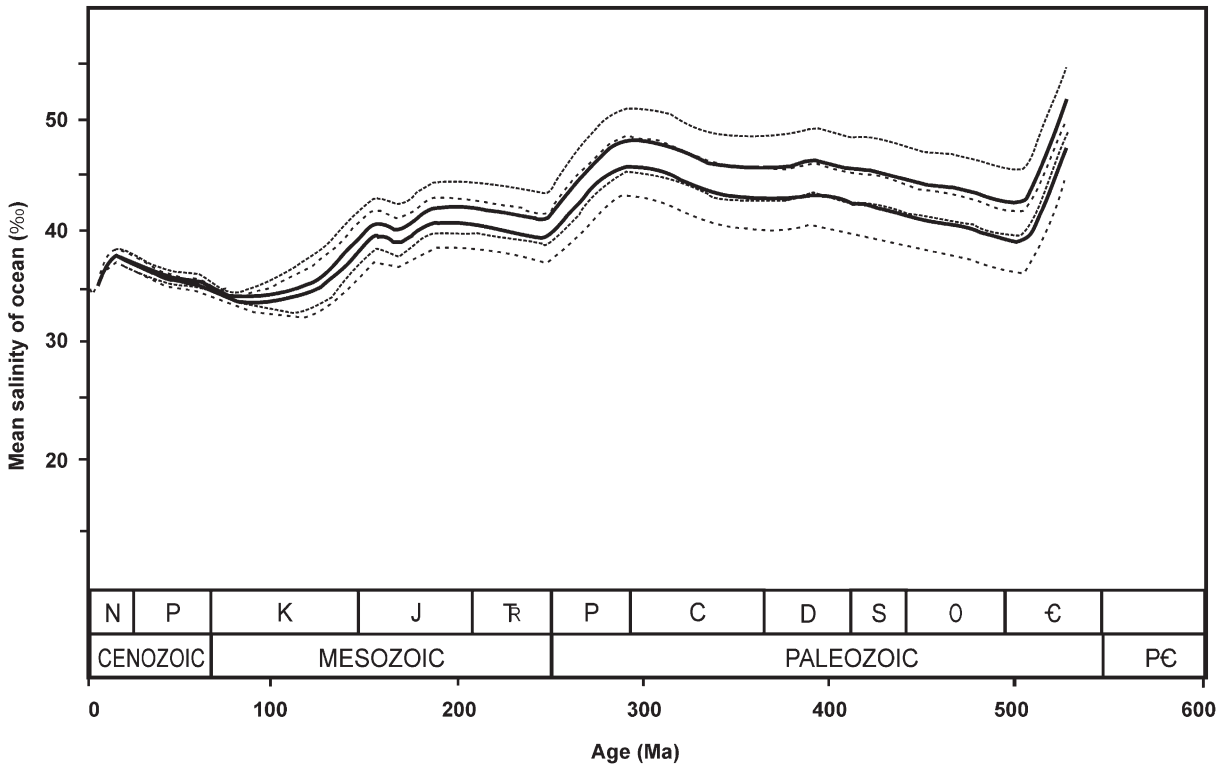

Fig. 7. Four models reconstructing the mean salinity of the ocean during the Phanerozoic. The short-dashed lines are the maximum and minimum estimates based on water Model A (no loss of water through subduction); the upper solid line is the average for Model A. The long-dashed lines are the maximum and minimum estimates based on water Model B (water steadily lost through subduction); the lower solid line is the average for Model B. In the Palaeozoic, the average for Model A nearly coincides with the maximum for Model B, and the average for Model B nearly coincides with the minimum for Model A.

higher salinities in the early Neogene after initiation of the glaciation of Antarctica and before the extractions into the Persian Gulf, Red Sea, Mediterranean and Carpathian regions. The maximum and minimum evaporite models diverge in the Mesozoic, primarily because of the uncertainties involved in estimating the size of the salt deposits in young ocean basins. The large decline in ocean salinity through the Mesozoic is related to the major salt extractions into the Gulf of Mexico and Atlantic, and indicate that in the early Mesozoic salinities would have been in the high 30's to low 40's (‰) depending on the minimum or maximum evaporite model. Palaeozoic salinities were in the low to high 40's and reached the 50's (‰) in the Early Cambrian, depending on the evaporite data. Water mass model B reduces the salinities by about 5‰ for both maximum and minimum evaporite models. Assuming that salts were subducted along with the water would bring the salinities back up almost to the level of the constant water mass model A, implying only a change in the mass of seawater. There would be a small difference because the seawater subducted early in the Phanerozoic would have been somewhat more saline than that in the later Phanerozoic.

8. Implications

Salinity and temperature affect a number of the physical properties of seawater, including its density, specific heat, saturation vapor pressure, and osmotic pressure. The largest effects are related to the density where there is a complex interplay between temperature and salinity. These relationships are described by the equation of state for seawater (Millero et al., 1980; Millero and Poisson, 1981), which is highly non-linear. The Millero et al. (1980) and Millero and Poisson (1981) equation of state is a polynomial with 17 terms, one of which is the bulk modulus. The bulk modulus is described by another polynomial with 25 terms. This equation of state is thought to be valid for the range T= −7 °C–50 °C and S=0–60‰ (Millero, personal communication). Salinity causes only a minor effect on specific heat which decreases by about 9% from a salinity of 0‰ to 60‰. This is unlikely to have any

detectable influence on climate. Similarly, saturation vapor pressure is overwhelmingly dominated by the effect of temperature. Increased salinity lowers the saturation vapor pressure but only very slightly, so that it is unlikely to have any effect on climate. Osmotic pressure varies directly with salinity and might be expected to have a major effect on organisms.

8.1. The effect of ocean salinity differences on circulation

Rooth (1982) called attention to the fact that the mean salinity of the ocean has profound implications for the behavior of the ocean. To understand the implications of differences in mean ocean salinity for the thermohaline circulation, one needs to only consider what would happen if the salinity of the ocean were significantly lower than it is today. Fig. 8 is a graphical representation of the equation of state for seawater (Millero and Poisson, 1981). Below a salinity of 27.4‰, the maximum density of seawater lies above the freezing point, and it behaves like fresh water in that the coldest water will float. This in fact occurs today along the Arctic shelf off Siberia, so that region has become the "ice factory" from the Arctic Ocean. In geologic perspective polar regions with lower than average salinities could become excluded as major sites of deep water formation even if they are very cold. This situation has existed periodically in the Arctic since the Arctic Ocean Basin became isolated from the Pacific in the Cretaceous (see palaeogeographic maps of Kazmin and Napatov, 1998). By contrast, for seawater with salinities greater than 27.4‰, the maximum density lies below the freezing point. It might be expected that ice formation could not occur unless the entire ocean was chilled to the freezing point, but near the freezing point salinity plays a critical role. It is thought that sea-ice formation in the open ocean requires freshening of a minute surface layer, probably through precipitation in the form of snowflakes. The snowflakes themselves can serve as nuclei for ice formation.

With present day ocean salinities, density changes due to temperature become very small as the freezing point is approached. At salinities of 30–35‰ the maximum density of seawater is just below the freezing point. The temperature change as the seawater cools from 0EC to the freezing point (about −2EC) has almost no effect on its density. As a result of this peculiar situation the formation of sea ice becomes an important factor in increasing the density of sea water. Sea ice initially has a salinity of about 7‰, so that as it freezes salt is expelled into the surrounding water, increasing its density. For this reason, most of the high latitude sites where deep water is generated involve sea-ice formation.

The temperature–salinity–density relation becomes significantly different when ocean salinities are significantly higher than at present. When the salinity reaches

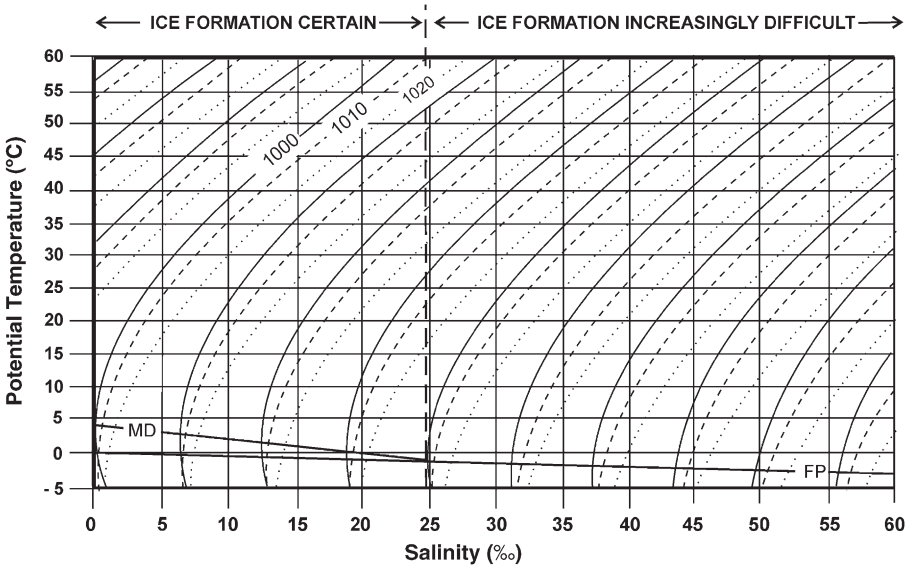

Fig. 8. Graphical representation of the equation of state of seawater showing the relation between temperature, salinity, pressure, and density. Solid lines are density at the surface beneath one atmosphere of pressure. Long-dashed lines are density at a pressure of 2000 dbar (=depth of approximately 2 km). Short-dashes lines are density at a pressure of 4000 dbar (=depth of approximately 4 km). After Millero et al. (1980), and Millero and Poisson (1981). See text for discussion.

40‰, the density curve never approaches the vertical, but slopes down to the freezing point. This means that the densest water in the ocean will be the coldest water. As the salinity increases, temperature becomes more and more dominant in controlling the density of seawater. This has profound implications for formation of high-latitude bottom waters in the past.

Another factor that plays an important role in deep water formation is the way in which its volume changes in response to pressure changes, sometimes termed compressivity. This is described by its bulk modulus, which is a strongly non-linear function (Millero and Poisson, 1981) that is required for the equation of state to determine the density of seawater below the sea surface. Like the density, the bulk modulus changes with both temperature and salinity. Fig. 8 shows the isopycnals (density lines) for the surface, 2000 dbar and 4000 dbar, corresponding approximately to depths of 2 and 4 km. The isopycnals are almost parallel at temperatures above 20EC. However, they converge at cooler temperatures. The convergence is the expression of the fact that colder water is more compressible than warmer water even if the temperature differences are very small. This phenomenon is very important in deep water formation in the ocean today. As two surface waters having the same density but slightly different temperatures begin to sink, the cooler water will be compressed more rapidly. Hence its density will become greater and it will "win the race" to the bottom, and will become the bottom water. The warmer water will stop sinking at an intermediate level. The compressibility also changes with salinity; as shown in Fig. 8 the salinity increases, the surface, 2000 dbar and 4000 dbar lines become more parallel as they approach the freezing point. At higher salinities the difference in compressibility of colder water becomes less important in deep water formation.

Today the thermohaline circulation is driven by small density differences (Hay, 1993) and this has undoubtedly been true in the past. Today, formation of the deep waters that drive thermohaline circulation requires a density increase through salinization, and this involves phase changes. At high latitudes this salinization results from the phase change from seawater to sea ice, and involves about 0.34×10^6 J/kg. Dense water can also form at low latitudes, as in the Mediterranean today. There it involves salinization through evaporation; the phase change is from water to vapor and involves about 2.5×10^6 J/kg. At higher salinities deep water formation can be achieved simply by cooling the water, which requires only 0.0042×10^6 J/kg.

Changing mean ocean salinity implies significant changes in the thermohaline circulation. If salinization is not required to produce deep water, the energy required by the phase changes at the atmosphere–ocean surface is eliminated. The phase changes required to increase seawater density today act as a flywheel on the ocean–atmosphere system, consuming energy and thereby slowing down the rate at which deep water formation can take place. At higher ocean salinities these phase changes are not required, and much less energy is needed to drive the thermohaline circulation. A more saline ocean could convect much more readily than it does today.

8.2. The effect of salinity on marine life

Many palaeontologists assume that conditions in the ocean have remained much as they are today, but some obvious changes have occurred. Stanley and Hardie (1998, 1999) have described the alternations between calcite and aragonite secreting organisms through the Phanerozoic, attributed to changing relative proportions of Ca^{2+} and Mg^{2+} in seawater. However, it has generally been assumed that most marine organisms cannot tolerate salinities much higher that those of the open ocean today. Interestingly, coral reefs in the northern part of the Red Sea are among the most diverse on Earth in terms of both corals and fish (Schuhmacher, 1991). Today they thrive in salinities ranging between 41‰ and 43‰, and their ancestors must have survived even higher salinities during the Last Glacial Maximum. It may be that at present many marine animals and plants are living nearer their low salinity tolerance limit rather than their high limit.

Palaeozoic fossils present a special opportunity to explore the hypothesis that ocean salinities then were significantly higher than today. There are very few Palaeozoic fossils, such as inarticulate brachiopod *Lingula*, that have modern counterparts, and those are almost always found in peculiar environments. It must be recalled that the fossil record prior to the Jurassic is almost exclusively from epeiric and shelf seas. These areas are fundamentally different from open ocean in that their salinity depends on local fresh water balance. The fresh water balance is an expression of the supply of fresh water through precipitation and runoff and loss of water to evaporation. Fresh water balance is negative in mid-latitudes where it is reflected in deserts on land and higher salinity marginal seas such as the Mediterranean. Fresh water balance is positive at high latitudes where marginal seas such as the Baltic and Hudson Bay have low salinities. The epeiric seas of the geologic past,

some of which have very diverse assemblages of fossils probably reflect abnormal conditions, having salinities either higher or lower than the mean of the world ocean at the time.

The best record of oceanic salinity would be in pelagic deposits, but these are almost unknown for the early Mesozoic and Palaeozoic. As far as is known, acritarchs were a major constituent of the Palaeozoic ocean plankton, but are rare in younger deposits (Mendelson, 1993). The evolution of the calcareous nannoplankton (Brown et al., 2004) fits well with the hypothesized decline in ocean salinity during the Mesozoic. Jurassic calcareous nannoplankton are mostly found in shelf deposits, and the invasion of the ocean proper seems to have occurred in mid- and Late Cretaceous. The planktonic foraminifera have a similar history (Culver, 1993). One peculiar group is the Radiolaria, which are known from the Cambrian on. Curiously Palaeozoic radiolaria are known from shallow water deposits (Casey, 1993), whereas today they are strictly inhabitants of the open ocean.

There is a question why the organic carbon-rich deposits of the Late Jurassic and Early Cretaceous are such prolific producers of petroleum. The coincidence of petroleum-prone organic carbon-rich deposits and sharply declining ocean salinity may not be unrelated. In many instances Cyanobacteria are important contributors of organic carbon in these deposits. It may be that the rapidly declining salinities of these times, when very large salt extractions were occurring in the Gulf of Mexico and South Atlantic, were instrumental in favoring an abundance of these organisms.

9. Summary and conclusions

The reconstructions presented here closely resemble those that have been published previously based on less complete data (Holser et al., 1980; Hay and Wold, 1997; Hay et al., 1998; Floegel et al., 2000; Hay et al., 2001). The data suggest that there have been significant changes in the mean salinity of the ocean during the Phanerozoic. The biggest changes are related to major extractions of salt into the young ocean basins which developed as Pangaea broke apart. Unfortunately, these salt deposits are the least well known. The last big extractions were those of the Miocene, and they occurred just after there had been a large scale extraction of water from the ocean to form the ice cap of Antarctica. However, these two modifications of the masses of H_2O and salt in the ocean followed in sequence and did not cancel each other out. Accordingly, salinities during the Early Miocene were between 37‰ and 39‰.

The Mesozoic was a time of generally declining salinity associated with the deep sea salt extractions of the North Atlantic and Gulf of Mexico (Middle to Late Jurassic) and South Atlantic (Early Cretaceous). Although none of these salt layers have been penetrated by drilling, the extent and thickness of salt in the Gulf of Mexico is relatively well known. The thin edge of that in the South Atlantic has been drilled along the Brazilian margin, but is known to thicken offshore. The North Atlantic salt deposits are known only though seismic interpretation. The decline in salinity corresponds closely to the evolution of both planktonic foraminifera and calcareous nannoplankton. Both groups were restricted to shelf regions and in the Jurassic and early Cretaceous, but spread into the open ocean in the mid-Cretaceous. Their availability to inhabit the open ocean may be directly related to the decline in salinity.

The earliest of the major extractions of the Phanerozoic occurred during the Permian and involved both halite and unusually large amounts of gypsum/anhydrite. These may have created stress for marine organisms and may have been a factor contributing to the end-Permian extinction. There were few major extractions of salt during the Palaeozoic. The models suggest that this was a time of relatively stable but slowly increasing salinities ranging through the upper 30 and low 40‰ range into the lower 50‰ concentrations in the Early Cambrian.

The modeling suggests that there was a major salinity decline from the Late Precambrian to the Cambrian, and it is tempting to speculate that this may have been a factor in the Cambrian explosion of life. However, the Late Precambrian salt deposits of the Hormuz region cannot be precisely dated, and the apparent sharp decline before the Cambrian may be an artifact of the lack of better information.

The largest uncertainties in the reconstruction of past ocean salinities lie first in the knowledge of the history of water on Earth. Has the mass of free water remained nearly constant or has it grown or decreased with time? Is the recycling of saline basin waters significant? How much of the salt in subducted seawater is returned to the ocean? Is there a steady flux of juvenile chlorine from the mantle, or a steady loss to the mantle? Are the deep sea deposits of salt as large as we think, or are there possible other deep sea deposits that remain undiscovered? Is there an unknown mechanism for regulating the salinity of the ocean? The answers to these questions must lie in innovative new approaches to understanding the history of seawater.

Acknowledgements

This work was carried out with the support from the Deutsche Forschungsgemeinschaft through grant HA 2891/1-2. We thank Robert Berner and Klaus Wallmann for thoughtful reviews and helpful suggestions.

References

Allen, P.A., 1997. Earth Surface Processes. Blackwell Science, Oxford.

Anderson, A.T., 1974. Chlorine, sulfur, and water in magmas and oceans. Geological Society of America Bulletin 85, 1485–1492.

Bartels, O.G., 1972. An estimate of volcanic contributions to the atmosphere and volcanic gases and sublimates as the source of radioisotopes ^{10}Be, ^{35}S, ^{32}P, and ^{23}Na. Health Physics 22, 387–392.

Berner, R.A., 2004. A model for calcium, magnesium and sulfate in seawater over Phanerozoic time. American Journal of Science 304, 438–453.

Berner, E.K., Berner, R.A., 1987. The Global Water Cycle: Geochemistry and Environment. Prentice-Hall, Englewood Cliffs, N.J.

Brown, J., Colling, A., Park, D., Phillips, J., Rothery, D., Wright, J., 1989. Seawater: Its Composition, Properties and Behaviour. Open University, Pergamon Press, Oxford.

Brown, P.R., Lees, J.A., Young, J.R., 2004. Calcareous nannoplankton evolution and diversity through time. In: Thierstein, H.R., Young, J.R. (Eds.), Coccolithophores — from Molecular Processes to Global Impact. Springer Verlag, Berlin, pp. 481–508.

Budyko, M.I., Ronov, A.B., Yanshin, A.L., 1987. History of the Earth's Atmosphere. Springer-Verlag, New York.

Burke, K., 1975. Atlantic evaporites formed by evaporation of water spilled from Pacific, Tethyan, and Southern Oceans. Geology 3, 613–616.

Burke, K., Sengor, A.M., 1988. Ten metre sea-level change associated with South Atlantic Aptian salt deposition. Marine Geology 83, 309–312.

Casey, R.E., 1993. Radiolaria. In: Lipps, J.H. (Ed.), Fossil Prokaryotes and Protists. Blackwell Scientific Publications, Oxford, pp. 249–284.

Correns, C.W., 1956. The geochemistry of the halogens. In: Ahrens, L.H., Rankama, K., Runcorn, S.K. (Eds.), Physics and Chemistry of the Earth, vol. 1. Pergamon Press, London, pp. 181–233.

Culver, S.J., 1993. Foraminifera. In: Lipps, J.H. (Ed.), Fossil Prokaryotes and Protists. Blackwell Scientific Publications, Oxford, UK, pp. 203–247.

Denton, G.H., Hughes, T.J., 1981a. The Last Great Ice Sheets. Wiley Interscience, New York.

Denton, G.H., Hughes, T.J., 1981b. The Arctic ice sheet: an outrageous hypothesis. In: Denton, G.H., Hughes, T.J. (Eds.), The Last Great Ice Sheets. Wiley Interscience, New York, pp. 437–467.

Drever, J.I., 1982. The Geochemistry of Natural Waters. Prentice-Hall, Englewood Cliffs, NJ.

Drever, J.I., Li, Y.-H., Maynard, J.B., 1988. Geochemical cycles: the continental crust and the oceans. In: Gregor, C.B., Garrels, R.M., Mackenzie, F.T., Maynard, J.B. (Eds.), Chemical Cycles in the Evolution of the Earth. John Wiley & Sons, New York, pp. 17–53.

Duplessy, J.C., Labeyrie, L., Juillet-Leclerc, A., Maitre, F., Duprat, J., Sarnthein, M., 1991. Surface salinity reconstruction of the North Atlantic Ocean during the last glacial maximum. Oceanologica Acta 14, 311–324.

Duplessy, J.C., Bard, E., Labeyrie, L., Duprat, J., Moyes, J., 1993. Oxygen isotope records and salinity changes in the northeastern Atlantic Ocean during the last 18,000 years. Paleoceanography 8, 341–350.

Einsele, G., 1992. Sedimentary Basins: Evolution, Facies, and Sediment Budget. Springer-Verlag, New York.

Emiliani, C., 1992. Planet Earth. Cambridge University Press, Cambridge, UK.

Ewing, W.M., Worzel, J.L., Burk, C.A., 1969. Regional aspects of deep water drilling in the Gulf of Mexico, east of the Bahama Platform, and on the Bermuda Rise. In: Ewing, W.M., Worzel, J.L., Beall, A.O., Berggren, W.A., Bukry, J.D., Burk, C.A., Fischer, A. G., Pessagno Jr., E.A. (Eds.), Initial Reports of the Deep Sea Drilling Project, vol. 1, pp. 624–640.

Feth, J.H., 1981. Chloride in natural continental water — a review. U. S. Geological Survey Water-Supply Paper 2176, 1–30.

Flint, R.F., 1971. Glacial and Quaternary Geology. John Wiley & Sons, New York.

Floegel, S., Wold, C.N., Hay, W.W., 2000. Evolution of sediments and ocean salinity. Abstracts Volume, 31st International Geological Congress, Rio de Janeiro — Brazil, August 6–17, 2000. 4 pp., CD-ROM.

Frank, L.A., Sigwarth, J.B., 2001. Detection of small comets with a ground-based telescope. Journal of Geophysical Research 106, 3665–3683.

Frank, L.A., Sigwarth, J.B., Craven, J.D., 1986. On the influx of small comets into the Earth's upper atmosphere: I. Observations. Geophysical Research Letters 13, 303–306.

Garrels, R.M., Mackenzie, F., 1971. Evolution of Sedimentary Rocks. W. W. Norton, New York.

Gill, R., 1989. Chemical Fundamentals of Geology. Unwin Hyman, London.

Gilluly, J., 1969. Geological perspective and the completeness of the geologic record. Geological Society of America Bulletin 80, 2303–2312.

Gradstein, F.M., Ogg, J., 1996. A Phanerozoic time scale. Episodes 19, 3–5.

Gradstein, F.M., Ogg, J.G., Smith, A.G., Agterberg, F.P., Bleeker, W., Cooper, R.A., Davydov, V., Gibbard, P., Hinnov, L., House, M.R., Lourens, L., Luterbacher, H.-P., McArthur, J., Melchin, M.J., Robb, L.J., Shergold, J., Villeneuve, M., Wardlaw, B.R., Ali, J., Brinkhuis, H., Hilgen, F.J., Hooker, J., Howarth, R.J., Knoll, A.H., Laskar, J., Monechi, S., Powell, J., Plumb, K.A., Raffi, I., Röhl, U., Sanfilippo, A., Schmitz, B., Shackleton, N.J., Shields, G.A., Strauss, H., Van Dam, J., Veizer, J., van Kolfschoten, Th., Wilson, D., 2004. A Geologic Time Scale 2004. Cambridge University Press, Cambridge, UK.

Hallam, A., 1992. Phanerozoic Sea-level Changes. Columbia University Press, New York.

Hardie, L.A., 1996. Secular variation in seawater chemistry: an explanation for the coupled secular variation in the mineralogies of marine limestones and potash evaporites over the past 600 m.y. Geology 24, 279–283.

Hardie, L.A., 2003. Secular variations in Precambrian seawater chemistry and the timing of Precambrian aragonite seas and calcite seas. Geology 31, 785–788.

Hay, W.W., 1993. The role of polar deep water formation in global climate change. Annual Review of Earth and Planetary Sciences 21, 227–254.

Hay, W.W., 1994. Pleistocene–Holocene fluxes are not the Earth's norm. In: Hay, W.W. (Ed.), Material Fluxes on the Surface of the Earth. National Academy Press, Washington, D.C., pp. 15–27.

Hay, W.W., 1999. Carbonate sedimentation through the late Precambrian and Phanerozoic. Zentralblatt für Geologie und Paläontologie, Teil I, 1998, Heft 5–6, 435–445.

Hay, W.W., Leslie, M.A., 1990. Could possible changes in global groundwater reservoir cause eustatic sea-level fluctuations. In: Revelle, R. (Ed.), Sea-Level Change. National Academy Press, Washington, D.C., pp. 161–170.

Hay, W.W., Wold, C.N., 1997. Preliminary reconstruction of the salinity of the ocean in the Cenozoic and Mesozoic. Freiberger Forschungshefte, C 468 Geowissenschaften-Paläontologie, Paläontologie, Stratigraphie, Fazies, Heft 5, Karl-Armin-Tröger-Festschrift, 119–127.

Hay, W.W., Sloan II, J.L., Wold, C.N., 1988. The mass/age distribution of sediments on the ocean floor and the global rate of loss of sediment. Journal of Geophysical Research 93, 14933–14940.

Hay, W.W., Wold, C.N., DeConto, R.M., 1998. The role of salinity in circulation of the Cretaceous ocean. Zentralblatt für Geologie und Paläontologie 1996 (11/12), 1445–1454.

Hay, W.W., Wold, C.N., Söding, E., Flögel, S., 2001. Evolution of sediment fluxes and ocean salinity. In: Merriam, D.F., Davis, J.C. (Eds.), Geologic Modeling and Simulation: Sedimentary Systems. Kluwer Academic/Plenum Publishers, Dordrecht, The Netherlands, pp. 153–167.

Holland, H.D., 1974. Marine evaporites and the composition of sea water during the Phanerozoic. In: Hay, W.W. (Ed.), Studies in Paleo-Oceanography. Society of Economic Paleontologists and Mineralogists Special Publication, vol. 20. Society of Economic Paleontologists and Mineralogists, Tulsa, Oklahoma, pp. 187–192.

Holland, H.D., 1978. The Chemistry of the Atmosphere and Oceans. Wiley, New York.

Holland, H.D., 1984. The Chemical Evolution of the Atmosphere and Oceans. Princeton University Press, Princeton, NJ.

Holser, W.T., 1977. Catastrophic chemical events in the history of the ocean. Nature 267, 403–498.

Holser, W.T., 1985. Gradual and abrupt shift in ocean chemistry during Phanerozoic time. In: Holland, H.D., Trendall, A.F. (Eds.), Patterns of Change in Earth Evolution. Dahlem Konferenzen 1984. Springer Verlag, Berlin, Germany, pp. 123–143.

Holser, W.T., Hay, W.W., Jory, D.E., O'Connell, W.J., 1980. A census of evaporites and its implications for oceanic geochemistry. Abstracts with Programs - Geological Society of America 12/7, 449.

Humphris, S.E., McCollom, T., 1998. The cauldron beneath the sea floor. Oceanus 18/2, 18–21.

Japakasetr, T., Workman, D.R., 1981. Evaporite deposits of Thailand. In: Halbouty, M.T. (Ed.), Energy Resources of the Pacific Region. American Association of Petroleum Geologists, Tulsa, Oklahoma, pp. 179–187.

Joly, J., 1899. An estimate of the geological age of the Earth. Transactions of the Royal Society of Dublin 2 (7), 23–66.

Joly, J., 1925. The Surface History of the Earth. Clarendon Press, Oxford, UK.

Junge, C.E., Werby, R.T., 1958. The concentration of chloride, sodium, potassium, calcium, and sulfate in rain water over the United States. Journal of Meteorology 15, 417–425.

Kazmin, V.G., Napatov, L.M. (Eds.), 1998. The Paleogeographic Atlas of Northern Eurasia. Institute of Tectonics of the Lithospheric Plates, Russian Academy of Natural Sciences, Moscow, Russia.

Knauth, L.P., 1998. Salinity history of the Earth's early ocean. Nature 395, 554–555.

Knauth, L.P., 2005. Temperature and salinity history of the Precambrian ocean: implications for the course of microbial evolution. Palaeogeography, Palaeoclimatology, Palaeoecology 219, 53–69.

Kurlansky, M., 2002. Salt — A World History. Walker and Company, New York.

Land, L.S., 1995. The role of saline formation water in crustal cycling. Aquatic Geochemistry 1, 137–145.

Lisitzin, A.P., 1974. Osadkovrazovanie v Okeanach. Izdatelstvo "Nauka", USSR, Moscow.

Livingston, D.A., 1963. Chemical composition of rivers and lakes, Chapter G. In: Fleischer, M. (Ed.), Data of Geochemistry. U.S. Geological Survey Professional Paper, vol. 440-G. 64 pp.

Lord Kelvin, W.T., 1864. On the secular cooling of the earth. Transactions of the Royal Society of Edinburgh 23, 157–170.

Lowenstein, T.K., Timofeeff, M.N., Brennan, S.T., Hardie, L.A., Demicco, R.V., 2001. Oscillations in Phanerozoic seawater chemistry: evidence from fluid inclusions. Science 294, 1086–1088.

Marcinek, J., Rosenkranz, E., 1989. Das Wasser der Erde: Lehrbuch der geographischen Meeres- und Gewässerkunde. Verlag Harri Deutsch, Thun, Switzerland.

McArthur, J.M., Howarth, R.J., Bailey, T.R., 2001. Strontium isotope stratigraphy: LOWESS Version 3: best fit to the marine Sr-isotope curve for 0–509 Ma and accompanying look-up table for deriving numerical age. Journal of Geology 109, 155–170.

Mendelson, C.V., 1993. Acritarchs and prasinophytes. In: Lipps, J.H. (Ed.), Fossil Prokaryotes and Protists. Blackwell Scientific Publications, Oxford, UK, pp. 77–104.

Meybeck, M., 1979. Concentrations des eaux fluviales en éléments majeurs et apports en solution aux océans. Revue de Géologie Dynamique et de Géographie Physique 21, 215–246.

Meybeck, M., 1983. Atmospheric inputs and river transport of dissolved substances. International Association of Hydrological Sciences Special Publication 141, 173–192.

Meybeck, M., 1987. Global chemical weathering from surficial rocks estimated from river dissolved loads. American Journal of Science 287, 401–428.

Millero, F.J., Poisson, A., 1981. International one-atmosphere equation of state for sea water. Deep-Sea Research 28A, 625–629.

Millero, F.J., Chen, C.T., Bradshaw, A., Schleicher, K., 1980. A new high pressure equation of state for seawater. Deep-Sea Research 27A, 255–264.

Mueller, R.F., Saxena, S.K., 1977. Chemical Petrology: with Applications to Terrestrial Planets and Meteorites. Springer-Verlag, New York.

Parrish, T.J., Ziegler, A.M., Scotese, C.R., 1982. Rainfall patterns and the distribution of coals and evaporites in the Mesozoic and Cenozoic. Palaeogeography, Palaeoclimatology, Palaeoecology 40, 67–101.

Railsback, L.B., Anderson, T.F., Ackerly, S.C., Cisne, J.L., 1989. Paleoceanographic modeling of temperature–salinity profiles from stable isotopic data. Paleoceanography 4, 585–591.

Rankama, K., Sahama, Th.G., 1950. Geochemistry. Chicago University Press, Chicago, Illinois, USA.

Ronov, A.B., 1968. Probable changes in the composition of seawater during the course of geologic time. Sedimentology 10, 25–43.

Ronov, A.B., 1972. Evolution of rock composition and geochemical processes in the sedimentary shell of the earth. Sedimentology 19, 157–172.

Ronov, A.B., 1980. Osadochnaya Obolochka Zemli (Kolichestvennoe Zakonomernosti Stroeniya, Sostava y Evoliutsii. Izdatelstvo "Nauka", USSR, Moskva. 78 pp.

Ronov, A.B., 1982. The earth's sedimentary shell (Quantitative patterns of its structure, compositions, and evolution). International Geology Review 24, 1365–1388.

Ronov, A.B., 1993. In: Yaroshevskii, A.A. (Ed.), Stratisfera — Ili Osadochnaya Obolochka Zemli (Kolichestvennoe Issledovanie). Nauka, Moskva. 144 pp.

Ronov, A.B., 1994. Phanerozoic transgressions and regressions on the continents: a quantitative approach based on areas flooded by the sea and areas of marine and continental deposition. American Journal of Science 294, 777–801.

Ronov, A.B., Khain, V.Y., Seslavinsky, K.B., 1984. Atlas of Lithological–Paleogeographical Maps of the World: Late Precambrian and Paleozoic of the Continents. U.S.S.R. Academy of Science Press, Leningrad.

Ronov, A.B., Khain, V.E., Balukhovsky, A.N., 1989. In: Barsukhov, V. L., Laviorov, N.P. (Eds.), Atlas of Lithological–Paleogeographical Maps of the World: Mesozoic and Cenozoic of Continents and Oceans. Editorial Publishing Group, Moscow.

Rooth, C., 1982. Hydrology and ocean circulation. Progress in Oceanography 11, 131–149.

Rubey, W.W., 1951. Geologic history of sea water. Geological Society of America Bulletin 62, 1111–1148.

Ryan, J.A., Mukherjee, N.R., 1975. Sources of atmospheric gaseous chlorine. Reviews of Geophysics and Space Physics 11, 650–658.

Sandberg, P.A., 1983. An oscillating trend in Phanerozoic nonskeletal carbonate mineralogy. Nature 305, 19–22.

Scotese, C.R., Bambach, R.K., Barton, C., Van der Voo, R., Ziegler, A., 1979. Paleozoic base maps. Journal of Geology 87, 217–277.

Shackleton, N.J., 1987. Oxygen isotopes, ice volume and sea level. Quaternary Science Reviews 6, 183–190.

Shackleton, N.J., Kennett, J.P., 1975. Paleotemperature history of the Cenozoic and the initiation of Antarctic glaciation: oxygen and carbon isotope analyses on DSDP sites 277, 279, and 281. In: Kennett, J.P., Houtz, R.E., et al. (Eds.), Initial Reports of the Deep Sea Drilling Project, vol. 29. U.S. Government Printing Office, Washington, D.C., pp. 743–755.

Schuhmacher, H., 1991. Korallenriffe — Verbreitung, Tierwelt, Ökologie. BLV Verlagsgesellschaft mbH, München, Germany.

Southam, J.R., Hay, W.W., 1981. Global sedimentary mass balance and sea level changes. In: Emiliani, C. (Ed.), The Sea, v. 7, the Oceanic Lithosphere. Wiley-Interscience, New York, pp. 1617–1684.

Stallard, R.F., Edmond, J.M., 1981. Chemistry of the Amazon, precipitation chemistry and the marine contribution to the dissolved load at the time of peak discharge. Journal of Geophysical Research 86, 9844–9858.

Stanley, S.M., Hardie, L.A., 1998. Secular oscillations in the carbonate mineralogy of reef-building and sediment-producing organisms driven by tectonically forced shifts in seawater chemistry. Palaeogeography, Palaeoclimatology, Palaeoecology 144, 3–19.

Stanley, S.M., Hardie, L.A., 1999. Hypercalcification: paleontology links plate tectonics and geochemistry to sedimentology. GSA Today 9 (2), 1–7.

Sverdrup, H.U., Johnson, M.W., Fleming, R.H., 1942. The Oceans, Their Physics, Chemistry, and General Biology. Prentice-Hall, New York.

Tardy, Y., N'kounkou, R., Probst, J.-L., 1989. The global water cycle and continental erosion during Phanerozoic time (570 my). American Journal of Science 289, 455–485.

Turekian, K.K., 1968. Oceans. Prentice-Hall, Englewood Cliffs, NJ.

Veizer, J., Jansen, S.L., 1979. Basement and sedimentary recycling and continental evolution. Journal of Geology 87, 341–370.

Veizer, J., Jansen, S.L., 1985. Basement and sedimentary cycling — 2: Time dimension to global tectonics. Journal of Geology 93, 625–664.

Von Huene, R., Scholl, D.W., 1991. Observations at convergent margins concerning sediment subduction, subduction erosion, and the growth of continental crust. Reviews of Geophysics 29, 279–316.

Wallmann, K., 2001. The geological water cycle and the evolution of marine $\delta^{18}O$ values. Geochimica et Cosmochimica Acta 65, 2469–2485.

Wilkinson, B., 2005. Humans as geologic agents: a deep-time perspective. Geology 33, 161–164.

Wold, C.N., Hay, W.W., 1990. Estimating ancient sediment fluxes. American Journal of Science 290, 1069–1089.

Wold, C.N., Hay, W.W., 1993. Reconstructing the age and lithology of eroded sediment. Geoinformatics 4, 137–144.

Wold, C.N., Schwartz, G.J., Morrill, C., 1999. Digital database of modern evaporites and their predicted distribution based on results from an atmospheric general circulation model simulation. In: Harff, J., Lemke, W., Stattegger, K. (Eds.), Computerized Modeling of Sedimentary Systems. Springer, Berlin, pp. 149–167.

Zachos, J.C., Stott, L.D., Lohmann, K.C., 1994. Evolution of early Cenozoic marine temperatures. Paleoceanography 9, 353–387.

Zharkov, M.A., 1974. Paleozoickie Solenosn'ie Formatsii Mira. Nedra, Moscow, USSR.

Zharkov, M.A., 1981. History of Paleozoic salt Accumulation. Springer Verlag, New York.